EFFECT OF GASPERS ON AIRFLOW PATTERNS AND THE TRANSMISSION OF AIRBORNE CONTAMINANTS WITHIN AN AIRCRAFT CABIN ENVIRONMENT

by

MICHAEL D. ANDERSON

B.S., Kansas State University, 2010

A THESIS

submitted in partial fulfillment of the requirements for the degree

MASTER OF SCIENCE

Department of Mechanical and Nuclear Engineering
College of Engineering

KANSAS STATE UNIVERSITY
Manhattan, Kansas

2012

Approved by:

Co-Major Professor
Dr. Mohammad H. Hosni

Approved by:

Co-Major Professor
Dr. Byron W. Jones

Copyright

Abstract

Due to the high occupant density and large number of travelers on commercial aircraft, it is crucial to limit the transport of contaminants and pathogens amongst passengers. In order to minimize the exposure of passengers to various contaminants of different sizes and characteristic, all mechanisms influencing airflow movement within an aircraft cabin need to be understood. The use of personal gaspers on commercial aircraft and their relation to airborne contaminants and pathogens transport is one such mechanism that was investigated.

Tracer gas testing using carbon dioxide (CO_2) was conducted in a wide-body, 11-row Boeing 767 aircraft cabin mockup using actual aircraft components for air distribution. Three separate experiments were conducted investigating the effect of gaspers on the transport of contaminants. The first series of experiments focused on the effect of gaspers on longitudinal transport patterns within an aircraft cabin environment by measuring the concentration of tracer gas along the length of the aircraft cabin. The second experiment investigated what fraction of air a passenger inhales originates from a gasper in relation to the overall cabin ventilation. The final set of experiments determined if gaspers could limit close range person-to-person transmission of exhaled contaminants.

Three separate sets of conclusions were drawn, one for each series of experiments. The first conclusion is that gaspers disrupt the longitudinal transport of contaminants within the aircraft cabin. The second conclusion is that less than 5% of the air inhaled by a passenger is originating from a gasper even with a gasper directed at the passenger's face. This low percentage is a result of the turbulent airflow within the aircraft cabin causing the gasper jet to quickly mix with the overall cabin ventilation air. The last conclusion is that gaspers can reduce person-to-person transmission of exhaled contaminants as much as nearly 90% in some cases. In other cases the gaspers are found to have negligible or negative impact on the transmission of contaminants. These conclusions are dependent upon where the tracer gas plume emanated from, the sampling location, and the configuration of gaspers around the tracer gas release point.

Table of Contents

List of Figures ix

List of Tables xiv

Acknowledgements xvi

Chapter 1 - Introduction 1

Chapter 2 - Background and Literature Review 3

2.1 Standard Conditions of the Aircraft Cabin Environment 3

2.2 Air Supply System 3

2.3 Disease and Contaminant Transmission 5

2.4 Gaspers and Personal Ventilation 6

2.5 Tracer Gas Selection 7

2.5.1 Carbon Dioxide Tracer Gas Properties 7

2.5.2 Carbon Dioxide Sensor Selection 8

Chapter 3 - Testing Facilities and Equipment 9

3.1 Aircraft Cabin Simulator 10

3.1.1 Cabin Dimensions 11

3.1.2 Cabin Seat Dimensions 14

3.1.3 Thermal Manikins 16

3.1.3.1 Thermal Resistance Manikins 16

3.1.3.2 Thermal Observation Manikin 17

3.2 Cabin Air Supply and Ductwork 18

3.2.1 Ductwork 18

3.2.1.1 Main Supply Duct 18

3.2.1.2 . Aircraft Cabin Ductwork 20

3.2.2 Cabin Air Supply 21

3.2.3 Control System and Program 24

3.2.4 Gasper System 26

3.2.4.1 Installation of Gaspers 26

3.2.4.2 Gasper Air Supply 27

3.3 Tracer Gas Supply and Sampling 31

3.3.1 Tracer Gas Supply 31

3.3.2 Tracer Gas Sampling Tree 32

3.3.3 Tracer Gas Detection 33

3.3.4 Control Program 36

Chapter 4 - Testing Methods and Analysis 37

4.1 Cabin Traverse Testing 37

4.1.1 Testing Setup 37

4.1.2 Tracer Gas Injection 38

4.1.3 Test Procedure 39
4.1.4 Data Analysis Method 40
4.2 Gasper Air Inhalation Testing 40
4.2.1 Testing Setup 40
4.2.2 Tracer Gas Injection 41
4.2.3 Tracer Gas Sampling 42
4.2.4 Test Procedure 43
4.2.5 Data Analysis Method 44
4.3 Manikin Tracer Gas Release Testing 46
4.3.1 Testing Setup 47
4.3.2 Tracer Gas Release Mechanism 47
4.3.3 Intra-Row Testing Method 49
4.3.3.1 Tracer Gas Sampling and Release 49
4.3.3.2 Test Procedure 50
4.3.4 Two-row Testing Method 50
4.3.4.1 Tracer Gas Sampling and Release 51
4.3.4.2 Test Procedure 52
4.3.5 Data Analysis Method 53
Chapter 5 - Results 54
5.1 Cabin Traverse Testing Results 54

5.1.1 Row 11 Injection 54
5.1.2 Row 1 Injection 58
5.1.3 Row 6 Injection 60
5.2 Gasper Air Inhalation 63
5.3 Manikin Tracer Gas Release 64
5.3.1 Intra-row Method Seat 6B Release Point 65
5.3.2 Intra-row Method Seat 6A Release Point 73
5.3.3 Two-row Sampling with Seat 6A Release 81
5.3.4 Two-row Sampling with Seat 6B Release 86
Chapter 6 - Discussion 92
6.1 Cabin Traverse Testing 92
6.2 Gasper Air Inhalation Testing 92
6.3 Manikin Tracer Gas Release 94
6.3.1 Intra-row Method, Seat 6B Release 94
6.3.2 Intra-row Method, Seat 6A Release 95
6.3.3 Two-row Sampling, Seat 6A Release 96
6.3.4 Two-row Sampling, Seat 6B Release 97
6.3.5 Additional Discussion 97
Chapter 7 - Summary and Conclusions 98
Chapter 8 - Recommendations 100

References 101

Appendix A - Uncertainty Analysis 103

Appendix B - Changing of Interior CO_2 Sensors 112

List of Figures

Figure 2.1 Air Supply in Cabin (Hunt & Space, 1994) 4

Figure 2.2 Transmission of SARS on a Flight (Olsen et al., 2003) 5

Figure 3.1 Aircraft Cabin Simulator Enclosure (Beneke, 2010) 9

Figure 3.2 Exterior of Aircraft Cabin Simulator (Trupka, 2011) 11

Figure 3.3 Location of Linear Diffusers in Aircraft Cabin (Beneke, 2010) 12

Figure 3.4 Top View of Seat Layout in Aircraft Cabin, Rows 1-11, Seats A-G (Trupka, 2011). 13

Figure 3.5 Cross Sectional View of Aircraft Cabin 14

Figure 3.6 Double Seat Dimensions 15

Figure 3.7 Triple Seat Dimensions 15

Figure 3.8 Seat Dimensions 16

Figure 3.9 Cabin Interior with Seated Manikins (Beneke, 2010) 17

Figure 3.10 Thermal Observation Manikin (TOM) 18

Figure 3.11 Initial Duct Configuration (Beneke, 2010) 19

Figure 3.12 Dehumidification System and Current Duct Inlet 20

Figure 3.13 Connections of Cabin Ductwork, Flexible Tubing, and Linear Diffusers (Trupka, 2011) 21

Figure 3.14 Flow Diagram of Air Supply System (Beneke, 2010) 21

Figure 3.15 Components of Air Conditioning System (Beneke, 2010) 23

Figure 3.16 Current Air Supply Control System 26

Figure 3.17 Gasper clusters installed in cabin 27

Figure 3.18 Gasper Supply System Layout 28

Figure 3.19 Connections from Supply Lines to Gaspers 29

Figure 3.20 Gasper System Pressure Regulator 30

Figure 3.21 Needle Valve and Mass Flow Controllers 32

Figure 3.22 Tracer Gas Sampling Tree (Trupka, 2011) 33

Figure 3.23 CO_2 sensors: Inlet air sensor (top left), NOVA 420 (bottom), WMA-4 (top right) .. 34

Figure 3.24 Flow Balancing System 35

Figure 3.25 Sampling and Control Program used for Testing 36

Figure 4.1 Locations of Tracer Gas Release 38

Figure 4.2 Tracer Gas Injection Tube 39

Figure 4.3 Sampling Location for Gasper Inhalation 43

Figure 4.4 Comparison of Measured Background and Gasper CO_2 Concentrations 45

Figure 4.5 All CO_2 Measurements Taken during Gasper Inhalation 46

Figure 4.6 Tracer Gas Release Device 48

Figure 4.7 Tracer Gas Smoke Visualization 48

Figure 4.8 Release Manikin and TOM in Row 6 49

Figure 4.9 Sampling and Release Locations for Two-row Tests 51

Figure 4.10 Release and Sampling Layout for Two-row Testing 52

Figure 5.1 Row 11 Release with Gaspers Off 55

Figure 5.2 Row 11 Release with Gaspers On 56

Figure 5.3 Average Values of Row 11 Release with Gaspers On and Off 56

Figure 5.4 Average Values of Row 11 Release Trial 2 with Gaspers On and Off 58

Figure 5.5 Row 1 Release Gaspers Off 59

Figure 5.6 Row 1 Release Gaspers On 59

Figure 5.7 Average Values of Row 1 Release with Gaspers On and Off 60

Figure 5.8 Row 6 Release Gaspers Off 61

Figure 5.9 Row 6 Release Gaspers On 62

Figure 5.10 Average Values of Row 11 Release Gaspers On and Off 62

Figure 5.11 Run 1 Intra-row Method, Both Gaspers Off, Seat 6B Release 65

Figure 5.12 Run 2 Intra-row Method, Both Gaspers Off, Seat 6B Release 66

Figure 5.13 Run 3 Intra-row Method, Both Gaspers Off, Seat 6B Release 66

Figure 5.14 Run 1 Intra-row Method, Gasper 6A On, Seat 6B Release 67

Figure 5.15 Run 2 Intra-row Method, Gasper 6A On, Seat 6B Release 68

Figure 5.16 Run 3 Intra-row Method, Gasper 6A On, Seat 6B Release 68

Figure 5.17 Run 1 Intra-row Method, Gasper 6B On, Seat 6B Release 69

Figure 5.18 Run 2 Intra-row Method, Gasper 6B On, Seat 6B Release 69

Figure 5.19 Run 3 Intra-row Method, Gasper 6B On, Seat 6B Release 70

Figure 5.20 Run 1 Intra-row Method, Both Gaspers On, Seat 6B Release 70

Figure 5.21 Run 2 Intra-row Method, Both Gaspers On, Seat 6B Release 71

Figure 5.22 Run 3 Intra-row Method, Both Gaspers On, Seat 6B Release 71

Figure 5.23 Intra-row Method, Summary of Seat 6B Release..... 72

Figure 5.24 Run 1 Intra-row Method, Both Gaspers Off, Seat 6A Release 73

Figure 5.25 Run 2 Intra-row Method, Both Gaspers Off, Seat 6A Release 74

Figure 5.26 Run 3 Intra-row Method, Both Gaspers Off, Seat 6A Release 75

Figure 5.27 Run 1 Intra-row Method, Gasper 6B On, Seat 6A Release..... 76

Figure 5.28 Run 2 Intra-row Method, Gasper 6B On, Seat 6A Release..... 76

Figure 5.29 Run 3 Intra-row Method, Gasper 6B On, Seat 6A Release..... 77

Figure 5.30 Run 1 Intra-row Method, Gasper 6A On, Seat 6A Release..... 77

Figure 5.31 Run 2 Intra-row Method, Gasper 6A On, Seat 6A Release..... 78

Figure 5.32 Run 3 Intra-row Method, Gasper 6A On, Seat 6A Release..... 78

Figure 5.33 Run 1 Intra-row Method, Both Gaspers On, Seat 6A Release 79

Figure 5.34 Run 2 Intra-row Method, Both Gaspers On, Seat 6A Release 79

Figure 5.35 Run 3 Intra-row Method, Both Gaspers On, Seat 6A Release 80

Figure 5.36 Intra-row Method, Summary of Seat 6A Release 81

Figure 5.37 Two-row testing, All Gaspers Off, Seat 6A Release..... 82

Figure 5.38 Two-row testing, Gasper Location 1 On, Seat 6A Release..... 83

Figure 5.39 Two-row testing, Release Gasper On, Seat 6A Release..... 83

Figure 5.40 Two-row testing, Gasper Location 2 On, Seat 6A Release..... 84

Figure 5.41 Two-row testing, Gasper Location 3 On, Seat 6A Release..... 84

Figure 5.42 Two-row testing, Gasper Location 4 On, Seat 6A Release 85

Figure 5.43 Summary of Average Normalized CO_2 for Rows 5 and Sampling with Seat 6A Release 86

Figure 5.44 Two-row testing, All Gaspers Off, Seat 6B Release 87

Figure 5.45 Two-row testing, Gasper Location 1 On, Seat 6B Release 88

Figure 5.46 Two-row testing, Release Gasper On, Seat 6B Release 88

Figure 5.47 Two-row testing, Gasper Location 2 On, Seat 6B Release 89

Figure 5.48 Two-row testing, Gasper Location 3 On, Seat 6B Release 89

Figure 5.49 Two-row testing, Gasper Location 4 On, Seat 6B Release 90

Figure 5.50 Summary of Average Normalized CO_2 for Rows 5 and 7 Sampling with Seat 6B Release 91

Figure 6.1 Top View of TOM with Smoke Visualization of Airflow 93

List of Tables

Table 3.1 Components of Air Conditioning System (Trupka, 2011) 22

Table 3.2 Control and Feedback Information (Trupka, 2011)..... 25

Table 4.1 Intra-row Testing Gasper Configurations..... 50

Table 4.2 Configurations for Two-row Testing..... 53

Table 5.1 Average Normalized Concentrations for Row 11 Release 57

Table 5.2 Average Normalized Concentration for Row 11 Trial 2 58

Table 5.3 Average Normalized Concentrations for Row 1 Release 60

Table 5.4 Average Normalized Concentrations fro Row 11 Release 63

Table 5.5 Results of Gasper Focused Directly on Face of TOM..... 63

Table 5.6 Results of Gasper Focused on the Left Side of TOM's face..... 64

Table 5.7 Results of Gasper Focused on the Right Side of TOM's face..... 64

Table 5.8 Intra-row Method, Averaged Values of Seat 6B Release..... 72

Table 5.9 Intra-row Method, Averaged Values of Seat 6A Release..... 81

Table 5.10 Normalized Values for Rows 5 and 7 Sampling with Seat 6A Release 86

Table 5.11 Normalized Values for Rows 5 and 7 Sampling with Seat 6B Release 91

Table A.1 CO_2 Analyzer and DAQ Uncertainties..... 106

Table A.2 R-squared Values and Uncertainties of CO_2 Analyzers..... 107

Table A.3 Statistical Values for Row 11 Injection, Row 10 Sampling, Test Run 2, Gaspers Off 108

Table A.4 Example Values for Gasper CO_2 Concentration Measurement 110

Table A.5 Uncertainties of Averaged CO_2 Concentrations..... 110

Table A.6 Relative Uncertainties for Manikin Release, Two-row Testing Method, Seat 6A Release 111

Table A.7 Relative Uncertainties for Manikin Release, Two-row Testing Method, Seat 6B Release 111

Acknowledgements

I would like to acknowledge all of my family members and professors who supported me during my time in graduate school and made it possible for me to earn my Master's degree.

First, I would like to thank Dr. Hosni and Dr. Jones for allowing me to work on this project and taking time to give their assistance and input. Dr. Hosni encouraged me to pursue my graduate degree and helped me get started working at ACER as an undergraduate. Dr. Jones helped me immensely in the design of the gasper system as well as my testing methods. I would also like to thank Dr. Beck for all of the help he has provided me in my time at Kansas State both as an undergraduate and graduate student and being a part of my graduate committee. A thank you goes to Boeing, the FAA, and all of the corporate sponsors that make research at ACER a possibility.

I was also helped along the way by several undergraduate and graduate students working at ACER. Tristan Trupka showed me around the laboratory facilities and showed me how to work many of the systems used for testing. Jeremy Beneke, Tanner Marshall, Drew Manker, and Robert Powell provided assistance whenever I needed extra help in setting up tests and equipment.

Finally, I would like to thank my parents and brother for all of their advice and support over the duration of my college career.

This research was funded by the U.S. Federal Aviation Administration (FAA) Office of Aerospace Medicine through the National Air Transportation Center of Excellence for Research in the Intermodal Transport Environment under Cooperative Agreement 07-C-RITE-KSU. Although the FAA has sponsored this project, it neither endorses nor rejects the findings of this research. The publication of this information is in the interest of invoking technical community comment on the results and conclusions of the research.

Chapter 1 - Introduction

In 2011, 730 million people traveled on commercial aircraft domestically (BTS, 2012). These passengers are confined to the same high occupant density space for sometimes as long as twenty hours depending on flight length. This large volume of travelers combined with their time spent in close proximity during flights increases the potential for transmitting diseases such as severe acute respiratory syndrome (SARS), tuberculosis, swine influenza (H1N1), and avian influenza (H5N1). The potential also exists for intentional dispersal of gaseous contaminants or biological agents by passengers with malicious intent.

The Air Transportation Center of Excellence for Airliner Cabin Environment Research (ACER) team was formed to address these concerns as well as to investigate transport phenomena within aircraft cabins. The two investigative methods used by ACER are the use of computational fluid dynamic (CFD) analysis, and the collection of experimental data in simulated aircraft cabins. The experimental data is important for verification of any CFD results. Past and current research conducted at ACER has been focused on what role the aircraft cabin environment itself has on causing pandemics and spreading contaminants amongst passengers. With focus being placed not only on whether the current systems of air distribution are adequate, but what improvements could possibly be made in mitigating contaminant transmission in the future. This thesis focuses on how airflow patterns within an aircraft are affected by the use of personal gaspers. Results are also presented on the ability of gaspers to provide protection to passengers from contaminants within the aircraft cabin.

All testing was performed in an 11-row mockup of a Boeing 767-300 located at the ACER laboratory at Kansas State University in Manhattan, KS. Previous research conducted has utilized tracer gas, fine particle dispersal, and CFD techniques to analyze flow patterns and contaminant dispersal within the cabin (Jones, 2009; IER, 2008; Trupka, 2011; Beneke, 2010; Lebbin, 2006). These are the first results focusing on the potential impact gaspers have on the health of passengers and crew as well as their influence on airflow patterns. Tracer gas is used to represent contaminants released by passengers as well as to detect the amount of gasper air inhaled by passengers. The results of three separate testing methods are presented, first using

tracer gas to determine how gaspers influence airflow patterns within the aircraft, secondly investigating the amount of gasper air a passenger typically inhales, and finally the protection a gasper provides a passenger from contaminants.

Chapter 2 - Background and Literature Review

The high occupant density of passengers and potential for spreading contaminants among passengers is a major issue for the aircraft cabin environment. The harsh outdoor environmental conditions of an aircraft at high altitude pose more issues in generating a comfortable environment for passengers. As such, the aircraft cabin environment is subject to rigorous regulations from the Federal Aviation Administration (FAA) to keep it safe.

2.1 Standard Conditions of the Aircraft Cabin Environment

The aircraft cabin environment is unique in terms of public and commercial transport. It is a high altitude environment, with the goal to condition a space to FAA standards subjected to external temperatures as low as -55°C (-67°F) and pressures one-fifth of atmosphere (Zhang & Chen, 2007). These standards include provisions for temperature, pressure, and contaminant levels within the air. From FAA regulation 25.831, the ventilation system is required to provide 0.25 kg/min (0.55 lb/min) of fresh air per passenger (FAA, 1996). This amount corresponds to an airflow rate of 3.75 l/s (7.5 cfm) at sea level and 5 l/s (10 cfm) at 8000 feet cabin altitude. This standard also limits CO_2 concentration during flight to not exceed 5000 ppm with CO concentrations remaining under 50 ppm in air. Under section 25.841, the pressure altitude within the cabin at which this air is provided must not exceed 2438 m (8,000 ft). While the external air must be brought up to a temperature in the ranges of 19.4-22.8°C (67-73°F) in winter and 22.8-26.1°C (73-79°F) in summer with a variation of no more than 3°C (5.4°F) between the ankles and head of a passenger according to ASHRAE standard 55-2004 (O'Donnell et al. 1991).

2.2 Air Supply System

In order to maintain these standards, air is completely exchanged within an aircraft cabin at an extremely high rate, approximately 20 to 30 times per hour (Hunt & Space, 1994). Typically providing 10 l/s (20 cfm) of fresh air per passenger; double what is called for in FAA regulation 28.831. The high exchange rate is necessary for greater control of temperature gradients within the environment and to prevent stagnant areas of air from forming. It is also meant to help in

prevention of disease transmission amongst different zones of the cabin by quickly exhausting any contaminants.

In a typical aircraft this air is supplied at the top of the cabin through a system of linear diffusers and ducts along the center of the cabin. It is then exhausted through the exhaust vents located on the side walls near the floor, creating a circular flow pattern. Theoretically, the recirculation of air in this manner generates side-to-side circulation with little front-to-back motion within the cabin (Hunt & Space, 1994; Mangili & Gendreau, 2005). This airflow pattern is illustrated in Figure 2.1 below.

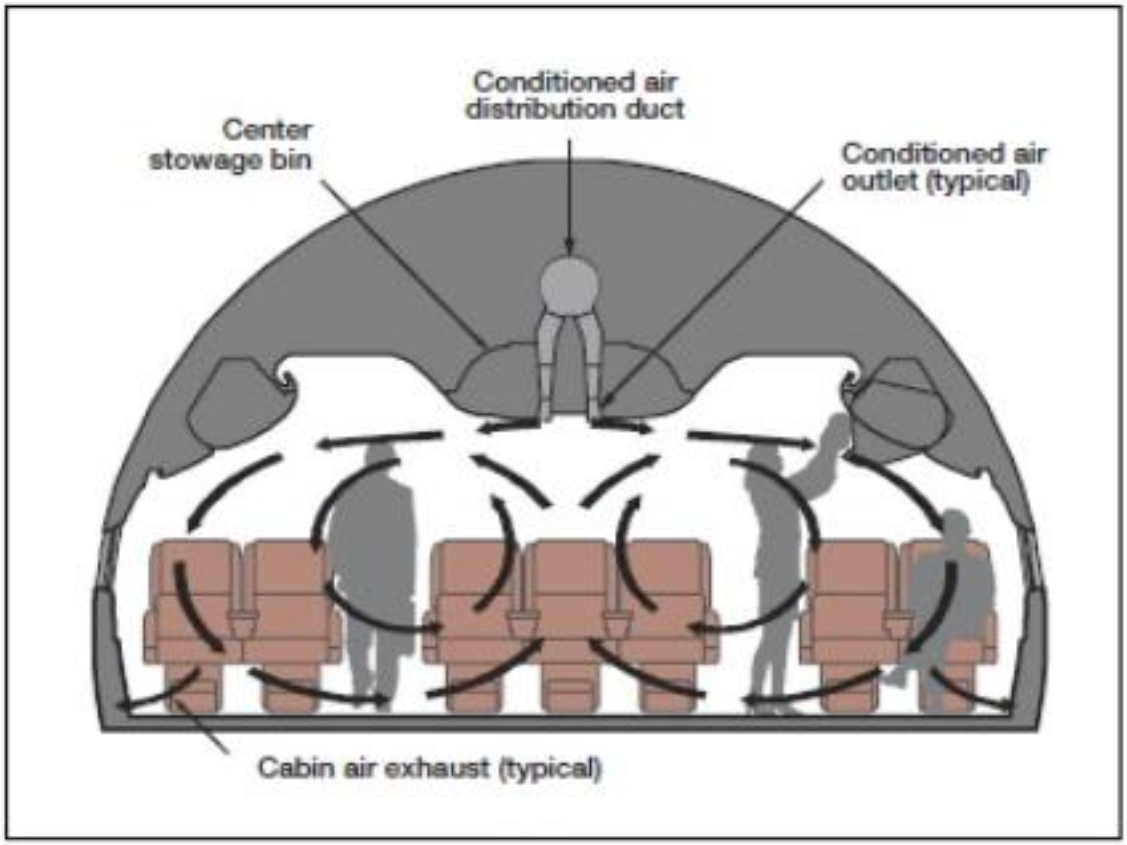

Figure 2.1 Air Supply in Cabin (Hunt & Space, 1994)

Approximately 50 percent of the air delivered is re-circulated for increased operational efficiency of the aircraft's air conditioning system and allows for the doubling of the ventilation rate over the FAA ventilation standard (Hunt & Space, 1994). This re-circulated air passes through high efficiency particulate air (HEPA) filters that remove between 94 and 99.97 percent of airborne particles (Mangili & Gendreau, 2005). HEPA filters have been found to remove particles 0.003

microns in diameter at efficiency greater than 99.9+ percent (Hunt & Space 1994). Typically viruses range from 0.02 to 0.3 microns in size with bacteria varying from 0.5 to 10 microns in size (Morawska, 2006). For instance, the SARS and influenza viruses of importance in this research range from approximately 0.075 to 0.16 microns in diameter (Morawska, 2006). The use of HEPA filters and high recirculation rate greatly reduces the possibility of spreading any disease or contaminant through a properly functioning recirculation system on an aircraft.

2.3 Disease and Contaminant Transmission

Diseases and contaminants are generally spread by contact amongst passengers, whether that is sneezing, coughing, breathing, or contact with fomites. Theoretically, the air distribution system only creates side-to-side circulation, but in actuality, large-scale eddies and non-uniform air distribution causes contaminants to spread along the length of the cabin and even accumulate in various locations (Wang et. al, 2006). During the SARS outbreak of 2003, Olsen et al. (2003) were able to document the spread of the disease on an actual flight of a Boeing 737-300. They documented that passengers as far as seven rows in front of the initial infected passenger were exposed and later infected with SARS. Figure 2.2 shows the results of their findings, showing how the disease transmitted throughout the cabin.

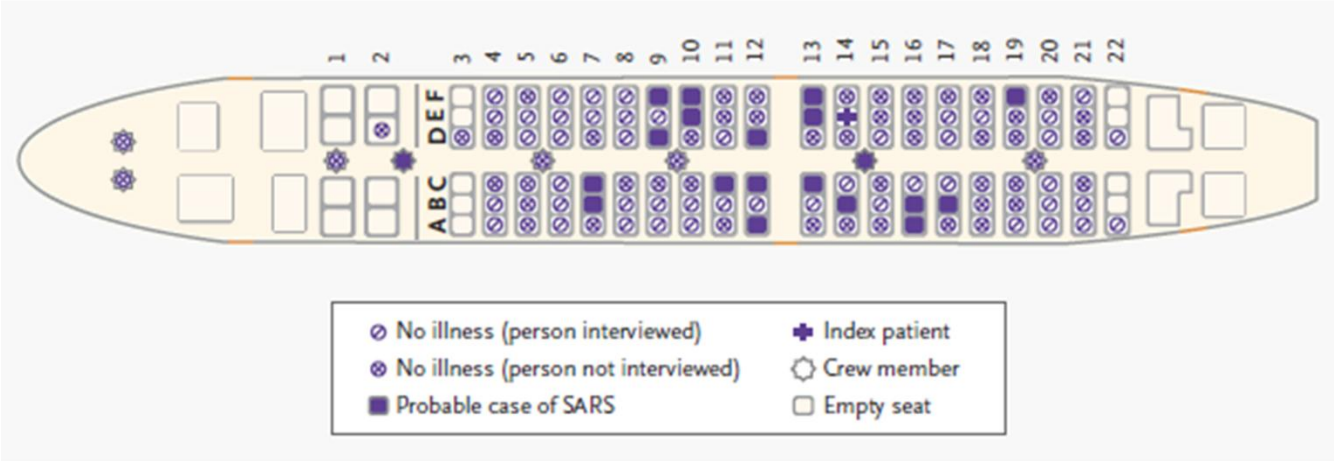

Figure 2.2 Transmission of SARS on a Flight (Olsen et al., 2003)

Previous testing conducted in mock up 5-row aircraft cabins (Wang, 2006) as well as at ACER (Lebbin, 2006; Jones, 2009; Beneke et al., 2011) show similar results of particles spreading along the length of the cabin. This transport is increased by the presence of a secondary airflow

pattern causing mixing along the length of the aircraft cabin (Beneke, 2010; Shehadi, 2010). It is important to better understand these flow patterns and eddies, and what systems on the aircraft can potentially alter this flow. The effect of the wake generated by beverage carts has already been researched (Trupka, 2011). Gaspers are another feature of most commercial aircraft cabins that possess the potential to alter airflow.

2.4 Gaspers and Personal Ventilation

Personal gaspers are adjustable nozzles found on most passenger aircraft above every seat. Their main purpose is for individual thermal comfort, allowing each passenger to control high velocity jets of air by adjusting the amount of airflow leaving the gasper (NRC, 2002). The air supplied to a gasper is dependent upon the make and model of an aircraft. Sometimes the air comes directly from the air conditioning packs, in other cases it is supplied with re-circulated air. They play a minor role in cabin ventilation, but their effect on airflow patterns within the cabin and ability to prevent disease transmission has yet to be assessed. The first set of results presented in this thesis addresses the effect of gaspers on overall airflow patterns within an aircraft cabin.

Research exists focusing on the use and development of personal ventilation systems in both office buildings and aircraft, systems analogous to gaspers (Bolashikov et al., 2009; Melikov, et al. 2002, Radim, et al 2006; Wang et al., 2006; Zhang & Chen, 2007; Zhang et al., 2012). Emphasis is placed on both thermal comfort and a reduction of disease transmission in these studies. In aircraft, the research covers novel air supply systems that could potentially be developed that reduce disease transmission by as much as 60% (Gao & Niu, 2008). In office buildings, some systems have been shown to reduce transmission by up to 90% (Bolashikov & Melikov, 2009).

The personal ventilation systems used in office buildings are not really applicable to aircraft due to the turbulent, mixing nature of aircraft ventilation compared to an office building air supply. Also, the novel systems being tested in aircraft are in developmental phases and not practical to currently install in all aircraft with most results coming from CFD analysis. However, the testing methods used in the papers previously mentioned to evaluate the effectiveness of personal

ventilation systems in office buildings as well as the novel aircraft personal ventilation are applicable to researching the influence of gaspers on disease transmission and airflow patterns.

These methods used tracer gas both as a pollutant emanating from individual manikins to simulate a plume of contaminant, and also as a source from personal ventilation devices to detect the amount of personal ventilation air inhaled. Both of these methods were directly applied with an installed gasper system in the Boeing 767-300 aircraft simulator at ACER lab. The tracer gas equipment necessary to perform testing already existed and was in place at ACER as it had been used in previous studies (Trupka, 2011; Lebbin, 2006; IER, 2008; Jones, 2009). Experimental results from tracer gas testing are important for future analysis of cabin airflow as airflows unaccounted for in current CFD models may be shown to develop. The use of tracer gas also simulates the travel of a contaminant plume well, making it suitable to use in determining if gaspers provide any protection from contaminants to airline passengers.

2.5 Tracer Gas Selection

In order to perform testing, a tracer gas needed to be selected to simulate gaseous contaminant plumes. The tracer gas needed to be readily available, nonhazardous, easily detectable, and mixes well with the cabin air supply (Lebbin, 2006; Trupka, 2011). Carbon dioxide (CO_2) was chosen as it displays all of these traits. Sulfur Hexafluoride (SF_6) is another common tracer gas; however it has not been utilized at ACER.

2.5.1 Carbon Dioxide Tracer Gas Properties

CO_2 is readily available on an industrial level, making it cheap to purchase. The large molecules of the gas itself also make it easily detectable. However, CO_2 is present in detectable levels in the atmosphere. The aircraft cabin simulator is supplied with outside, atmospheric air, meaning this background concentration must be differentiated from when performing testing. Also the molecular weight of CO_2 is far greater than that of atmospheric air, possibly causing problems with mixing. To remedy this, helium was used to mix with the CO_2 to increase the buoyancy to that of atmospheric air.

CO_2 can be harmful to humans in high enough concentrations. In order to maintain a safe testing environment, a CellarSafe CS100 CO_2 detector was installed in the cabin (Trupka, 2011). An alarm sounds if unsafe levels of CO_2 within the cabin are reached. A "GAS IN USE" sign on the exterior cabin is also illuminated to notify patrons within the lab that tracer gas testing is taking place in the aircraft cabin simulator.

2.5.2 Carbon Dioxide Sensor Selection

Non-dispersive infrared (NDIR) sensors were chosen to detect tracer gas CO_2 concentrations within the cabin. NDIR sensors were chosen because of their low cost and stable measurement of CO_2 concentrations (Trupka, 2011). The output of NDIR sensors is also highly linear, allowing the sensors to be calibrated easily using calibration gases.

NDIR sensors function by passing the sampled gas through a sensor with a filtered infrared light source at one end, and a light detector at the other. The amount of CO_2 present is then obtained using the Lambert-Beer law since the amount of light absorbed by the sample is proportional to its concentration. The intensity of the emitted light is measured before and after the sample passes through, giving the concentration of CO_2. Because of the large size of CO_2 molecules this process is accurate for concentrations between 100 ppm to 100% (Lebbin, 2006).

Chapter 3 - Testing Facilities and Equipment

The aircraft cabin simulator is located at the Airliner Cabin Environment Research (ACER) laboratory at Kansas State University located in Manhattan, Kansas. The cabin itself is housed in a 7.4 by 9.8 by 4.9 m (24.3 by 32.2 by 16.1 ft) enclosure and is ventilated with 100% outside air. This design allows for the aircraft cabin exhaust to be sealed during testing and allows for only the inlet air and tracer gas to be present within the cabin. The cabin enclosure is seen in Figure 3.1 below.

Within the enclosure, the cabin is surrounded by four spaces. Two hallways are located along the East and West sides of the cabin, allowing for storage and placement of instruments and access to the exterior of the cabin walls. A 1.2 m (3.9 ft) crawl space exists beneath the cabin, used for distribution of tracer gas supply cables and electrical wiring, as well as for more storage. The void created by these spaces serves as a plenum for the exhaust air leaving the cabin. The exhaust air is pulled out of the cabin using two exhaust fans that can be seen in Figure 3.1.

Figure 3.1 Aircraft Cabin Simulator Enclosure (Beneke, 2010)

Information presented in this chapter on the aircraft cabin simulator, cabin air supply, and controls system can be found in Trupka (2011), Beneke (2010), Lebbin (2006), and IER (2008). All of the results presented in these papers used the identical aircraft cabin setup with the exception of the change in air supply as described in section 3.2.1.1. Lebbin (2006) designed and installed the tracer gas system described, with Trupka (2011) continuing work on the system and make alterations in the controls program that was also used in this study.

3.1 Aircraft Cabin Simulator

The aircraft cabin simulator is meant to simulate a wide body aircraft with two aisles running the length of the cabin as would be seen in commercial economy class seating, with each seat installed being from an actual Boeing 767. This configuration divides each of the 11 rows into a 2-3-2 seat configuration, with 2 seats along each wall, and 3 seats between the sides.

The cabin simulator was created using plywood ribbing surrounded by formed sheet aluminum walls and ceiling with the interior being painted white. The front end of the cabin is plywood and also painted white on the interior. The aft end wall is also plywood painted white on the inside and equipped with two, standard 0.9 m (3 ft) wide doors to allow entrance into the cabin. The walls created by the ribs end are 180 mm (7.1 in.) above the plywood decking to create the exhaust gaps of the cabin simulator. The exterior of the cabin simulator can be seen in Figure 3.2 below.

Figure 3.2 Exterior of Aircraft Cabin Simulator (Trupka, 2011)

The sections below outline the dimensions of the interior of the cabin, seats used, as well as describing the thermal manikins used to simulate passengers.

3.1.1 Cabin Dimensions

The cabin itself has 77 seats laid out in the 2-3-2 configuration mentioned previously. The cabin is 9.6 m (31.5 ft) in length, with a width of 4.72 m (15.5 ft) where the seats are installed. Figure 3.4 displays the dimensions of the cabin from a top view looking toward the front. The column letters (A-G) and row numbers (1-11) are used later on when referencing specific locations within the cabin.

Air enters the cabin through two linear diffusers running along the length of the cabin. The linear diffusers are located 165 mm (6.5 in.) on either side of the cabin's centerline. The diffuser outlets are shown in Figure 3.3 below.

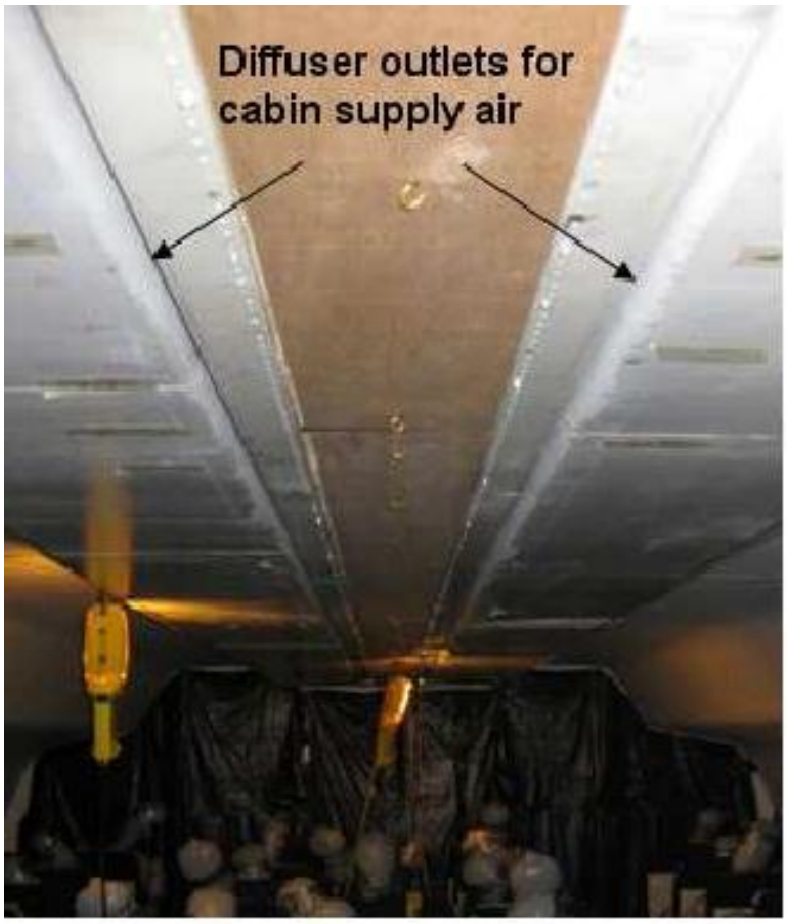

Figure 3.3 Location of Linear Diffusers in Aircraft Cabin (Beneke, 2010)

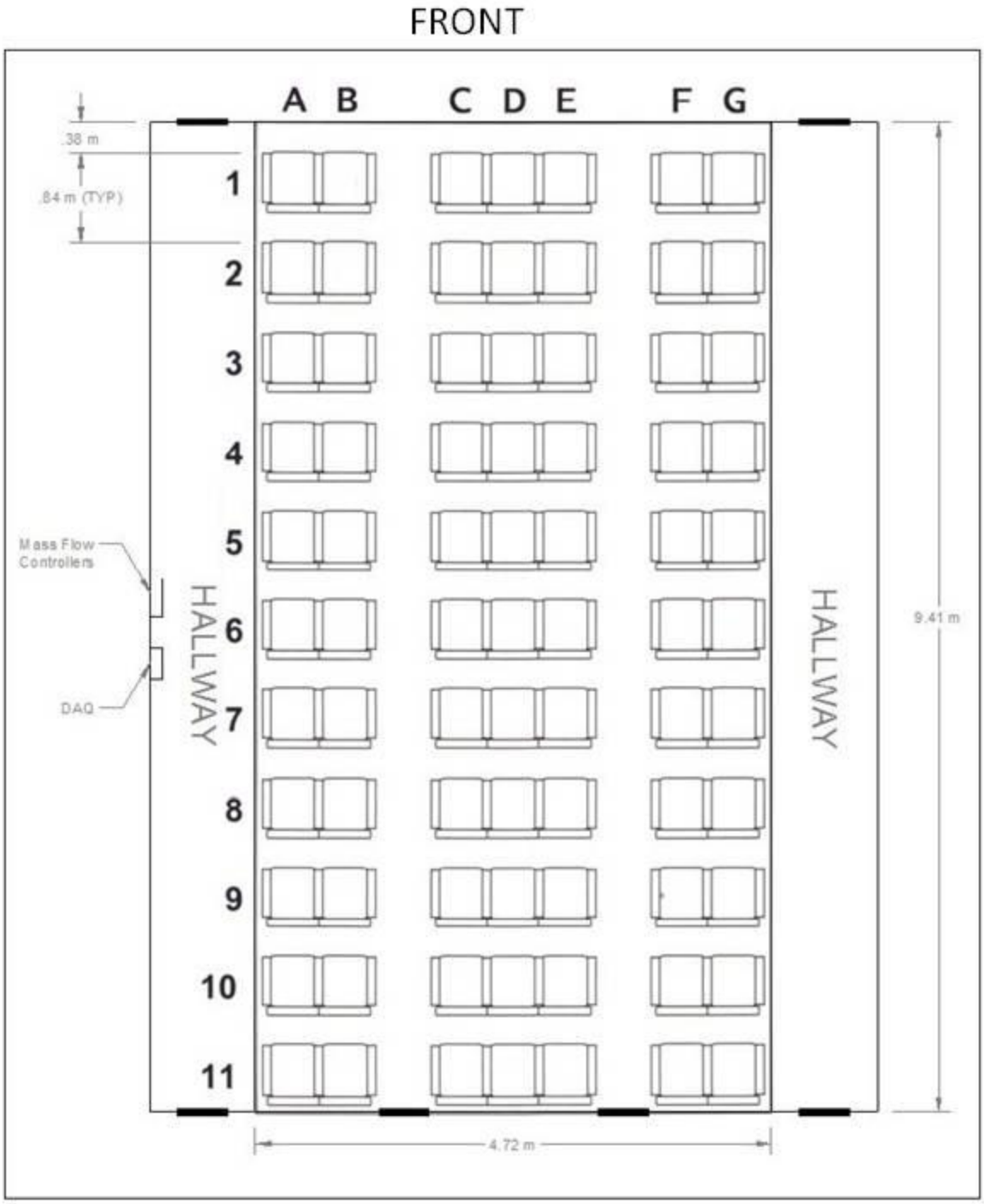

Figure 3.4 Top View of Seat Layout in Aircraft Cabin, Rows 1-11, Seats A-G (Trupka, 2011)

The cross sectional dimensions of the cabin are shown in Figure 3.5 below, the profile and dimensions are based on a mathematical formula derived by Lebbin (2006).

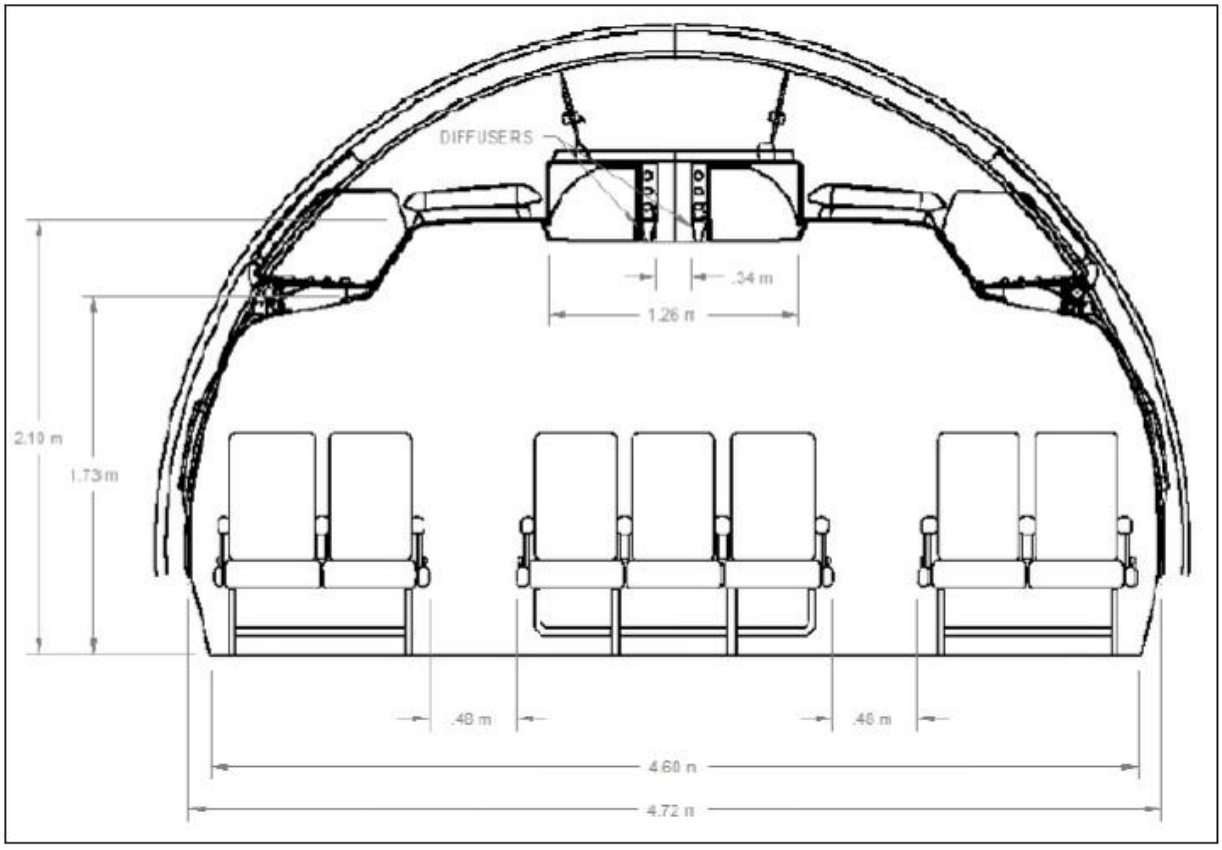

Figure 3.5 Cross Sectional View of Aircraft Cabin

3.1.2 Cabin Seat Dimensions

The seats used in the aircraft cabin are Boeing 767 seats, identical in structure with some differing in pattern or the fabric used. The seats are held to the floor of the cabin using an aluminum channel 25.4 mm (1 in.) by 19 mm (0.75 in.). Since the seats are laid out in a 2-3-2 configuration, two different seat clusters are used, one with two seats placed along the walls, the other with three seats along the center of the cabin. This arrangement is seen in both the cross sectional view and the overhead view of the cabin. The dimensions for the double and triple seat configurations as well as the dimensions of the actual seats can be seen in Figure 3.6, Figure 3.7, and Figure 3.8 below. These figures can also be found in IER (2008) and Trupka (2011).

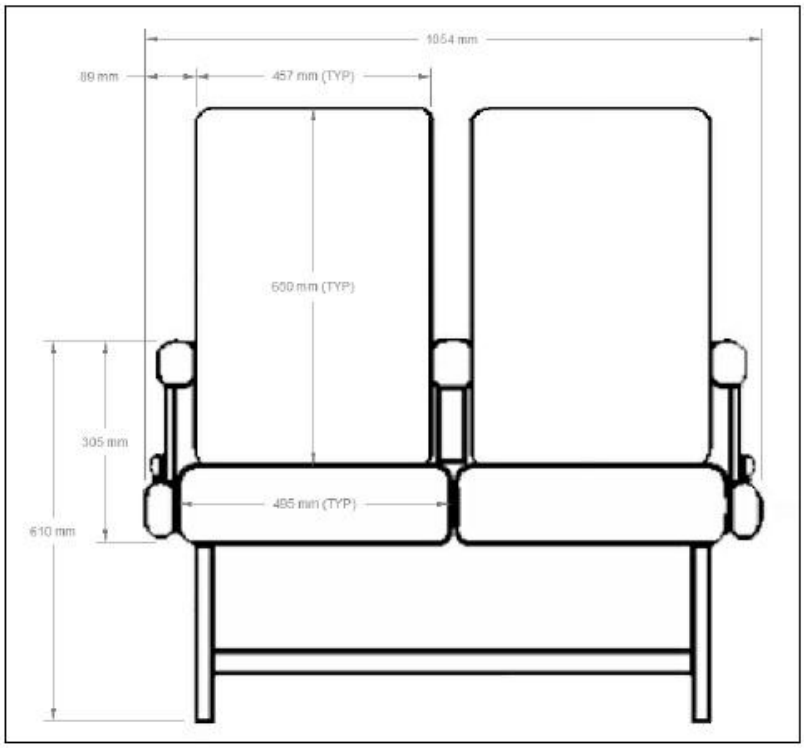

Figure 3.6 Double Seat Dimensions

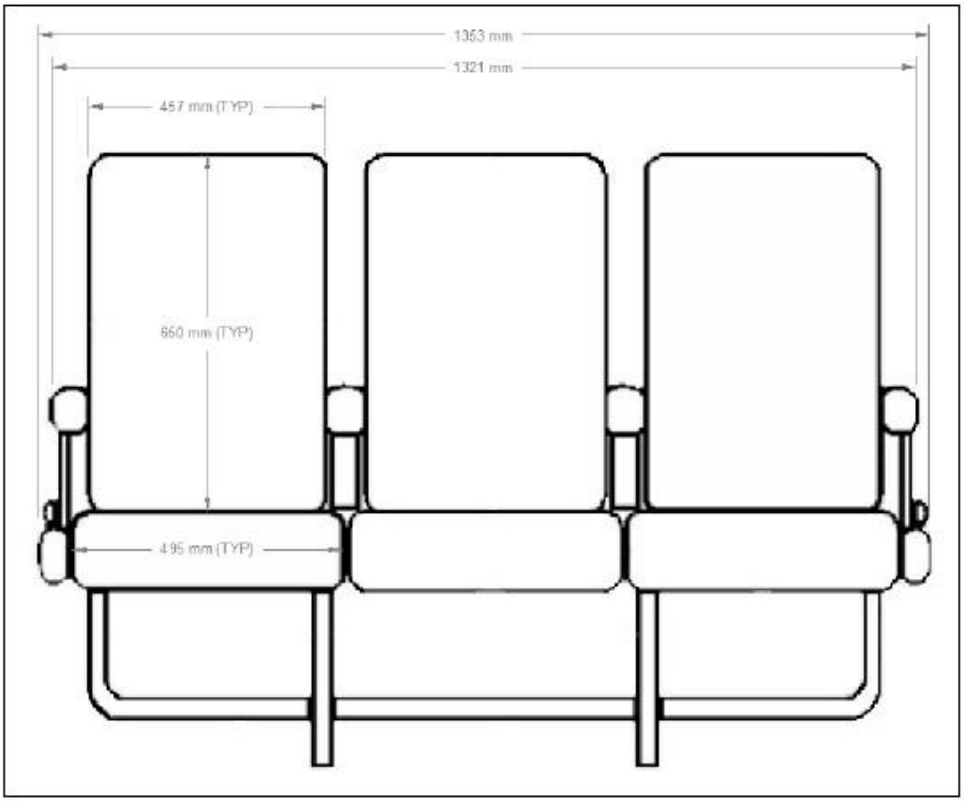

Figure 3.7 Triple Seat Dimensions

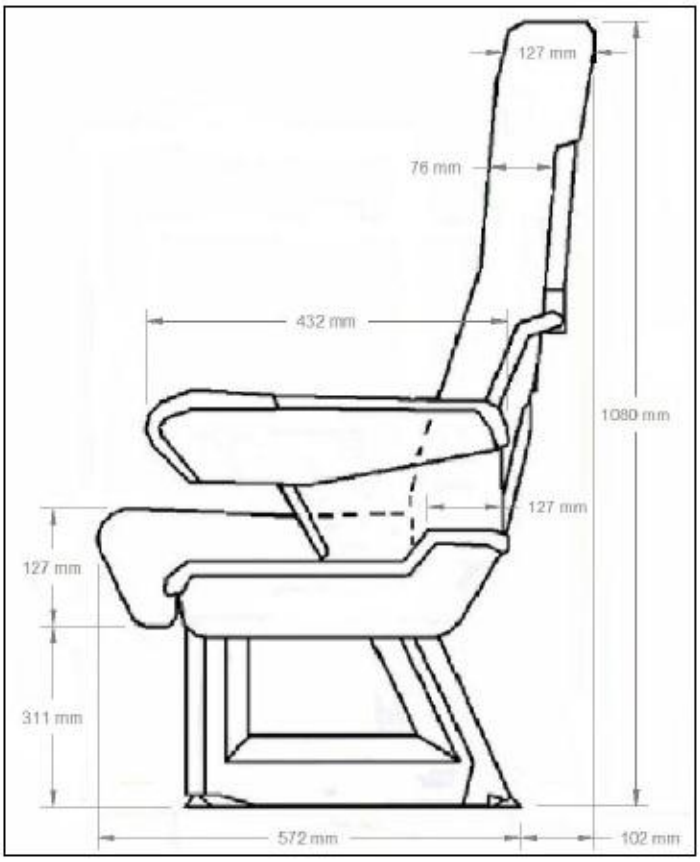

Figure 3.8 Seat Dimensions

3.1.3 Thermal Manikins

The seats of the aircraft cabin simulator were filled with thermal manikins to simulate the heat load of a typical passenger. The majority of the seats were filled with thermal manikins created in house using thermal resistance wire and inflatable manikins. However, a specialized thermal observation manikin (TOM) was utilized for testing when thermal boundaries were important.

3.1.3.1 Thermal Resistance Manikins

The thermal resistance manikins were created using Rubie's Costume Company model number 1724 inflatable manikins. 25 m (82 ft) of Omega TFCY-015 thermocouple wire was then evenly distributed around the manikin. The thermocouple wires, which served as resistance heating elements, were then connected to a 115 V AC power source. This configuration allows each manikin to generate 102 watts of heat, the heat load specified for a seated adult with a surface area of 1.8 m^2 (19.4 ft^2) as specified in ASHRAE standard 55-2004. To prevent the manikins

from overheating the cabin, safety measures were implemented. A pressure switch in the ductwork of the cabin prevents the manikins from turning on if the air supply is too low, while a thermostat at the back of the cabin shuts the power to the manikins down if the cabin temperature is too high. Seventy-six of the 77 seats in the cabin were filled using these thermal manikins. A view of the cabin interior with the seated manikins can be seen in Figure 3.9.

Figure 3.9 Cabin Interior with Seated Manikins (Beneke, 2010)

3.1.3.2 Thermal Observation Manikin

For the tests that simulated inhalation from the breathing zone of a person, a sophisticated Thermal Observation Manikin (TOM) was used to better recreate thermal boundary layers that would exist on a typical passenger. TOM is remotely controlled via a computer interface with the body being divided in to several zones. The computer controls and measures the heat flux leaving each zone, allowing for a specific skin temperature of 34°C (93.2°F) to be set. This skin temperature was the same for each zone of TOM. The inflatable manikins described before give off the same amount of heat overall, however, the heat fluxes are concentrated where the thermal wire was wrapped, causing an uneven temperature distribution along the surface of the manikin. TOM was moved to various locations depending on the test being conducted, swapping positions

with the inflatable manikins as will be described in the testing section of the paper. Figure 3.10 shows TOM in a seated position along the aisle.

Figure 3.10 Thermal Observation Manikin (TOM)

3.2 Cabin Air Supply and Ductwork

The aircraft cabin is supplied with air at a rate of 661 l/s (1400 cfm) conditioned to a temperature of 15.6°C (60°'F) through the use of a series of sensors and controls on air handling equipment. This air is supplied to the cabin using a fan and system of ducts.

3.2.1 Ductwork

There are two major components to the ductwork supplying air to the cabin. The first is the main duct supplying air to the structure enclosing the aircraft cabin. The second being the system of ducts and linear diffusers within the cabin supplying air to the interior of the aircraft cabin.

3.2.1.1 Main Supply Duct

Over the course of testing, alterations were made to the duct system supplying the cabin enclosure with air. In the initial configuration, outside air was brought in through an intake section leading up to a fan and air conditioning system. The intake section was 3.66 m (12 ft)

long with a diameter of 0.36 m (14 in.) and was insulated as were all sections of duct. After the air conditioning system, a 3.8 m (12.5 ft) section of duct 0.41 m (16 in.) in diameter led to a 90 degree bend connected to another 1.51 m (5 ft) of duct leading into a HEPA filter box. The air exits the HEPA filter box and entered a 90 degree bend leading into a 3.96 m (13 ft) long vertical section of duct 0.41 m (16 in.) in diameter. Another 90 degree bend is reached, connected to a 0.25 m (10 in.) diameter duct that enters the cabin enclosure. This configuration can be seen in Figure 3.11.

Figure 3.11 Initial Duct Configuration (Beneke, 2010)

In the fall of 2011, a dehumidification system was installed in the laboratory. The ductwork leading from the air conditioning system to the cabin enclosure was not altered. However, the inlet configuration was changed. Initially air was drawn into the duct through a louvered inlet placed under a closing garage door. When the dehumidifier was installed, the inlet was moved upward to supply the new system. The air then travels through the dehumidification system and enters the air conditioning system. The fan used in the dehumidification system operated independently of the actual dehumidification processing equipment, meaning the system could be set to use only for supplying air to the air conditioning system. An image of the dehumidification system and current inlet configuration is shown in Figure 3.12.

Figure 3.12 Dehumidification System and Current Duct Inlet

3.2.1.2 . Aircraft Cabin Ductwork

Once the air enters the cabin enclosure, it is supplied to the cabin itself using ductwork and connections from an actual Boeing 767. The 0.25 m (10 in.) diameter duct that enters the cabin enclosure runs along the length of the chamber along the centerline of the aircraft cabin. The duct is connected to the two linear diffusers using clear smooth plastic hoses coming from 34 separate ports along the length of the duct. The air then enters the cabin through these diffusers and leaves through the exhaust gaps at the base of the cabin walls into the east and west hallways. The air is drawn out of the enclosure by the fans on the south side of the cabin enclosure previously shown in Figure 3.1. The left side of Figure 3.13 shows the supply duct and its connections to the flexible tubing, while the right side shows the connection of the flexible tubing to the linear diffusers.

Figure 3.13 Connections of Cabin Ductwork, Flexible Tubing, and Linear Diffusers (Trupka, 2011)

3.2.2 Cabin Air Supply

The air supplied to the aircraft cabin is 100% outdoor air. In order to maintain the proper flow rate and temperature, the air being supplied to the cabin goes through a system consisting of a supply fan, pre-heating or cooling system dependent upon outdoor temperature, and an electric heater to fine tune the temperature. A schematic of this system is seen below in Figure 3.14.

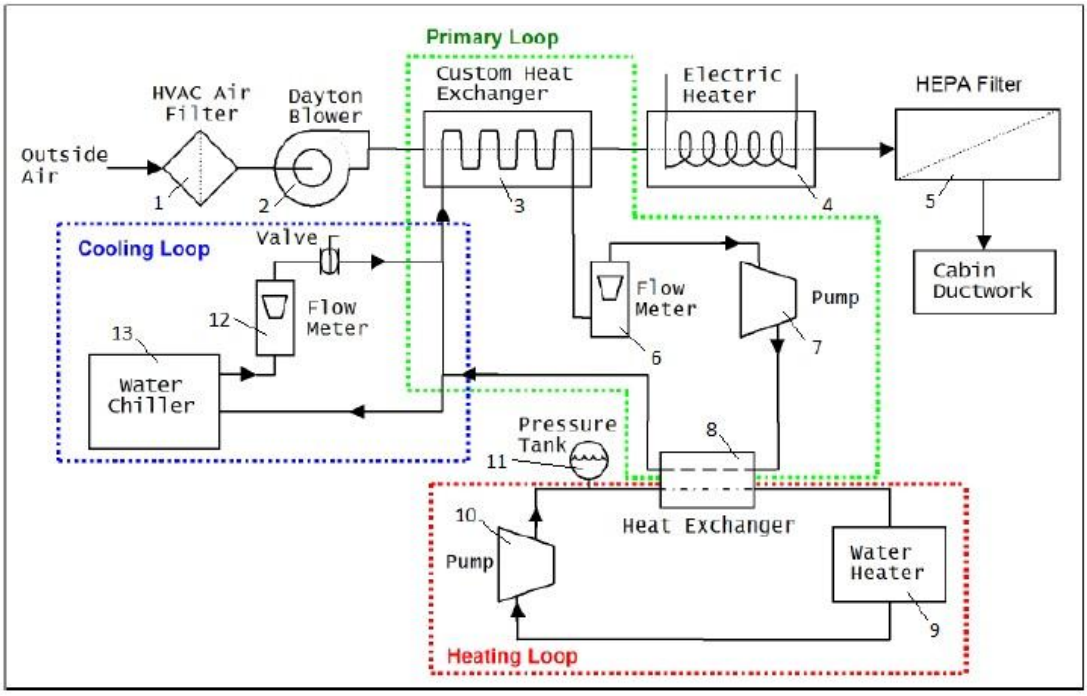

Figure 3.14 Flow Diagram of Air Supply System (Beneke, 2010)

A list of components corresponding to the flow diagram created by Trupka (2011) is presented in Table 3.1.

Table 3.1 Components of Air Conditioning System (Trupka, 2011)

No.	Item	Model	Notes
1	Air Filters	Ace 2025134	20" x 25" (2 filters in parallel)
2	Fan	12-1/4" Dayton Blower	Yaskawa GPD315/V7 VFD
3	Heat Exchanger	Custom 0.6 x 0.6 m	
4	Electric Heater	AccuTherm DLG-9-3	240 V, 3 ph., 9kW
5	HEPA Filter	Custom 1.1 m^2	99.97% to 0.3 µm efficiency
6	Flow Meter	Omega FL-7204	
7	Pump	Marathon CQM 56C34d212OF P	120 V, 3/4 HP
8	Heat Exchanger	Alfa Laval CB27-18H T06	
9	Water Heater	Rheem GT-199PV-N-1	19,000 - 199,900 BTU
10	Pump	FHP C4T34DC35A	Yaskawa GPD205-1001 VFD
11	Pressure Tank	Dayton 4MY57	6.5 gal @ 30 psi
12	Flow Meter	King 7205023133W	
13	Water Chiller	AccuChiller LQ2R15	PV-B311 condensing coils

With the installation of the of the dehumidification system, no components in the flow diagram were changed. A new 12-1/4" Dayton blower and Yaskawa controller were installed in the dehumidification system to supply outside air. A picture of the conditioning loop and components is shown in Figure 3.15. After system modifications, the air inlet was moved into the dehumidification system as indicated in Figure 3.12. The hot water heater used to supply the heating loop is not shown as it is located at the north end of the cabin enclosure.

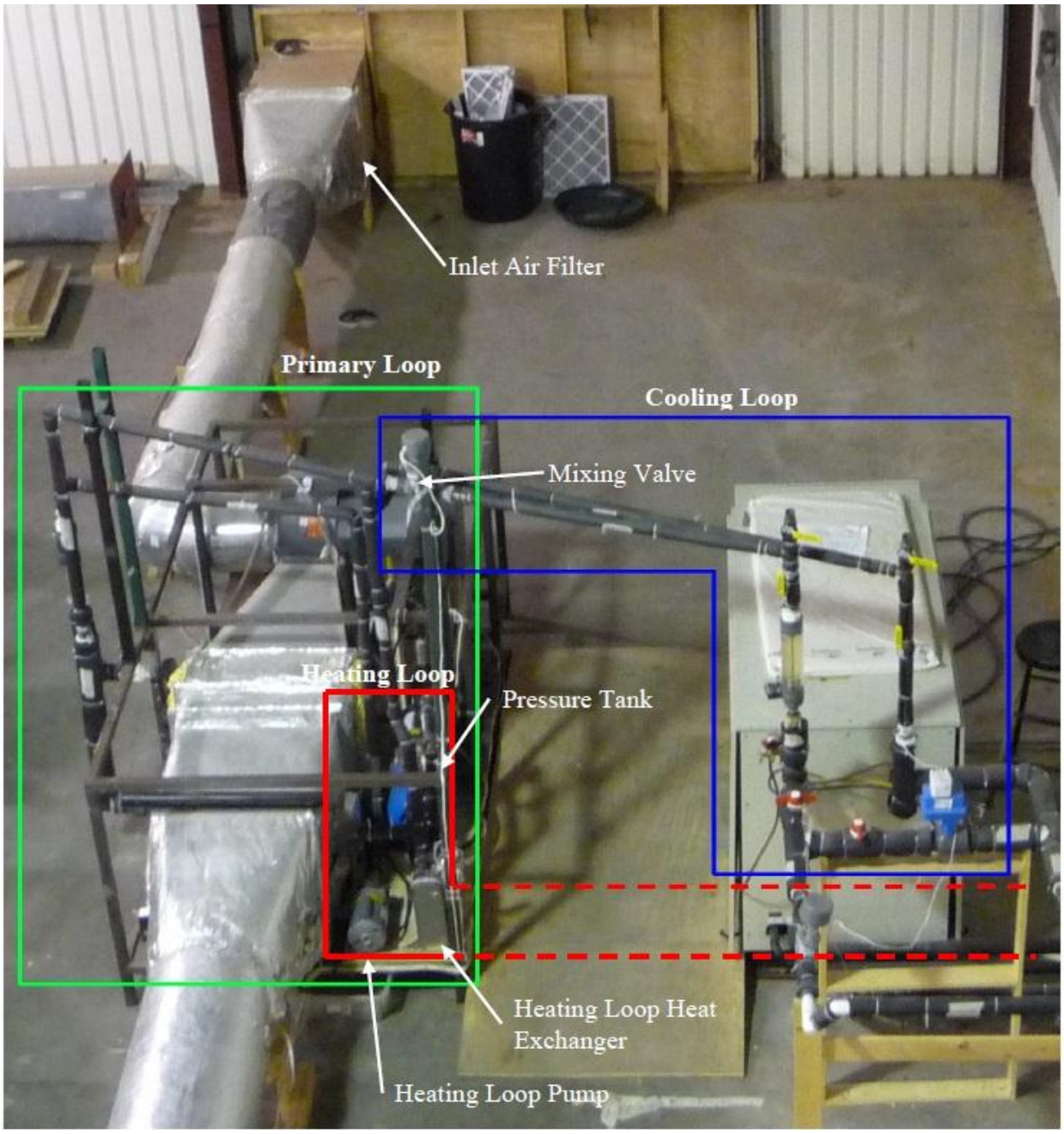

Figure 3.15 Components of Air Conditioning System (Beneke, 2010)

The air conditioning system is composed of three main loops that allow the air to be conditioned to a temperature of 15.6°C (60°F). The primary loop operates constantly to exchange heat with either the cooling or heating loop. The goal of the heating and cooling loops is to condition the air to slightly below the 15.6°C (60°F) set point. This allows for the electric heater located after the conditioning system to fine tune the temperature based on feedback response in the control system. The heating and cooling loops are operated based upon outdoor temperature. If the

outdoor air temperature was above 12.8°C (55°F), the cooling loop was operated, whereas below 10°C (50°F), the heating loop was used. If the outdoor air temperature was going to be stable during testing in the 10-12.8°C (50-55°F) range, only the electric heater was necessary to maintain set point temperature.

3.2.3 Control System and Program

The air handling system is controlled using National Instruments LabVIEW software and a series of feedback controls and sensors. Airflow rate and temperature of the air flowing into the chamber are measured and maintained using this system to maintain specific set points. Temperatures are also measured in six other locations in the primary, cooling, and heating loops. This section gives an overview of the controls system setup with more information on the system being available in Beneke (2010) and Trupka (2011).

Data is acquired through a computer interface using an Agilent 34970A and a National Instruments FP-1000 data acquisition system (DAQ). The output is controlled through a National Instruments FP-1000 with add-on modules PWM-520 and AO-210 for pulse width modulation and analog output (Trupka, 2011). Flow rate and temperature of the air are the primary objectives of the control system with other variables feeding into the PID controllers within the code.

Slight adjustments were made in the control system when the dehumidification system was installed. The most noticeable being the ability to turn the dehumidification system on or off. The user can also input whether the chiller loop, heating loop, or both loops are on, allowing for the program to control the mixing of water from the water heater and chiller. This allows for more precise temperature adjustments.

The temperature controls for the water chiller as mentioned before in Trupka (2011) are still manually set. On exceptionally hot days of over 37.8°C (100°F), the chiller was set at 2.2°C (36°F) in order to maintain air temperature. The chiller was always set at a point where the air was at a temperature below the 15.6°C (60°F) set point to allow for the electric heater to fine tune.

Trupka (2011) compiled a succinct outline of control and feedback parameters that can be seen in Table 3.2. Beneke (2010) presents a more in depth view on the specifications of each controller and sensor used. As mentioned, two different VI's were used over the course of testing, with the most recent version after the dehumidification system installation being shown in Figure 3.16. An image of the previous control program can be seen in Trupka (2011).

Table 3.2 Control and Feedback Information (Trupka, 2011)

Feedback	Notes	Control	Notes
Inlet Air Temp.	Near inlet filter	Blower VFD	
Electric Heater Temp.	Fast acting thermistor	Heating Loop Pump VFD	
Hot Water Temp.		Mixing Valves	Primary/cooling loop mixing
Glycol Supply Temp.	To heat exchanger	Duct Heater	Pulse-width-modulation
Glycol Return Temp.	From heat exchanger		
Heating Loop Heat Exchanger Temp.			
Supply Relative Humidity			
Supply Flow Rate			
Supply Air Temp.	Primary feedback		

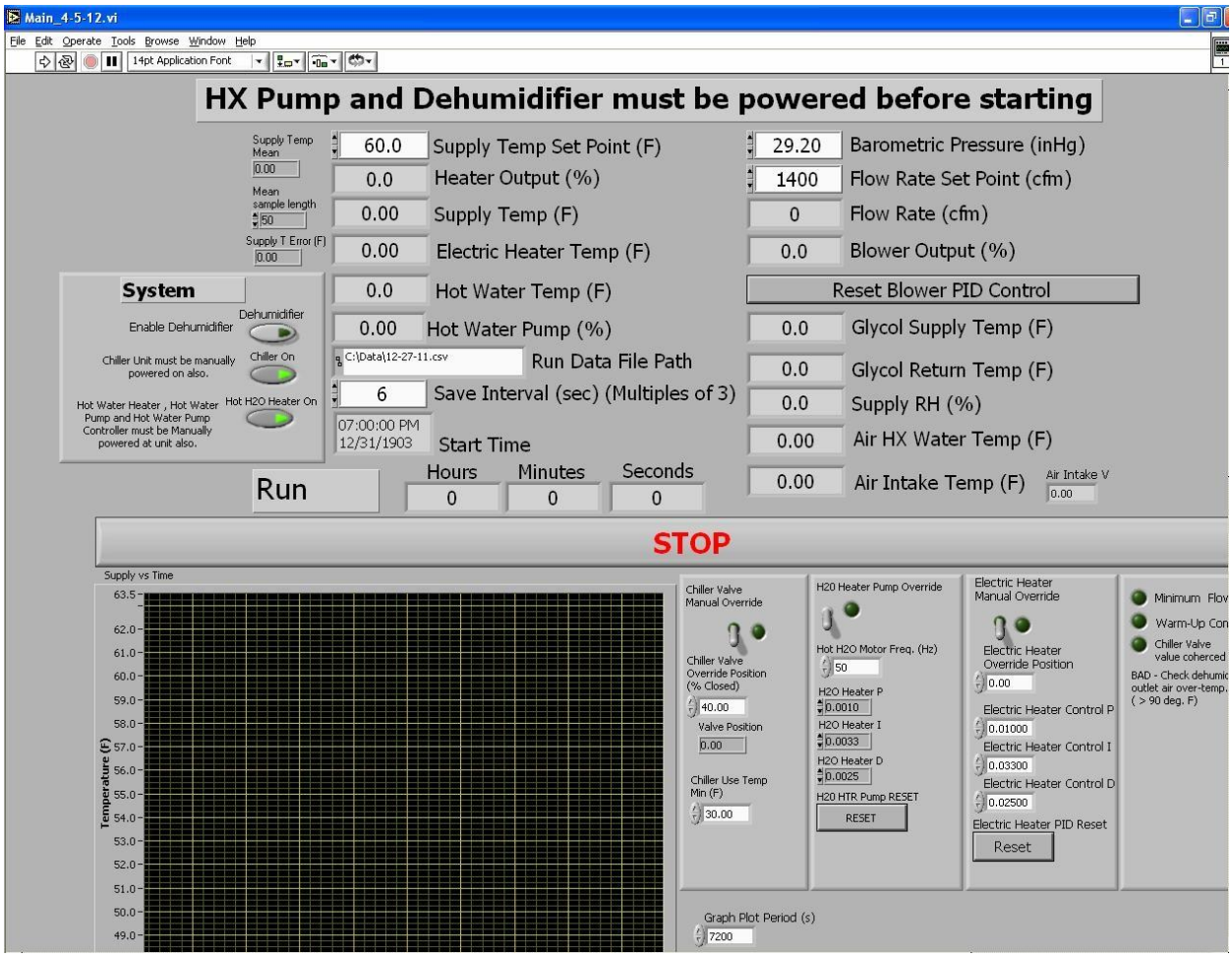

Figure 3.16 Current Air Supply Control System

3.2.4 Gasper System

The aircraft cabin simulator as originally built was not equipped with any gaspers. In order to conduct testing, a system of gaspers had to be installed within the cabin, and then an air supply system created to provide air flow to the gaspers.

3.2.4.1 Installation of Gaspers

Twenty-one gaspers specified for use in a Boeing-767 aircraft were purchased for installation from an airline parts manufacturer. This allowed for gaspers to be installed for each seat in rows 5-7 of the aircraft cabin. Specifications of the gaspers called for operation at a pressure of 2 inches water column. At this pressure and fully opened, the gaspers provide 1.6 l/s (3.2 cfm) of

flow and an air velocity of 0.6 m/s (118 fpm) 1.9 m (6.2 ft) away from the gasper opening. These values are specified by the manufacturer as a function of pressure drop.

In order to install the gaspers in the aircraft cabin ceiling, they were mounted in stainless steel plates in clusters of two and three. In each cluster, the gapers are separated 76 mm (3 in.) center to center. The clusters of three gaspers were placed above seats in the center of the cabin, while the clusters of two were installed above seats along the walls of the cabin. These gasper groupings are shown in Figure 3.17.

Figure 3.17 Gasper clusters installed in cabin

In total, three tri-gasper and six dual-gasper clusters were installed. Detailed drawings for the gasper installation were not available from the aircraft manufacturer. The arrangement and placement of the gaspers was based on photographs of an actual 767 cabin interior. In order for the gaspers to be supplied with air, each gasper was fitted on the back side of the plate with a flexible PVC pipe fitting that was adjust to fit around the inlet of the gaspers to minimize leakage.

3.2.4.2 Gasper Air Supply

The gaspers were supplied with the same HEPA filtered air that is used to supply the linear diffusers within the cabin. In order to provide the gaspers with air, a supply system was constructed using schedule-40 PVC pipe above the aircraft cabin within the cabin enclosure in the same space as the linear diffuser supply duct. The air used in the system was diverted from the main duct using a 4 in. PVC supply line connected to a ball valve and a Continental PRD08

radial pressure blower that provided the necessary pressure boost within the system. The blower and ball valve are used together to control the flow of air within the system. A pressure regulator based on a fixed water column kept the air pressure within the gasper system at 2 in. water column. Figure 3.18 shows the gasper air supply system overlaid onto the layout of the aircraft cabin, indicating the actual location of each component.

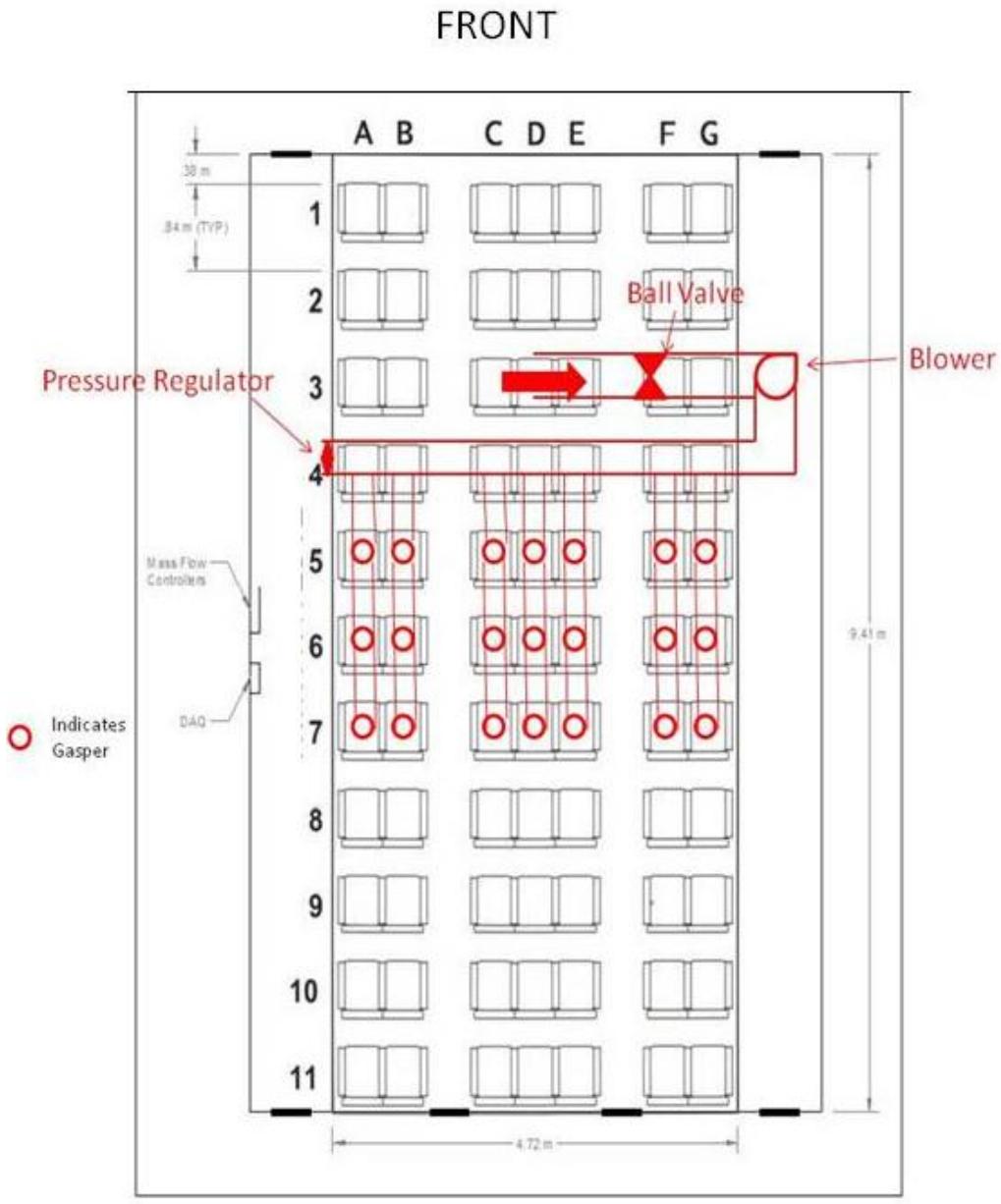

Figure 3.18 Gasper Supply System Layout

As can be seen in the layout, after the air leaves the blower, it enters a header made of 51 mm (2 in.) nominal diameter PVC pipe. The pressure regulator was placed at the end of this header. The header supplies seven separate 31.75 mm (1-1/4 in.) PVC lines which are each connected to three gaspers along their length. These lines are diverted into the individual gaspers through a tee fitting at each gasper location along the 31.75 mm (1-1/4 in.) PVC lines. Through these tee connections, 31.75 mm (1-1/4 in.) lines run vertically downward connecting to the gaspers through the flexible pipe fittings described earlier. The actual connection of the gasper and the tee connection can be seen in Figure 3.19.

Figure 3.19 Connections from Supply Lines to Gaspers

These vertical lines varied in length from 0.66 m (26 in.) to 1.02 m (40 in.), dependent upon the location in the cabin and obstructions present from support structures.

As mentioned before, the pressure within the system was kept at 2 in. water column using a custom pressure regulator. The custom pressure regulator was created by placing the outlet of the PVC header into a vertical PVC pipe filled with water to the point where it begins to bubble from the flow of air. In order to have the right amount of water in the regulator, it was calibrated using a pressure transducer. When the ball valve on the system was adjusted to the point where the pressure transducer read 2 in. water column, the pressure regulator was then filled. The regulator was filled slowly to the point where the water just started to bubble.

This allowed for quicker adjustments of the gasper air supply system flow rate. Opening and closing different combinations of gaspers caused the pressure within the system to either rise or fall, necessitating the adjustment of flow into the system. As long as the pressure regulator was bubbling, the pressure within the system was 2 in. water column. This bubbling was audible from the location of the ball valve. The pressure regulator can be seen in Figure 3.20. The ball valve at the base of the regulator allows for the water to be emptied if necessary.

Figure 3.20 Gasper System Pressure Regulator

PVC cement was not used to connect the sections of PVC pipe and fittings in case future alterations of the system were necessary. Each connection to a fitting was sealed initially using electrical tape and duct tape to minimize leaks in the system.

3.3 Tracer Gas Supply and Sampling

Three separate testing methods were utilized in this study. However, each testing method utilized the same tracer gas supply and sampling system. The tracer gas release methods used are explained in the next chapter on testing methods. The methods and equipment used for supplying the tracer gas and sampling the tracer gas are the same as used by Trupka (2011) and Lebbin (2006).

3.3.1 Tracer Gas Supply

The tracer gas used was a mixture of carbon dioxide and helium. Industrial grade CO_2 in 50 lb cylinders, and high purity He in type T cylinders were utilized as the supply of the gases. Each cylinder was equipped with its own pressure regulator, regulating the supply gas to 200 kPa. The cylinders were located outside the cabin, with vinyl tubing running underneath the cabin enclosure to mass flow controllers in the east hallway.

The mass flow controllers used allowed for the use of computers to control the injection rate of tracer gas during testing. It also enabled the computer to sync the release of the tracer gas with different periods of sampling. Two mass flow controllers were used for injection. For CO_2, an electric MKS 1559A-200L1-SV-S controller was used, while a pneumatic MKS 2179A00114CS controller was used for He (Trupka, 2011). The controllers are operated with the use of a MKS PR4000 power supply and RS-232 interface. This allows for the controllers to be connected to an Agilent 34970A DAQ, which allows for computer control of the mass flow rates. The PR4000 also makes it possible to manually set flow rates for use in smoke visualizations when the use of CO_2 sensors also run by the control program was unnecessary. When low flow rates below the range of the mass flow controllers were needed, a 1/4 in. 20-turn precision brass needle valve was used to control flow.

The flow rate of each gas was verified through the use of two rotameters, one for each gas. When the needle valve was used in place of an electronic flow controller, the corresponding rotameter was used to set the flow rate. Figure 3.21 shows the connection of the needle valve to the rotameter as well as the two mass flow controllers.

Figure 3.21 Needle Valve and Mass Flow Controllers

After the CO_2 and He exit the rotameters, they are mixed in a brass tee fitting which feeds vinyl tubing 12 mm (0.5 in.) in diameter. This vinyl tubing is then used to supply various injection apparatuses.

3.3.2 Tracer Gas Sampling Tree

For all tests conducted, a custom made sampling tree was used to supply samples of air taken within the cabin to a CO_2 sensor. The sampling tree has four 304 stainless steel sampling lines with inside diameters of 5 mm (0.2 in.). Each sampling line is connected to a SMC Pneumatics NVKF334V-3G two-way solenoid valve within a common manifold, allowing the line to be either opened or closed. The manifold allows the lines to be connected to a common outlet which is constantly drawing a sample.

In order for the air leaving the manifold to originate from only one line, the solenoids default to closed with the desired sampling line being open. The orientation of the solenoids is controlled using the same testing program that controls tracer gas release and CO_2 measurements connected with another. During a test, all sampling lines are cycled through, allowing all four locations to be sampled for equal amounts of time. The inlets of the sampling tree are spaced 840 mm (33 in.) apart, allowing four rows of the cabin to be sampled during a given test. The sampling tree can be seen in Figure 3.22.

Figure 3.22 Tracer Gas Sampling Tree (Trupka, 2011)

3.3.3 Tracer Gas Detection

All samples taken by the sampling tree were analyzed by a CO_2 analyzer located inside the aircraft cabin simulator. In order to account for any differences in background CO_2 concentration of air entering the cabin, a second CO_2 analyzer was used for measuring the concentration of air entering the cabin. This analyzer was placed on the top of the aircraft cabin enclosure next to the inlet duct. A third CO_2 analyzer was later purchased to use as a backup in the case one of the original analyzers failed. All CO_2 sensors were connected to an Agilent 34970A DAQ enabling analog voltage measurements to be taken and recorded in a LabVIEW program.

The CO_2 analyzer, located within the cabin and connected to the sampling tree, was a NOVA Analytical model 420 with a sampling range of 0 to 5000 ppm. This analyzer was equipped with several filtering elements that were deemed unnecessary as they masked the transient behavior of the tracer gas (Trupka, 2011). These filters were bypassed by reading the voltage output of the CO_2 sensor directly off of the sensor.

The analyzer located on the roof of the cabin enclosure that sampled air entering the cabin was a custom made analyzer that used an Edinburgh Instrument gas sampling card. This card was

connected to a 24 V power supply with 60 Hz noise filters. This analyzer had a range of 0 to 3000 ppm.

The third analyzer used was a PP Systems WMA-4 CO_2 analyzer. This analyzer had a range of 0 to 2000 ppm and was equipped with direct analog voltage outputs for connection to the DAQ with selectable voltage output range. It also came with a soda lime desiccant column which allowed for automatic zeroing of the system on regular intervals. The three analyzers can be seen in Figure 3.23.

Figure 3.23 CO_2 sensors: Inlet air sensor (top left), NOVA 420 (bottom), WMA-4 (top right)

Each CO_2 analyzer came equipped with a diaphragm pump that would ideally prevent any leakage of ambient air into the sample. However, leakage in the diaphragm pump was found to occur in previous research and resulted in the sampled air being diluted by the leaked air Trupka (2011). To solve this problem, the pumps within each system were bypassed, instead connecting all analyzers to a single vacuum pump downstream of the analyzers. To ensure the same flow rate to each analyzer, a balancing system was installed that used Omega FL-2012 flow meters to

verify the flow rate of each analyzer and merge these three lines to one to connect to the vacuum pump. The balancing system can be seen in Figure 3.24.

Figure 3.24 Flow Balancing System

Since all data recorded from the analyzers was output in analog voltages, a calibration curve was necessary to obtain the actual CO_2 concentration. As described earlier, NDIR sensors have a linear output relating to CO_2 concentration. This meant a simple linear regression could be performed to obtain an equation to convert voltage to CO_2 concentration. Each sensor was calibrated using calibration gases of 500, 1000, and 2000 ppm CO_2 concentration, covering the range of concentrations usually measured within the cabin. These calibration gases were plumbed to the analyzers using the normal sampling lines. The flow of calibration gas was controlled using a custom made device. This device ensured that undiluted calibration gas entered the sampling port but not at elevated pressure. In this way, any leaks in the sample line between the port and the instrument would become apparent during calibration.

To perform the calibration, voltages were acquired using the DAQ for each CO_2 analyzer. For each calibration gas, separate measurements were performed for each analyzer. Each measurement lasted for forty seconds, with one measurement being taken every two seconds, resulting in twenty data points. These data points were then averaged to give a corresponding average voltage for a given calibration gas. The three resultant data points for a given analyzer

were then analyzed using the data analysis regression feature within Microsoft Excel. This gave a separate regression curve for each sensor. In order to maintain the accuracy of the analyzers and prevent drift, calibrations were performed on a regular basis when testing was being conducted, typically every two weeks.

3.3.4 Control Program

The flow rate, release, and sampling of tracer gas, along with the measurement of CO_2 concentrations and temperatures within the cabin were controlled by one LabVIEW program. The duration and timing of the tracer gas injection were set within this program, along with the sampling duration for each location on the sampling tree, and recording interval for voltage measurements from the CO_2 analyzers. These values were altered depending upon the testing method being used. The control program utilized was the same used by Trupka (2011). All measurements taken were saved as a comma delimited file easily opened in Microsoft Excel.

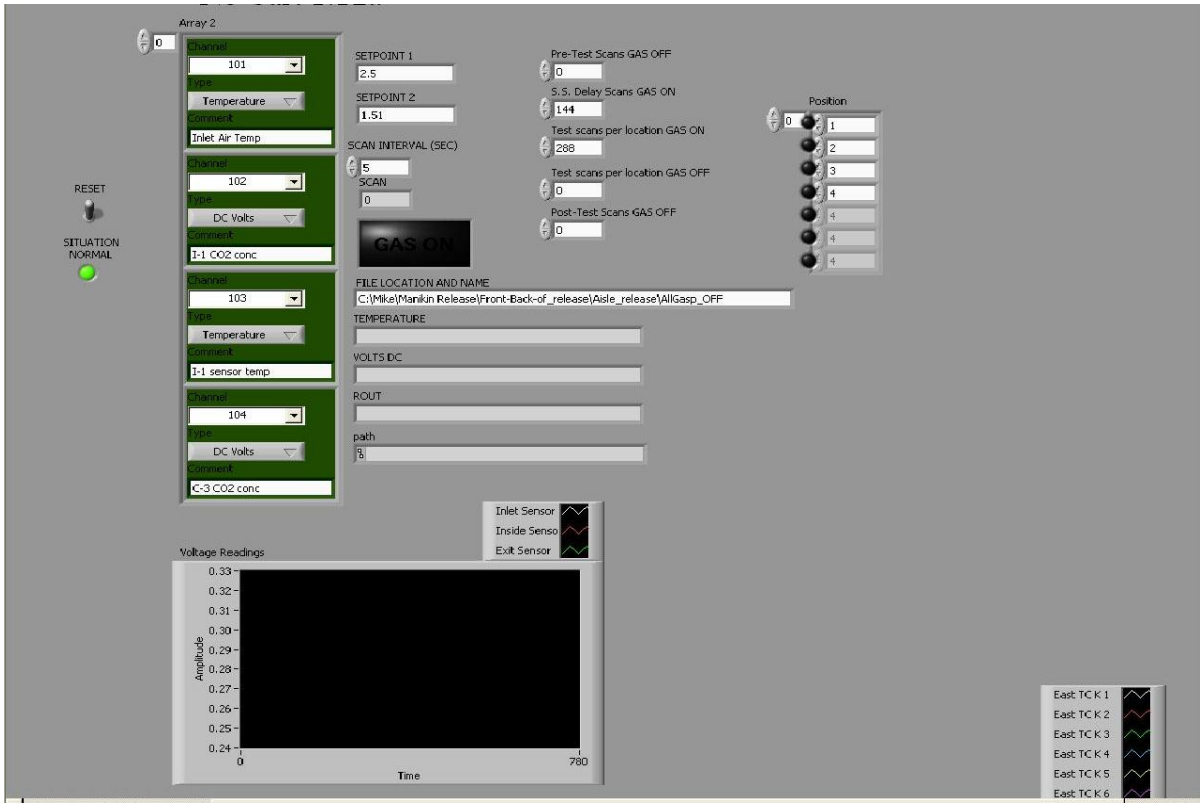

Figure 3.25 Sampling and Control Program used for Testing

Chapter 4 - Testing Methods and Analysis

Three separate tests were performed on the installed gaspers. Each test used a different method of sampling and releasing tracer gas within the aircraft cabin. Initially, the effect of gaspers on longitudinal contaminant transport within the aircraft cabin was investigated. Next, the portion of total inhaled air coming from a gasper in comparison to the overall airflow within the cabin was determined. Finally, the ability of gaspers to reduce the transmission of diseases amongst passengers was evaluated. The basic tracer gas supply and sensing equipment outlined above remained the same in all cases. The following sections describe the testing methods used in each scenario, as well as sampling location within the cabin.

4.1 Cabin Traverse Testing

The first sets of testing with the gasper system operational were to determine what effect, if any, gaspers had on the longitudinal contaminant transport within an aircraft cabin. Recall that the primary flow pattern was shown in Figure 2.1 and it is believed to be a side-to-side circulation with little front-to-back motion within the cabin. However, the turbulent nature of the air motion results in turbulent eddies that generate significant longitudinal contaminant transport. Additionally, there are secondary flow patterns that result in a horizontal rotation along the length of the cabin and have been illustrated in previous testing conducted at ACER (IER, 2008; Beneke, 2011).

4.1.1 Testing Setup

In order to examine these effects, tracer gas was injected vertically into the aircraft cabin at three separate locations along the centerline of the cabin in rows 1, 6, and 11 of seat D as indicated in Figure 4.1. However, only one injection location was tested at a time. CO_2 was injected at a rate of 7.5 lpm (0.265 cfm) and helium a rate of 4.5 lpm (0.159 cfm). These flow rates were chosen so that a detectable amount of tracer gas would be present throughout the cabin. This consideration was most necessary when sampling at the opposite end of the cabin from the release point. For cases when the release point was furthest away from the sampling tree, 7.9

lpm (0.279 cfm) of CO_2 was released, the maximum amount that could flow through the rotameters.

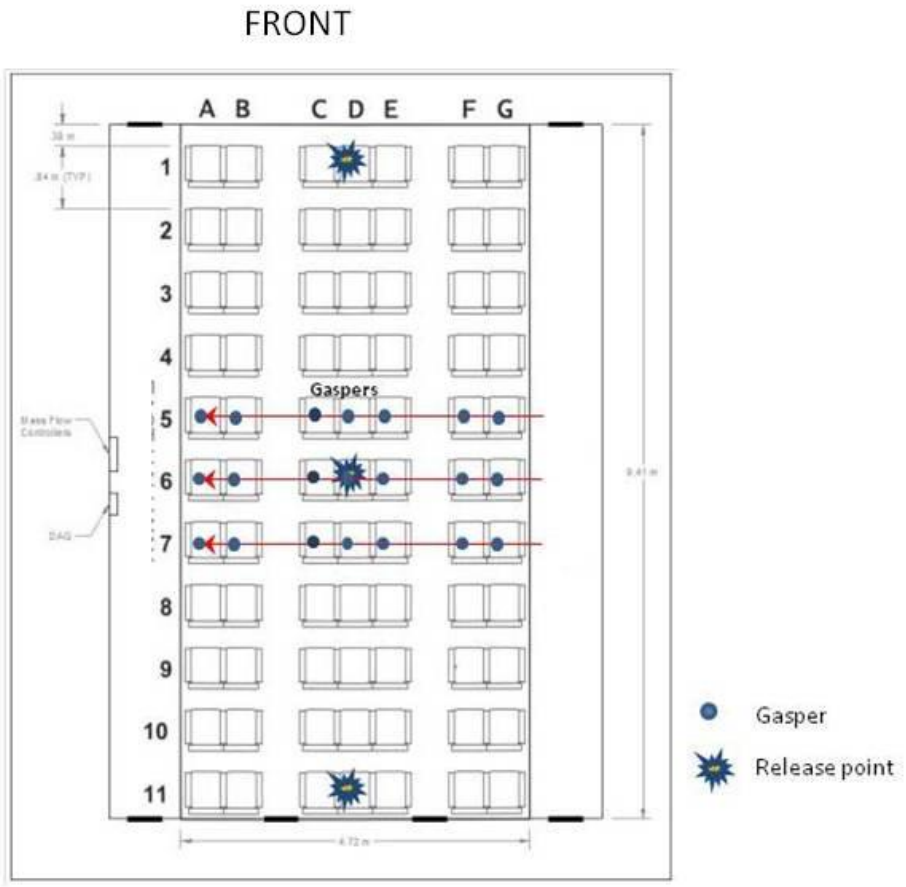

Figure 4.1 Locations of Tracer Gas Release

For each injection location, the sampling tree was then used to monitor the tracer gas concentrations along column D for rows 1-11. This approach allowed for the flow of the tracer gas along the length of the cabin to be sampled. The inlets of the sampling tubes on the sampling tree were 0.127 m (5 in.) above the seat backs. To establish the effect of the gaspers, two tests were performed for each release location, one with all gaspers off, and one with all gaspers fully opened with the nozzle pointed straight down.

4.1.2 Tracer Gas Injection

The tracer gas was injected through a vertical 500 mm (19.7 in.) long copper tube, 25.4 mm (1 in.) in diameter. The outlet of the tube was 127 mm (5 in.) above the seat backs of the location

in which it was attached. At the injection rates stated before, the tracer gas is leaving the apparatus at approximately 0.39 m/s (1.28 ft/s). For each injection location, the release tube was placed 178 mm (7 in.) in front of the sampling port on the sampling tree corresponding to that location. The injection tube and its relation to the sampling tree can be seen in Figure 4.2

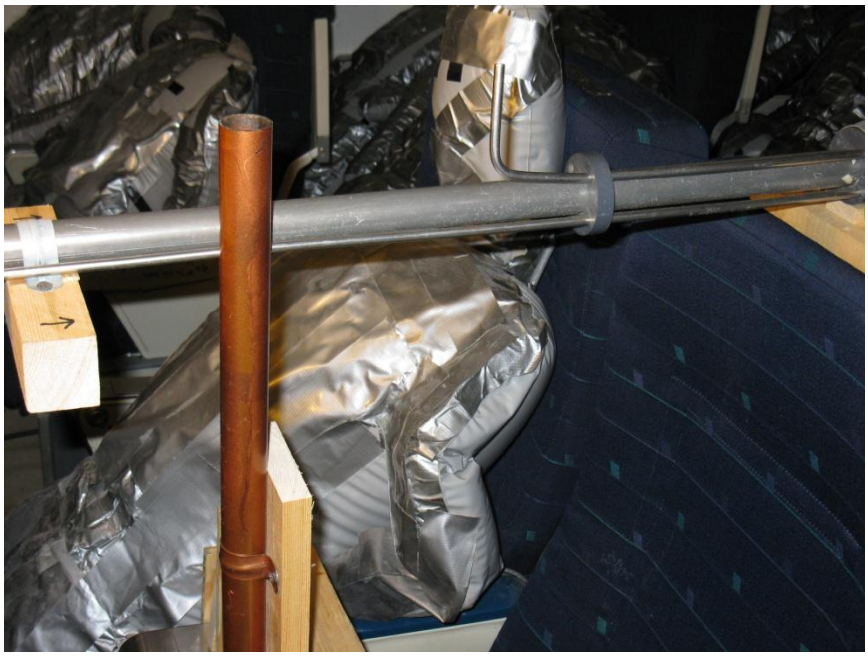

Figure 4.2 Tracer Gas Injection Tube

4.1.3 Test Procedure

If testing was being performed with gaspers off, all gaspers were simply turned to their fully closed positions. If testing was for gaspers on, all gaspers were turned to a fully open position and the gasper supply blower turned on. The ball valve was then adjusted to ensure a pressure of 2 in. water column within the gasper air supply system. After these adjustments were made, the cabin was allowed to settle for 30 minutes before testing. The actual testing began with allowing the aircraft cabin to reach a steady-state level of tracer gas; this was achieved by injecting the tracer gas for an initial 12 minute period of time. The amount of time required to reach steady-state was established in previous tracer gas studies performed at ACER (IER, 2008; Trupka, 2011).

The sampling tree only has four sampling ports, necessitating it be moved after a set of tests in order to sample all 11 seats along column D. Samples were taken at each seat location along

column D for 33 minutes with the first 3 minutes of sampling necessary for the line to purge of the previous location's sampled air. This process was repeated along the length of the cabin for rows 1-11 of column D for each tracer gas injection location. Sampling was conducted starting from the rear of the cabin, moving to the front for each release point. Rows 8-11 were sampled, and then rows 4-7, and finally rows 1-4. At each location of the sampling tree, the testing was repeated three times.

4.1.4 Data Analysis Method

For each individual testing run, the normalized concentration values were averaged for a 30 minute period of time. The measured concentrations were normalized using Equation (4.1).

$$N = \frac{(C_{interior} - C_{inlet})}{\left(\frac{V_{CO2}}{V_{Vent}}\right)} \tag{4.1}$$

Where V_{vent} is the total volume of air entering the aircraft cabin, V_{CO2} is the total volume of CO_2 being released, $C_{interior}$ is the measured CO_2 concentration taken from the sampling tree, and C_{inlet} is the CO_2 concentration of the ventilation air entering the cabin. Equation (4.1) eliminates the effect of fluctuations in background CO_2 along with showing observed results independent of the amount of tracer gas injected. The three test runs conducted for each situation were averaged together to give a normalized value for each seat located in column D for all release locations with gaspers both on and off.

4.2 Gasper Air Inhalation Testing

After testing the effect of gaspers on the overall longitudinal contaminant transport within the cabin, focus was placed on determining the effectiveness of gaspers at reducing the spread of contaminants amongst individual passengers. The first test involved measuring the amount of gasper air inhaled relative to the overall aircraft cabin ventilation.

4.2.1 Testing Setup

In order to know how much air from a gasper is reaching the inhalation zone of a typical passenger, tracer gas needed to be injected into an individual gasper, with the CO_2 concentration

of the air exiting the gasper being known. To accomplish this, a CO_2 injection system was installed for the gasper located in row 6 seat column B, this location can be seen in Figure 3.4. This location was chosen because the gaspers along the sides of the aircraft cabin are closest to the passengers due to the aircraft cabin's geometry. Along column B, the gaspers are 0.48 m (19 in.) vertically above a manikin's inhalation zone, while for seat columns C, D, and E in the center of the cabin; they are 0.84 m (33 in.) above the inhalation zone. Using the closer gasper distance was based on the logic that if no real effect was observed for the closer distances from gasper to inhalation zone, then even less of a measurable result would be observed from a gasper twice as far away.

4.2.2 Tracer Gas Injection

To supply tracer gas, the schedule 40 1-1/4 in. supply line connected to gasper 6B was replaced with 3/4 in. schedule 40 PVC to increase the air velocity and turbulence of the air being supplied to the gasper to increase mixing of the tracer gas. This helped the air exiting the gasper to have a uniform CO_2 concentration. CO_2 was directly injected into this supply line without the need for helium because of the turbulent mixing within the supply line. In order to create proper mixing with the turbulent flow, the injection point was placed at a length of 0.61 m (24 in.) away from the actual gasper, resulting in a mixing length of 29 diameters.

The fact that the flow was turbulent was based upon assuming a flow rate of 90 lpm (3.18 cfm) using the gasper specifications. Using this flow rate with the known nominal diameter of 3/4 in. schedule 40 PVC pipe, the Reynolds number of the flow is approximately 6250, past the transition region from laminar to turbulent flow which has a limiting Reynolds number of 4000. This Reynolds number is for the specified flow rate, even if the flow rate is dropped to 30 lpm (1.06 cfm), the flow would still be transitioning to a turbulent flow.

The CO_2 was injected into the supply line through a vinyl-hose barb 12.7 mm (0.5 in.) in diameter. This barb was connected to a 12.7 mm (0.5 in.) vinyl tube being supplied with CO_2. A 6.35 mm (0.25 in.) vinyl-hose barb was then placed at the bottom of the gasper supply line to sample the concentration of the air being released through the gasper using the sampling tree

during testing. A 6.35 mm (0.25 in.) vinyl tube was connected to this sampling port and strung back into the cabin and connected to a port on the sampling tree.

At the injection barb, the flow of CO_2 was regulated to 0.1 lpm (0.0035 cfm) using a 20 turn precision needle valve in conjunction with the CO_2 flow meter to ensure the flow rate was correct. The needle valve used was previously shown in Figure 3.21. The electronic flow controllers were not utilized for this testing because the necessary flow rate was below what could be stably maintained by the controllers. This amount was chosen through trial and error, varying the flow of CO_2 until a concentration of around 3000 ppm for the gasper air was reached. The high CO_2 concentration was chosen to enable better detection since the volume of gasper air is small relative to the overall airflow within the cabin. This concentration is also within the span of the NOVA CO_2 sensor used with the sampling tree.

4.2.3 Tracer Gas Sampling

In order to determine the amount of gasper air reaching a passenger's inhalation zone, the Thermal Observation Manikin (TOM) was used to simulate a passenger and placed under gasper 6B. TOM was used as the sampling site because it is a far more sophisticated manikin with a more equal temperature distribution than the thermal resistance manikins used throughout the rest of the cabin. This enables TOM to better simulate any thermal boundary layer effects that may be observed in the inhalation zone of a typical human being.

To sample the tracer gas, the sampling tree and corresponding analyzer were again used. However, in order to create a sampling zone the inhalation region of TOM, a 6.35 mm (0.25 in.) diameter vinyl tube was placed between the nose and mouth of TOM and connected to sampling port 2 of the sampling tree. The inlet of the sampling tube was placed 0.9 m (35.4 in.) above the floor and 0.51 m (20 in.) to the side of the manikin in seat 6A. The inlet of the sampling tube was a distance of 0.53 m (21 in.) away from the outlet of the gasper in Figure 4.3. Gasper 6B was focused directly on the inhalation and breathing zone of TOM to begin with.

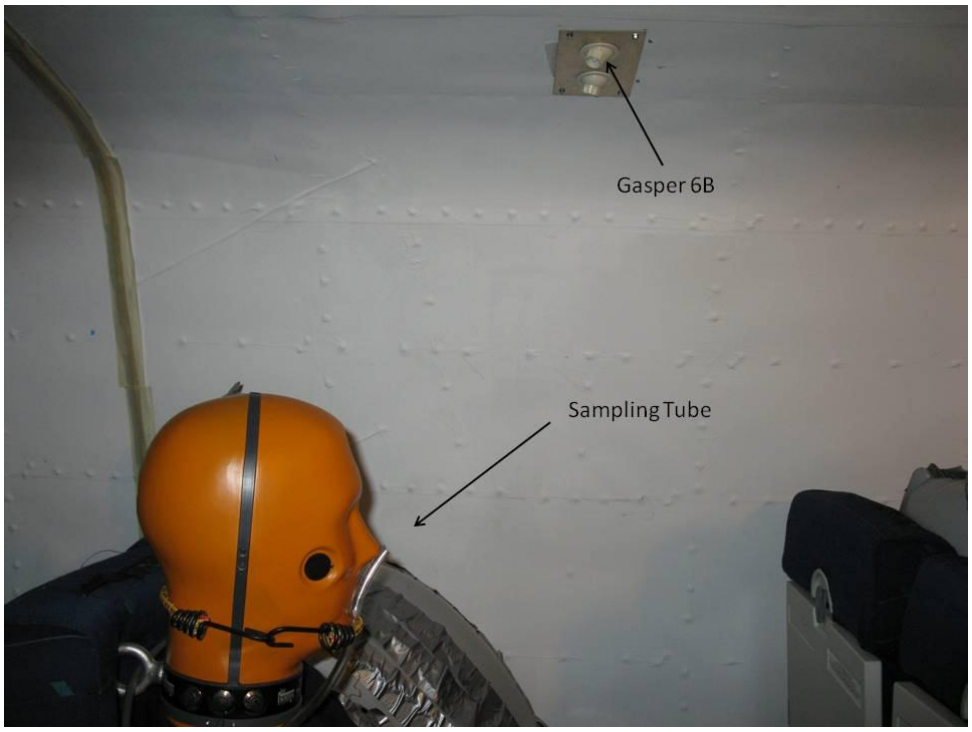

Figure 4.3 Sampling Location for Gasper Inhalation

Since the sampling tree had four separate ports, all four were utilized. Port 1 was used to sample the concentration of the air entering the gasper, Port 2 was used for sampling at the manikin, Port 3 was connected to a sampling tube sampling air upstream of the injection port within the gasper system, and port 4 was placed at the front of the cabin to measure the steady state CO_2 concentration of the cabin away from the gasper. The length of the sampling tubes were different, but the flow rate was kept the same in each sampling tube because all sample were drawn using the same flow balancing system described in section 3.3.3. Since the aircraft cabin reaches steady-state CO_2 concentration, the upstream values taken from the sampling tree allowed for direct comparison of measurements using the interior CO_2 sensor only, eliminating the need to use the CO_2 sensor measuring ventilation concentration in analysis and calculations.

4.2.4 Test Procedure

Measurements were again recorded with the same testing program as in the cabin traverse testing. Initially, the tracer gas was injected into the gasper for 12 minutes to allow the aircraft cabin to reach a steady-state concentration of CO_2. Each port was then sampled for 18 minutes

with the first 3 minutes of data being ignored as the transition time to clear the sampling lines from the previous sampled port.

Three separate adjustments of the gasper were performed during testing. Initially, the gasper was directed straight at the sampling port in the inhalation zone of TOM. Two other configurations were then performed with the gasper focused slightly to the left and slightly to the right of the sampling tube. In all configurations, the gasper was fully opened and testing was repeated three times. Aiming was performed with the use of smoke visualization from the gasper.

4.2.5 Data Analysis Method

The effectiveness of the gasper was determined by comparing the CO_2 concentration in air sampled at the manikin with the steady-state concentration of ventilation air within the cabin. Through the sampling of air at the front of the cabin it was possible to determine that the steady-state concentration within the cabin is no different than the concentration of air entering the cabin. This is due to the fact that when the 0.1 lpm (0.0035 cfm) of CO_2 is fully mixed with the cabin ventilation air it increases the overall concentration by only 2.5 ppm. Therefore, the only source of tracer gas observed at the manikin is the 3000 ppm by volume air entering through the gasper. The other amounts of CO_2 present are simply background values typically around 400 ppm in concentration, fluctuating slightly with nearby traffic density.

The background concentration was taken into account by taking the difference between the gasper CO_2 concentration and the background CO_2 concentration as the actual value of new CO_2 to which the thermal manikin was exposed. A similar method was used by Radim et al. (2006) in their analysis of personal ventilation systems. Figure 4.4 illustrates this difference, showing the transient results of the sampling location for one testing run. As can be seen from the figure, this difference is typically 2600-2700 ppm.

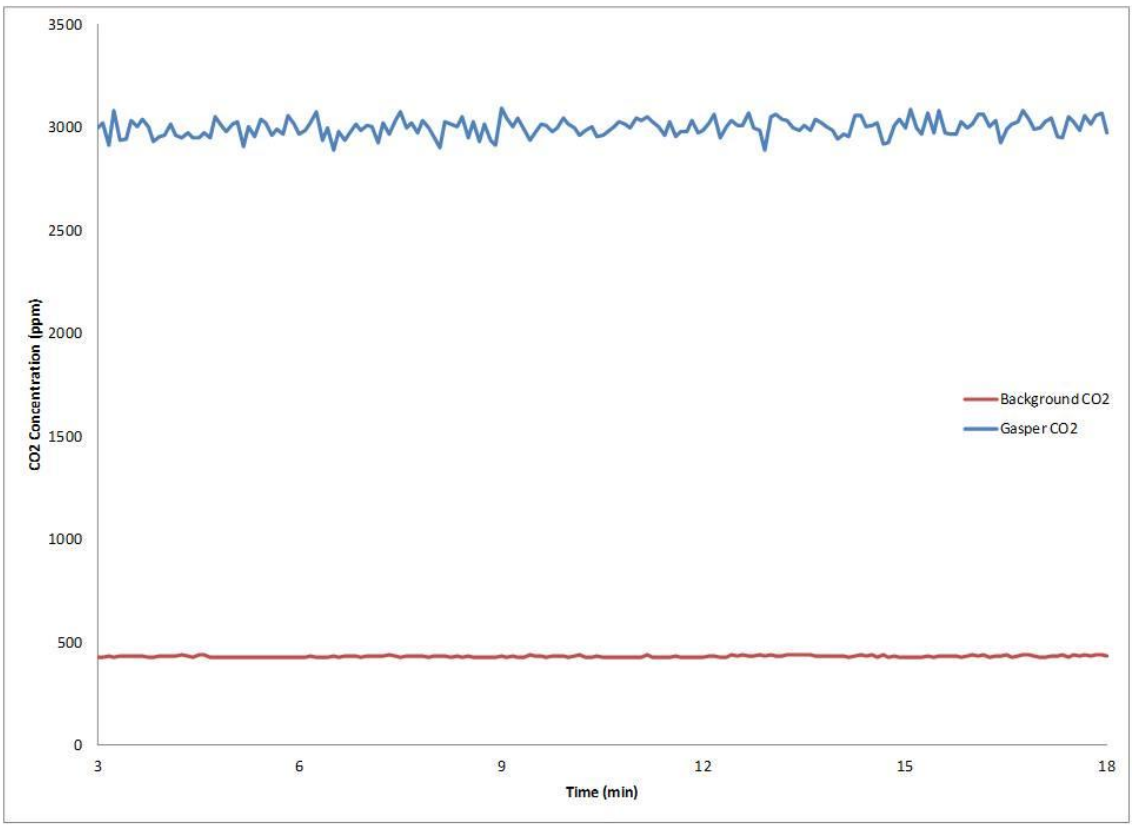

Figure 4.4 Comparison of Measured Background and Gasper CO_2 Concentrations

In each test, this difference was then used as the baseline for maximum exposure as seen at the manikin sampling site. Any value above background was assumed to be air inhaled at the sampling location coming from the gasper. This value was then compared to the maximum exposure level to derive a percent based inhalation level for the manikin. For instance, if the difference between background and the sample taken at the manikin was the same as the difference between the background and sample taken at the gasper, 100% of the air sampled at the manikin would be coming from the gasper. Figure 4.5 shows all three transient CO_2 measurements for a given test to illustrate these differences. For each test and gasper configuration, all measured results were similar in pattern to this figure, with the only difference being in the value of the measured CO_2 concentrations.

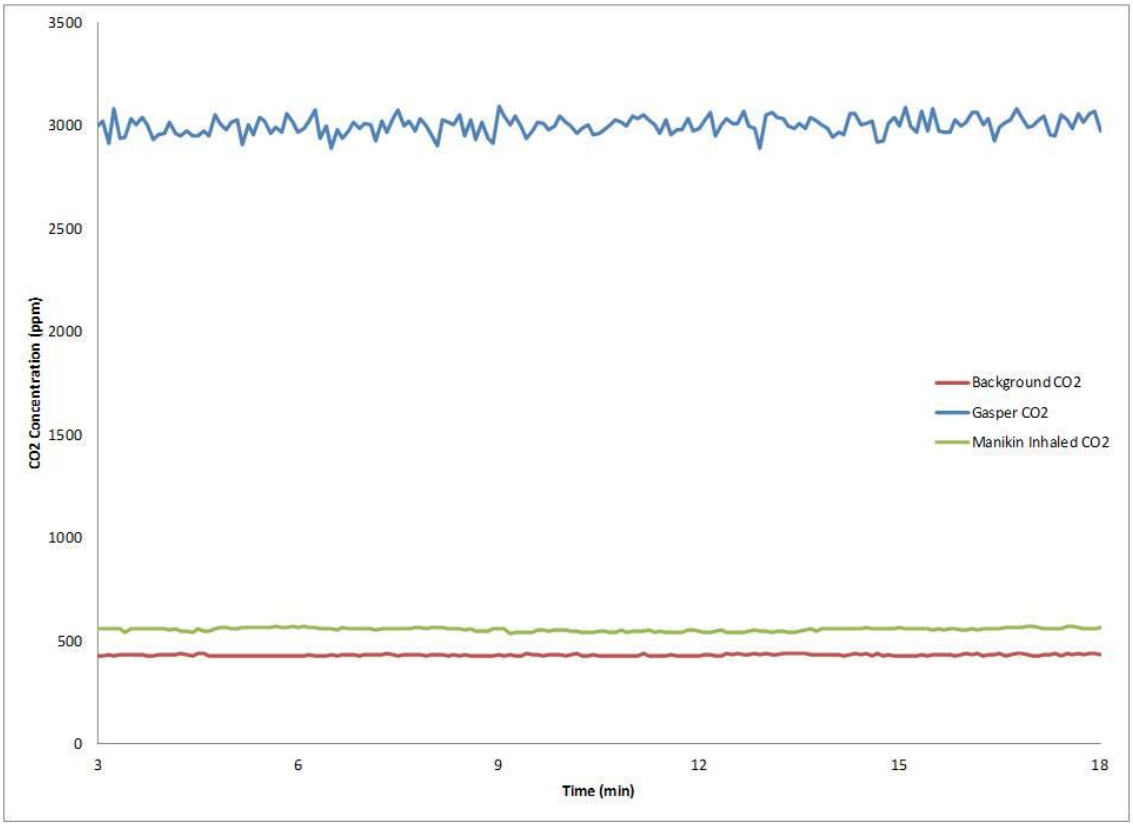

Figure 4.5 All CO_2 Measurements Taken during Gasper Inhalation

For each 18 minute test run, the final 15 minutes of sampled concentrations were averaged to generate a concentration value for each measurement location. After these averages were taken, the gasper exposure was calculated using Equation (4.2).

$$Exp = \frac{C_{Manikin} - C_{background}}{C_{gasper} - C_{background}} \tag{4.2}$$

Where $C_{Manikin}$ is the CO_2 concentration taken in the inhalation zone of TOM, C_{gasper} is the concentration of air exiting the gasper, and $C_{background}$ is the steady-state CO_2 concentration of the aircraft cabin simulator.

4.3 Manikin Tracer Gas Release Testing

Finally, a series of tests were performed to evaluate the influence of gaspers on contaminant transmission between adjacently seated passengers. Two separate configurations of testing were focused on, with initial results evaluating transmission between passengers seated side-by-side in

row 6, and then on passengers seated in-front and behind the simulated contaminated passenger. The scope of the experiment was limited to one location within the cabin where alterations in the airflow patterns or that area could be observed. The testing and sampling methods for the data sets were developed with the slow travel of tracer gas plumes in mind. Two separate experiments were performed with varying gasper configurations and sampling locations along with varying the location of the tracer gas release mechanism. To simplify the explanation of the testing method, the manikin with the release mechanism attached to it will be referred to as the "release" manikin.

4.3.1 Testing Setup

The testing for this part of the overall experiment was performed in rows 5-7 along the left side of the aircraft cabin simulator in seats A and B. Since the geometry and physical configuration of the cabin dictated the location of the gaspers when they were installed, the gaspers being tested were further away from the breathing zone than typically expected in an aircraft cabin. To overcome this, the rows of seats being focused on were moved slightly closer to the gaspers above the seats. This enabled rows 5 and 7 to be the same distance from the gaspers as row 6 used in the gasper inhalation testing.

4.3.2 Tracer Gas Release Mechanism

In each testing scenario, for the sampling within row 6 and sampling in rows 5 and 7, tracer gas was released in a manner meant to slowly emit the tracer gas in plumes to better simulate exhalation. To accomplish this, the base of a soft drink cup 76.2 mm (3 in.) in diameter at the top, and 63.5 mm (2.5 in.) diameter at the base, with a depth of 76.2 mm (3 in.) was utilized. The cup was faced with the open end outwards, strapped to a thermal resistance wire manikin in what was approximated to be the breathing zone of a typical passenger. This location was 1 m (39 in.) above the floor of the cabin. In order to supply tracer gas to the breathing zone, a 12 mm (0.5 in.) diameter vinyl tube was run into the back of the cup. This configuration can be seen in Figure 4.6.

Figure 4.6 Tracer Gas Release Device

Again, a mixture of CO_2 and helium was used as the tracer gas, this time at a rate of 2.5 lpm (0.088 cfm) for CO_2, and 1.51 lpm (0.0533 cfm) for helium. At these rates, the tracer gas was injected into the breathing apparatus at approximately 0.66 m/s (2.16 ft/s). As the tracer gas was injected, the volume of tracer gas would build up within the breathing apparatus, eventually causing plumes of tracer gas to be displaced that then dispersed throughout the cabin. These plumes can be seen in Figure 4.7 emanating from the release manikin using smoke visualization.

Figure 4.7 Tracer Gas Smoke Visualization

The tracer gas release mechanism was used in both testing cases and kept within row 6. The only change in the release location was moving the release manikin between seats 6A and 6B.

4.3.3 Intra-Row Testing Method

The first set of tests performed focused on sampling the released tracer gas as it travelled within row 6. This test placed emphasis on protecting a passenger seated directly adjacent to a passenger exhaling contaminants.

4.3.3.1 Tracer Gas Sampling and Release

The release manikin was initially placed in seat 6A with TOM being placed in the aisle seat (6B), directly next to the release manikin. In order to determine the effect gaspers had on the tracer gas plume emanating from the release manikin, TOM was again used as the sampling location similar to the gasper inhalation tests. The configuration of the release manikin and TOM can be seen in Figure 4.8.

Figure 4.8 Release Manikin and TOM in Row 6

To sample the tracer gas, the sampling tree and corresponding CO_2 analyzer were again utilized. Similar to the gasper inhalation testing, a sampling zone was created in the inhalation region of TOM by placing a 6.35 mm (0.25 in.) diameter vinyl tube between the nose and mouth of TOM and connecting it to sampling port 1 on the sampling tree. The inlet of the sampling tube was

placed 0.9 m (35.4 in.) above the floor and 0.51 m (20 in.) to the side of the release device. The rest of the sampling ports were left open to evaluate the steady-state CO_2 concentration within the aircraft cabin. These measurements were necessary to ensure observed results weren't attributed to recirculation of increased background concentrations of tracer gas. The inlet of the sampling tube was a distance of 0.53 m (21 in.) away from the outlet of the gasper, the same distance as in the gasper inhalation testing. The gaspers were focused directly on the inhalation and breathing zone of both the release and sampling manikins.

4.3.3.2 Test Procedure

For the side-by-side testing, only the two gaspers located above the release manikin and TOM in seats 6A and 6B were of interest. To determine the effect of each gasper, separate configurations of the gaspers both on and off were tested. In all cases where the gaspers are turned on, the gaspers were fully opened. Table 4.1 lists the separate gasper configurations utilized, with the state of each gasper as either on or off. The release gasper refers to the gasper located above the release point while TOM gasper refers to the gasper located above TOM. All other gaspers within the aircraft were turned off.

Table 4.1 Intra-row Testing Gasper Configurations

Configuration	Release Gasper State	TOM Gasper State
Both Gaspers OFF	OFF	OFF
TOM Gasper ON	OFF	ON
Release Gasper ON	ON	OFF
Both Gaspers ON	ON	ON

For each of the configurations, three separate tests were run in order to verify results. Samples were again taken continuously through the sampling tree CO_2 analyzer. For each test, 24 minutes worth of sampling were taken from the inhalation location on TOM after allowing the aircraft cabin to reach a steady-state background concentration of CO_2. The entire method was then repeated with the release manikin being placed in seat 6B and TOM being placed in seat 6A.

4.3.4 Two-row Testing Method

The next set of testing utilized the same tracer gas dispersion device and dispersion locations as the intra-row method. However, the sampling locations were located in seats 5A, 5B, 7A, and 7B ahead and behind the release location.

4.3.4.1 Tracer Gas Sampling and Release

The sampling tree enabled four locations to be sampled consecutively at steady-state during a test run. Figure 4.9 indicates how each sampling location is numbered when referencing the results.

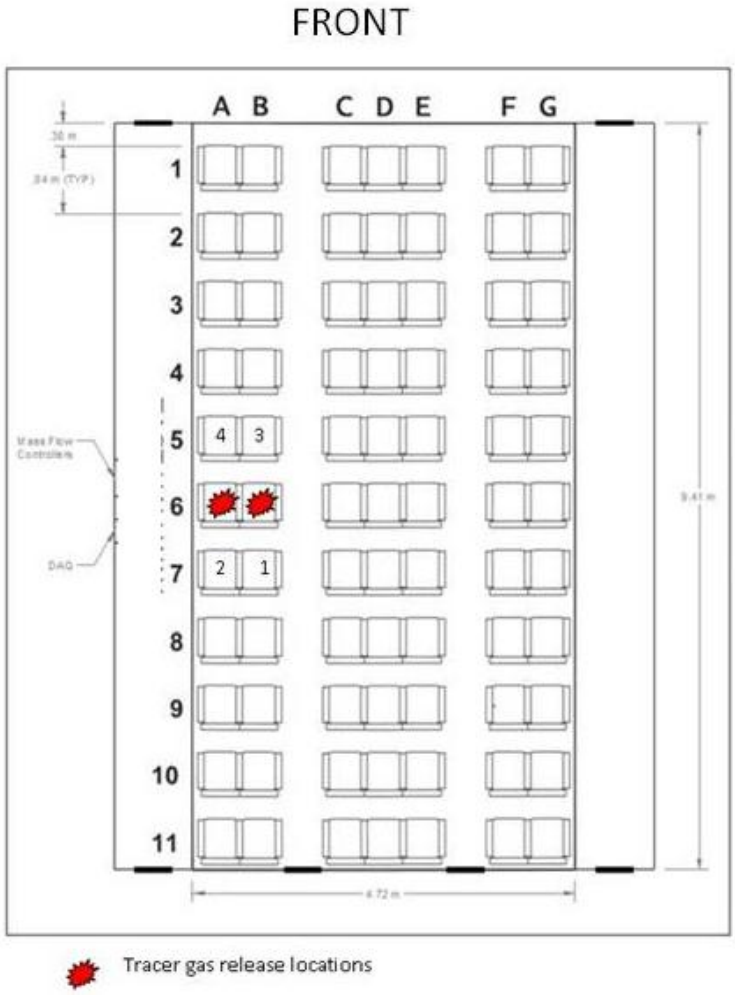

Figure 4.9 Sampling and Release Locations for Two-row Tests

Each sampling location matches with its assigned sampling port number on the sampling tree. Sampling location 1 is indicated as being seat 5B, location 2 corresponds with seat 5A, location 3 with 7B, and location 4 with 7A.

TOM was left in row 6 of the aircraft cabin, again alternating between seats 6A and 6B. The 6.35 mm (0.25 in.) diameter sampling tubes were placed in the inhalation zones of inflatable

manikins and connected to the sampling tree. This was done to keep consistency in thermal boundary effects for sampling due to the fact that four sampling locations were used and only one TOM is in the cabin. Again, to keep consistency, the inlets of the sampling tubes were all placed 0.9 m (35.4 in.) above the floor of the simulator and separated by 0.51 m (20 in.) within the rows. Each sampling tube was also evenly spaced to have 0.84 m (33 in.) of space between rows. Figure 4.10 illustrates the spacing of the sampling manikins as well as the location of the release manikin.

Figure 4.10 Release and Sampling Layout for Two-row Testing

Again, for each sampling and release location the gasper above a given seat was focused directly onto the sampling port and release mechanism at a total distance of 0.53 m (21 in.) away.

4.3.4.2 Test Procedure

For the two-row test configuration, two separate sets of tests were again conducted, initially with the release manikin in seat 6B, then with the release manikin moved to seat 6A. During these two test runs, six different gasper configurations were examined, evaluating a single gasper's effect on airflow patterns within the area outlined in Figure 4.9. In reference to testing and data, each gasper is labeled by its seat number from Figure 4.9. Table 4.2 indicates the label given to

each test for a configuration along with the gasper state during a given test configuration. In all cases the gasper above TOM was left off. The second run of tests used the same gasper configurations, simply changing the location of the release manikin from seat 6B to seat 6A and moving TOM from seat 6A to 6B.

Table 4.2 Configurations for Two-row Testing

Test	Gasper 1 State	Gasper 2 State	Gasper 3 State	Gasper 4 State	Release Gasper State
All Gaspers OFF	OFF	OFF	OFF	OFF	OFF
Gasper 1 ON	*ON*	OFF	OFF	OFF	OFF
Gasper 2 ON	OFF	*ON*	OFF	OFF	OFF
Gasper 3 ON	OFF	OFF	*ON*	OFF	OFF
Gasper 4 ON	OFF	OFF	OFF	*ON*	OFF
Release Gasper ON	OFF	OFF	OFF	OFF	*ON*

Three separate tests were conducted for each of the above gasper configurations for both manikin release locations. Each sampling location was again sampled for 24 minutes, with the first 3 minutes of sampling being eliminated due to possible contamination from the previous sampling port. The cabin was again allowed to reach a steady-state tracer gas concentration for 12 minutes prior to sampling at individual locations.

4.3.5 Data Analysis Method

For both testing methods, the interior CO_2 analyzer values were again normalized using the background CO_2 concentration of air entering the aircraft cabin seen in Equation (4.1). The normalized value for a given location was taken to be the average normalized value over the sampling period. Data were analyzed in both transient and averaged manners for comparison. Transient analysis allowed for the visualization of when plumes of tracer gas reach the sampling tube. The spike in the normalized value on a transient plot as will be seen in the results chapter indicates when the tracer gas plumes are reaching the sampling location.

Chapter 5 - Results

The results of each test above are presented in a manner dependent on the focus of the test. The average normalized CO_2 concentrations over the entire testing runs were considered of most importance. Testing over long enough periods of time allows for a steady-state concentration of tracer gas at a given location to be evaluated since the release amount is continuous. Using an averaged normalized value also greatly reduces the uncertainty of the normalized tracer gas values at locations due to the large number of data points. Transient results are presented for the intra-row testing because of some interesting patterns in the data that occurred at repeated intervals.

5.1 Cabin Traverse Testing Results

The analyzed results for the cabin traverse testing are presented below in groups by release point, row 1 injection with gaspers on and off, row 6 injection with gaspers on and off, and row 11 injection with gaspers on and off. Row 1 injection is considered the front of the cabin, row 6 the middle, and row 11 the rear of the cabin, all corresponding to the layout in Figure 3.4. The uncertainties of the normalized values increase with decreasing normalized value. Uncertainties of the values nearest the release pointed are listed in the results tables.

5.1.1 Row 11 Injection

The first tests were performed with the injection point in row 11 as seen in Figure 4.1. The normalized readings at each location for the gasper system turned off can be seen in Figure 5.1. The horizontal-axis in each plot indicates the row number the sampling occurred in, again corresponding to Figure 4.1. The plot in Figure 5.2 is for the same injection point with the gasper system turned on. The normalized values appear to be much larger near the injection point with the gasper system on. In order to directly compare the gaspers off and on results, the three separate runs at each seat location were averaged and then plotted against each other as seen in Figure 5.3. These averaged values can be seen in

Table 5.1. The plots of normalized readings appear to indicate the tracer gas distributed through the cabin more so with gaspers off than gaspers on.

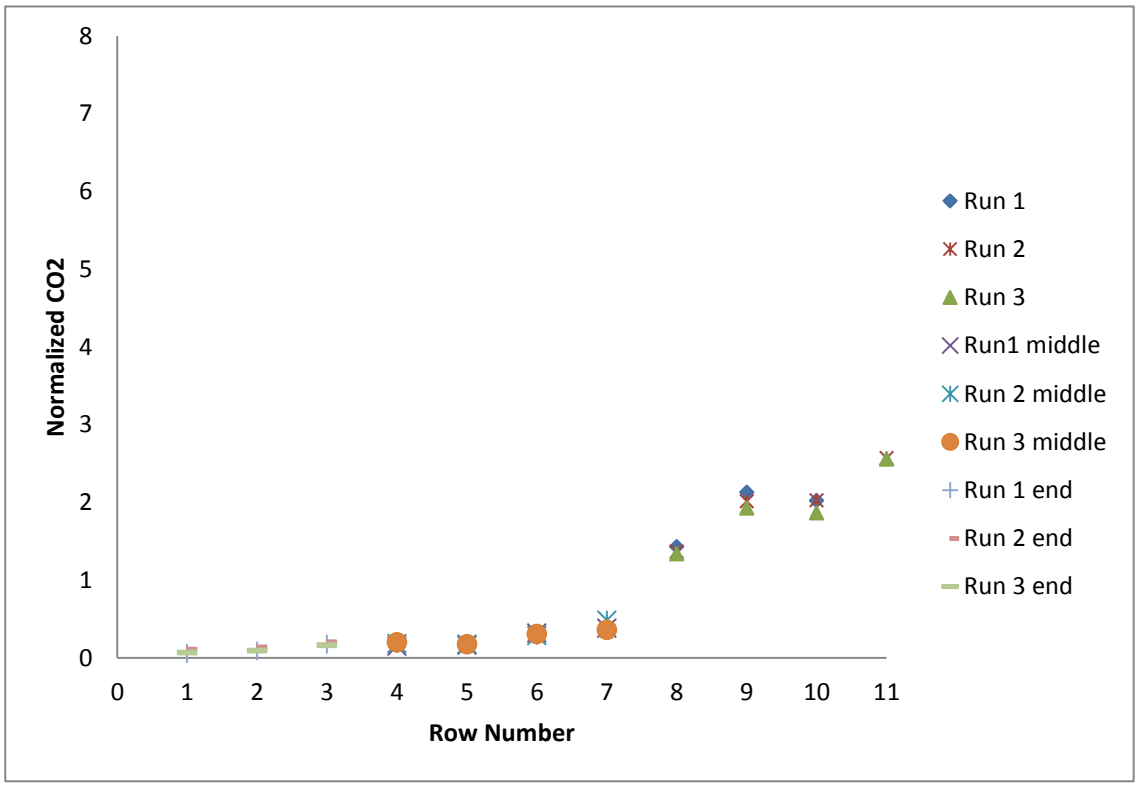

Figure 5.1 Row 11 Release with Gaspers Off

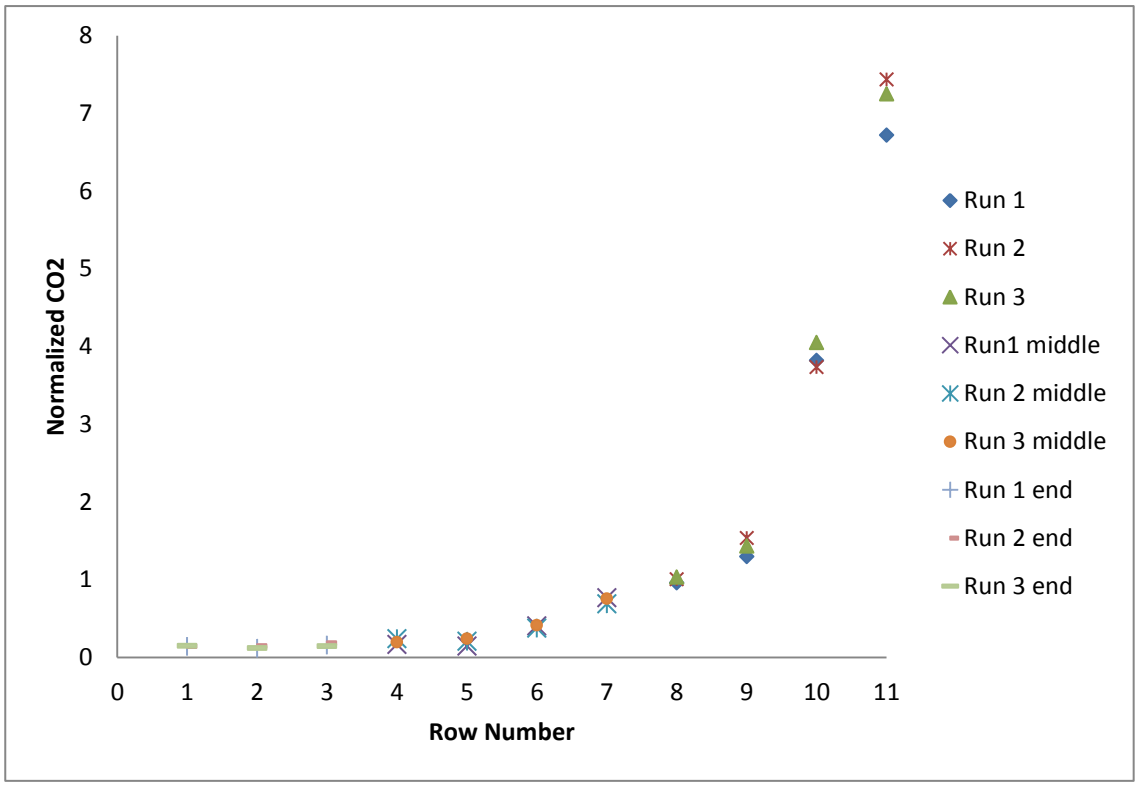

Figure 5.2 Row 11 Release with Gaspers On

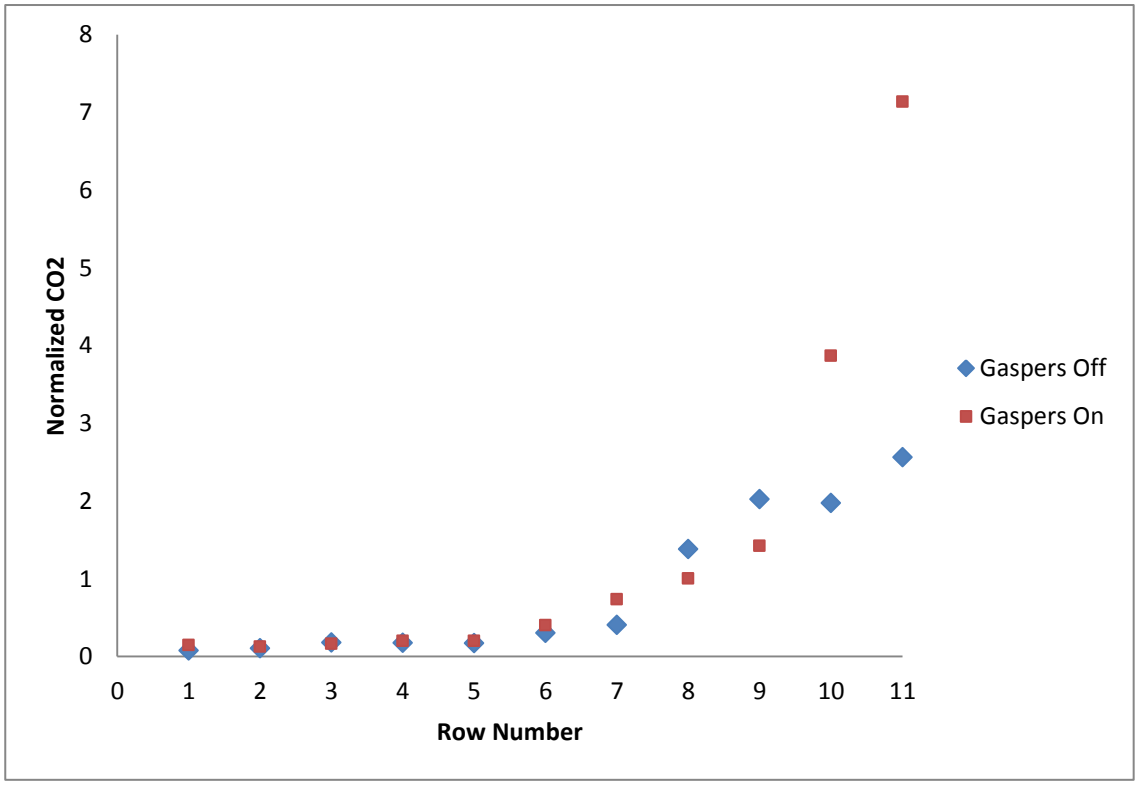

Figure 5.3 Average Values of Row 11 Release with Gaspers On and Off

Table 5.1 Average Normalized Concentrations for Row 11 Release

Average Normalized CO_2				
Row	**Gaspers OFF**	**Relative Uncertainty**	**Gaspers ON**	**Relative Uncertainty**
1	0.07		0.14	
2	0.1		0.13	
3	0.18		0.16	
4	0.18		0.2	
5	0.17		0.2	
6	0.3		0.4	
7	0.41		0.73	
8	1.38	±13%	1.00	±16%
9	2.02	±8%	1.42	±10%
10	1.97	±6%	3.87	±6%
11	2.56	±7%	7.14	±6%

As can be seen in the plots, the only locations where noticeable amounts of tracer gas were present were near the release location. Since this was the initial test location, a second trial was performed re-measuring the normalized concentrations in rows 8-11, again with three separate tests for gaspers turned on and off. It was an attempt to verify the sudden increase in concentration seen when the gaspers were turned on. No sampling was conducted in rows 1-7 for this second trial. The conditions and setup were identical to the initial testing; only the testing took place three weeks later. These averaged results can be seen in Figure 5.4 with the values being presented in Table 5.2. The results show a similar impact on tracer gas dispersal as the initial testing.

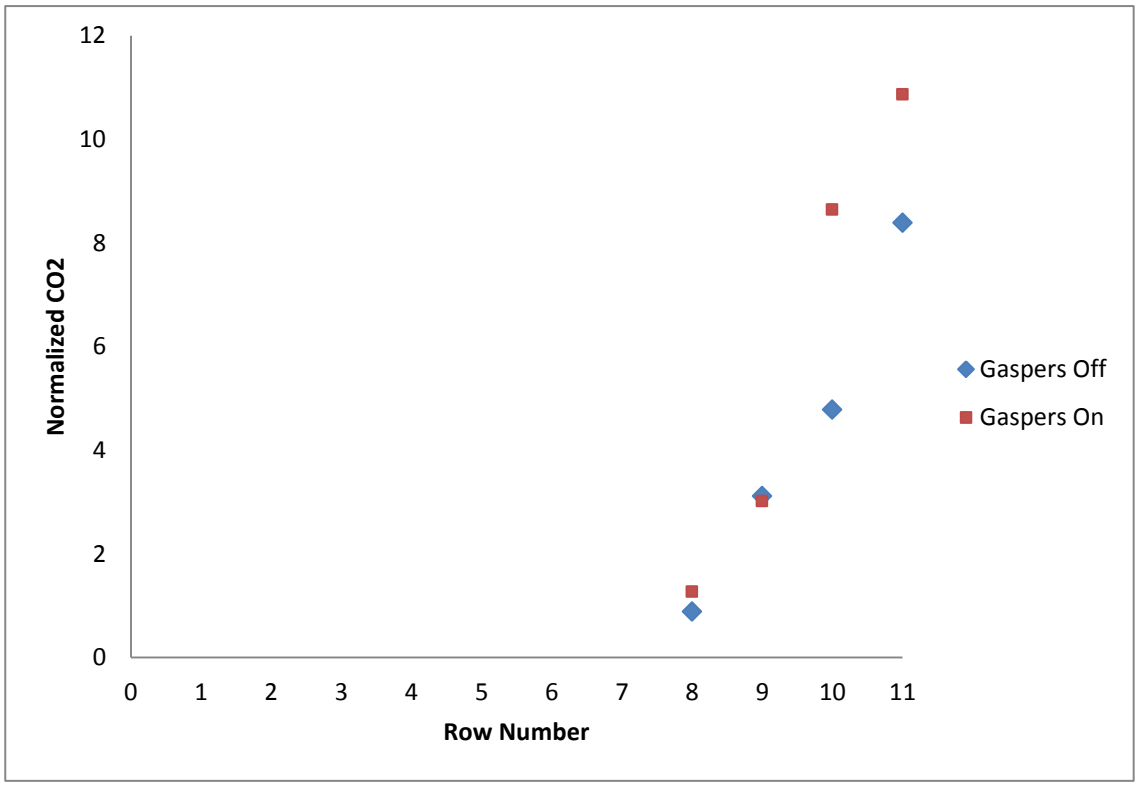

Figure 5.4 Average Values of Row 11 Release Trial 2 with Gaspers On and Off

Table 5.2 Average Normalized Concentration for Row 11 Trial 2

Average Normalized CO_2				
Row	**Gaspers OFF**	**Relative Uncertainty**	**Gaspers ON**	**Relative Uncertainty**
8	0.88	±19%	1.26	±15%
9	3.10	±7%	3.01	±8%
10	4.48	±7%	8.35	±7%
11	7.54	±9%	10.42	±9%

5.1.2 Row 1 Injection

After injecting the tracer gas at the rear of the cabin, the injection point was moved to the front of the cabin in row 1. The normalized values for injection with the gaspers off can be seen in Figure 5.5. The results with the gaspers turned on are shown in Figure 5.6. Again, an averaged plot comparison of gaspers on and off is shown in Figure 5.7, showing the tracer gas dispersing along the length of the cabin less with the gaspers on than off. These values are shown in Table 5.3. While not nearly as dramatic as the rear injection results, the results again indicate the gaspers decrease the dispersion of the tracer gas along the length of the aircraft cabin simulator.

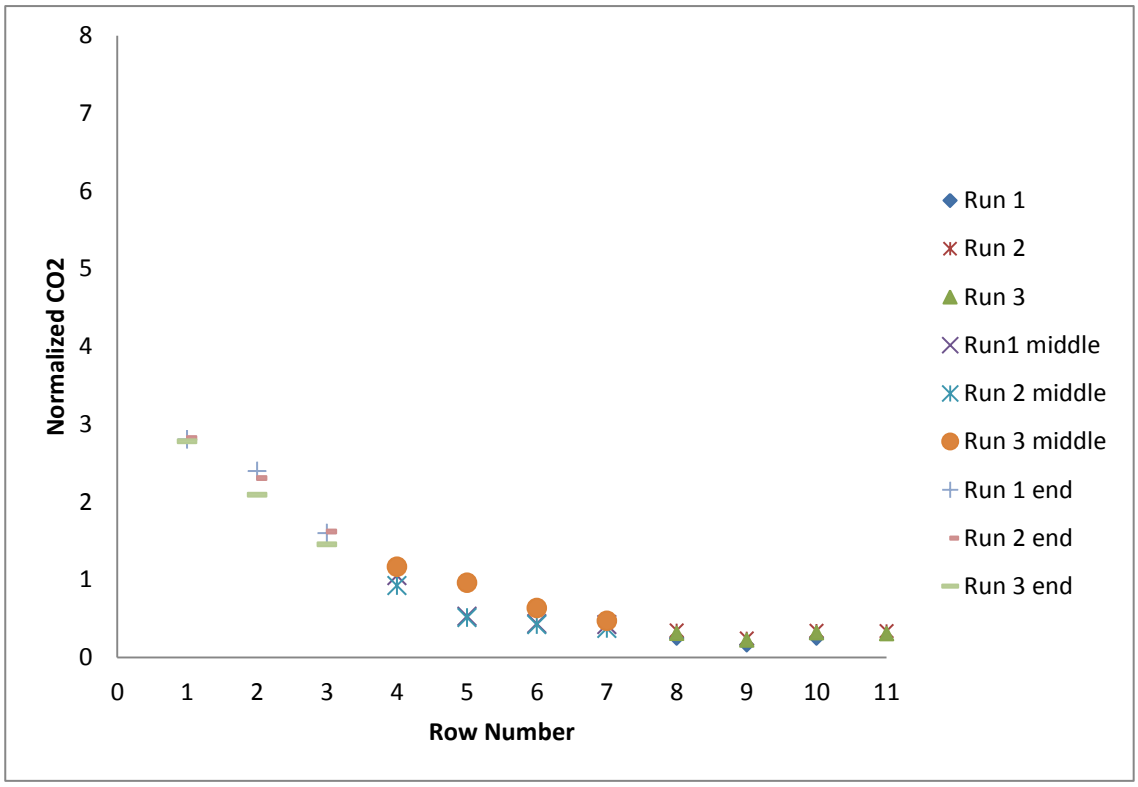

Figure 5.5 Row 1 Release Gaspers Off

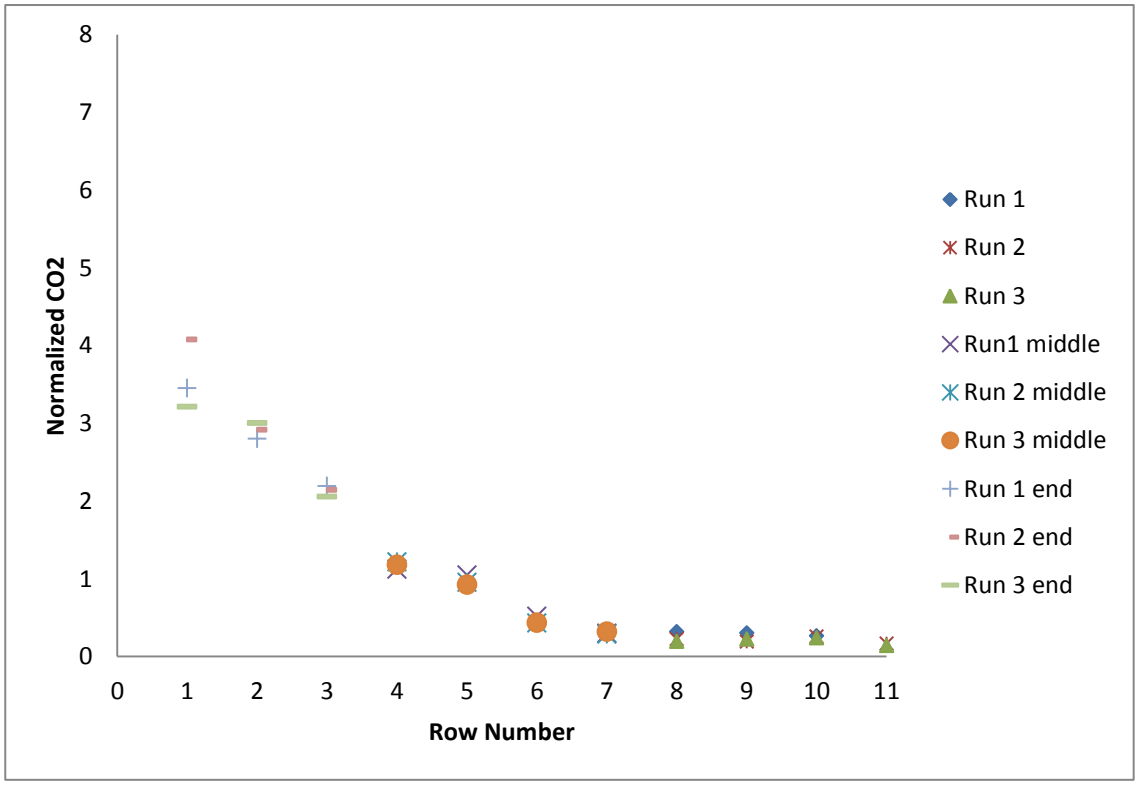

Figure 5.6 Row 1 Release Gaspers On

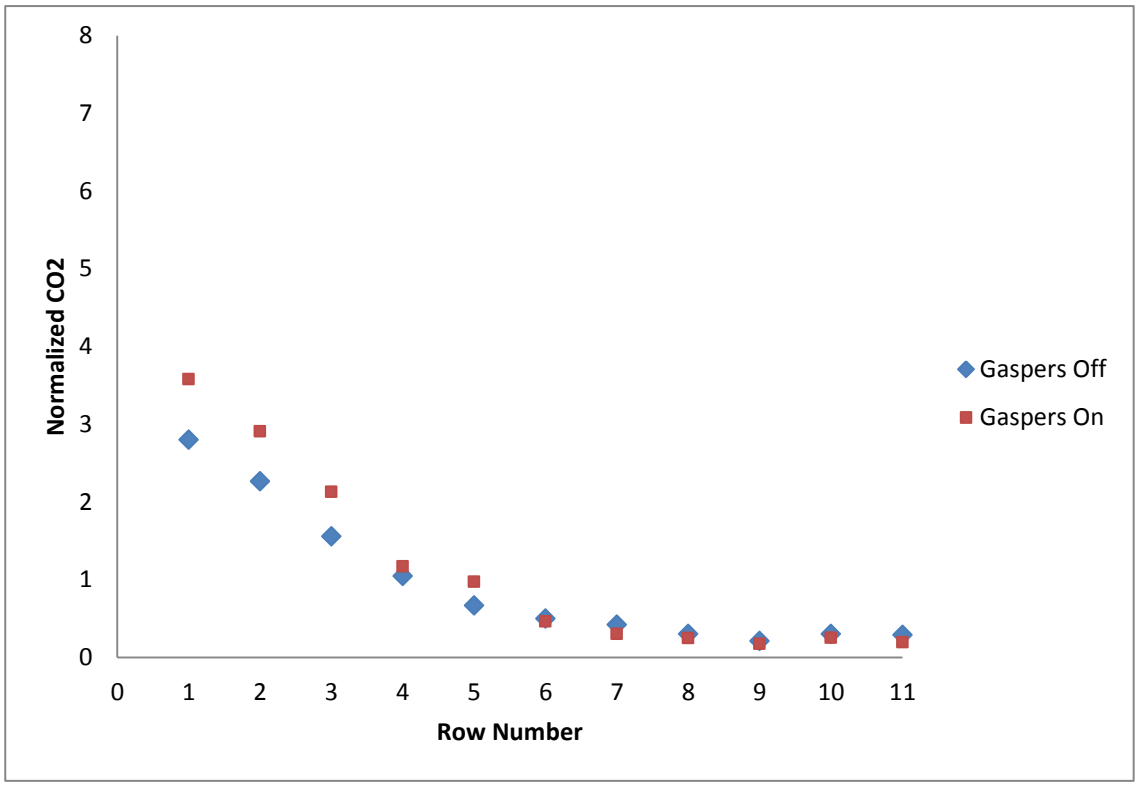

Figure 5.7 Average Values of Row 1 Release with Gaspers On and Off

Table 5.3 Average Normalized Concentrations for Row 1 Release

Average Normalized CO_2				
Row	**Gaspers OFF**	**Relative Uncertainty**	**Gaspers ON**	**Relative Uncertainty**
1	2.80	±7%	3.58	±6%
2	2.27	±8%	2.91	±7%
3	1.56	±6%	2.13	±7%
4	1.05	±6%	1.17	±5%
5	0.67		0.97	
6	0.5		0.46	
7	0.42		0.30	
8	0.30		0.25	
9	0.21		0.17	
10	0.30		0.25	
11	0.29		0.19	

5.1.3 Row 6 Injection

The final injection site used was the middle of the aircraft in row 6. Figure 5.8 shows the normalized values with the gasper system off. The normalized values with the gaspers on are

seen in Figure 5.9, and Figure 5.10 shows the comparison of averaged values. While the peak value is about the same in both cases, the peak appears sharper and the distribution is more consistent with gaspers on. This result indicates the gaspers increase the local mixing as would be expected. Table 5.4 shows values of the normalized averages plotted in Figure 5.10.

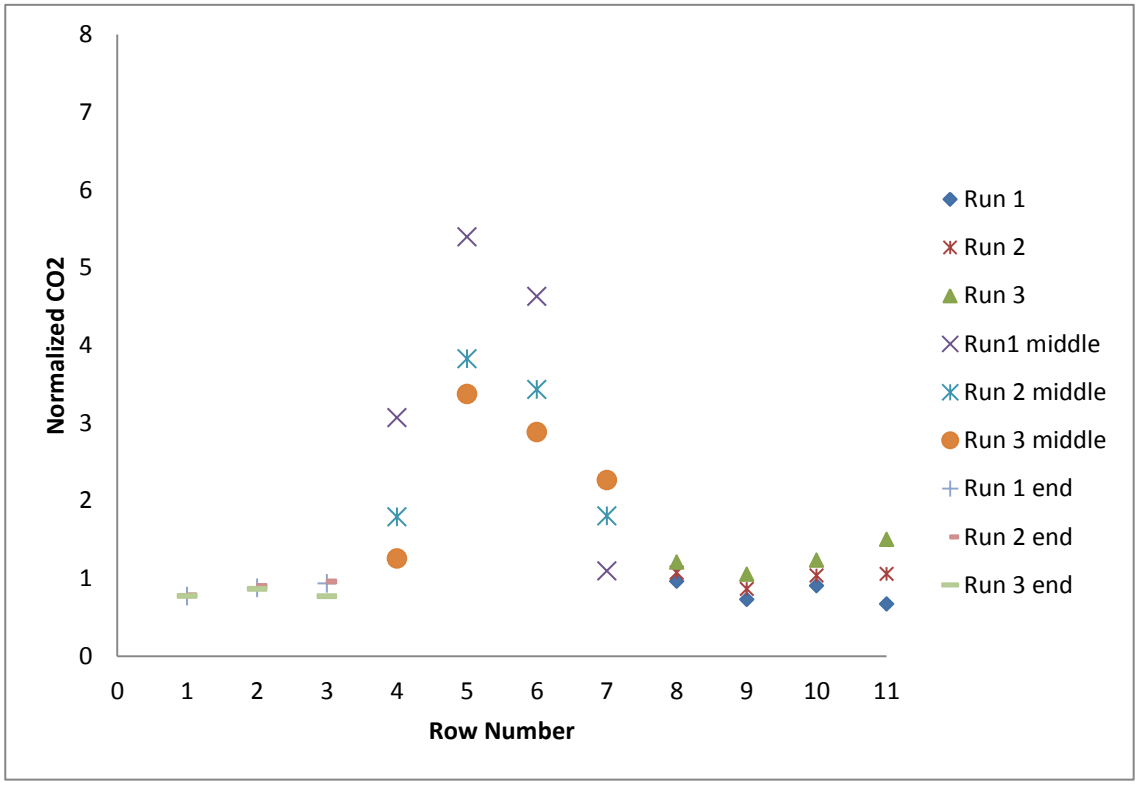

Figure 5.8 Row 6 Release Gaspers Off

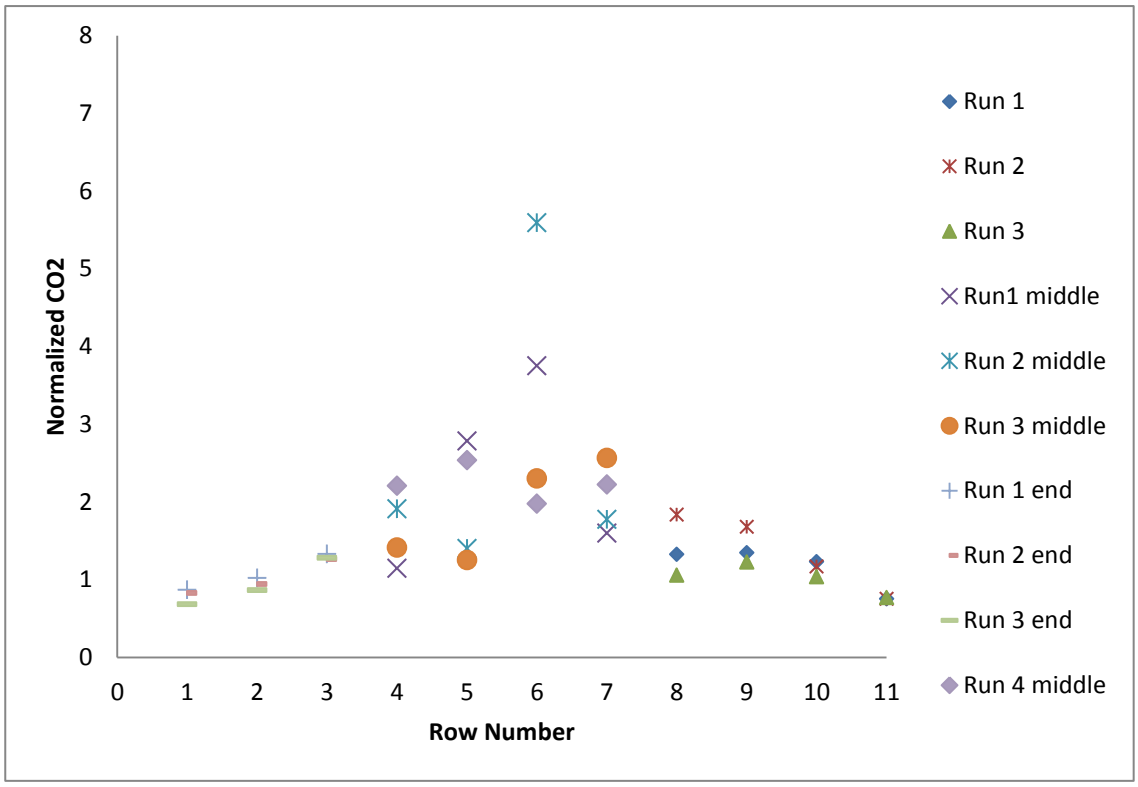

Figure 5.9 Row 6 Release Gaspers On

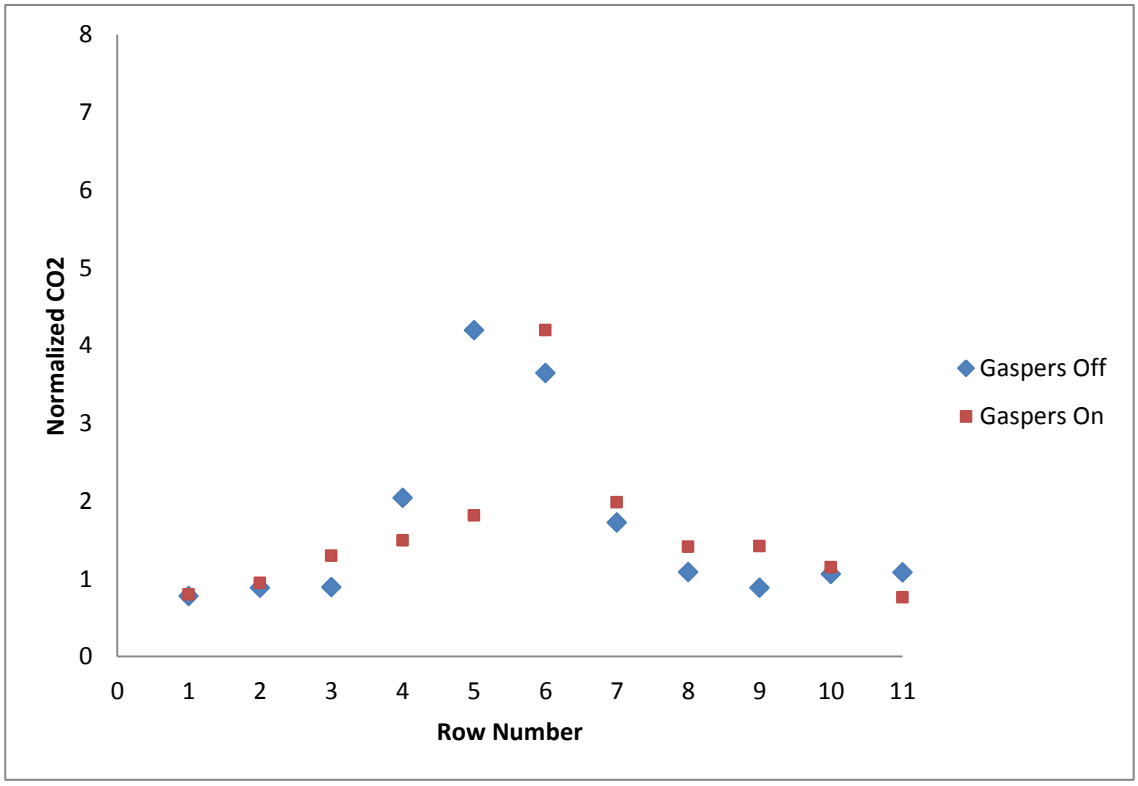

Figure 5.10 Average Values of Row 11 Release Gaspers On and Off

Table 5.4 Average Normalized Concentrations fro Row 11 Release

Average Normalized CO_2				
Row	**Gaspers OFF**	**Relative Uncertainty**	**Gaspers ON**	**Relative Uncertainty**
1	0.78		0.79	
2	0.88		0.94	
3	0.89		1.29	
4	2.04	±7%	1.49	±9%
5	4.20	±7%	1.81	±7%
6	3.65	±8%	4.20	±7%
7	1.72	±9%	1.98	±9%
8	1.08		1.41	
9	0.88		1.42	
10	1.06		1.15	
11	1.08		0.76	

5.2 Gasper Air Inhalation

Table 5.5, Table 5.6, and Table 5.7 give the results of the gasper air inhalation testing, indicating measured CO_2 concentrations at each location along with the percentage of gasper air inhaled at the sampling location relative to the overall cabin ventilation. For the separate gasper directional configurations, the gasper was aimed using smoke visualization to give a relative location of the jet exiting the gasper. It was by no means perfect, but a general aim of right, left, or directly on the face could be obtained. The exposure values in the tables below were obtained by converting equation (4.2) to a percentage.

Table 5.5 Results of Gasper Focused Directly on Face of TOM

	Background CO_2 (ppm)	**Gasper CO_2 (ppm)**	**Manikin CO_2 (ppm)**	**Exposure (%)**
Run 1	433	3204	557	4.5
Run 2	424	3165	582	5.7
Run 3	436	3108	591	5.8

Table 5.6 Results of Gasper Focused on the Left Side of TOM's face

	Background CO_2 (ppm)	Gasper CO_2 (ppm)	Manikin CO_2 (ppm)	Exposure (%)
Run 1	423	2971	520	3.8
Run 2	426	3059	530	4.0
Run 3	429	3009	529	3.9

Table 5.7 Results of Gasper Focused on the Right Side of TOM's face

	Background CO_2 (ppm)	Gasper CO_2 (ppm)	Manikin CO_2 (ppm)	Exposure (%)
Run 1	430	3044	487	2.2
Run 2	428	3017	486	2.3
Run 3	422	3002	468	1.8

Table 5.7 shows the results for the gasper aimed directly on the manikin's face. The results for this indicate only a small fraction of the air inhaled at the manikin is actually emanating from the gasper. The small fraction of gasper air being inhaled seems to indicate the gasper air mixes quickly with the surrounding air within the cabin. Table 5.6 is for the gasper focused slightly to the left of the face of TOM. Again, the exposure is relatively low, even lower than when the gasper was aimed directly at the face of TOM. Table 5.7 is for the gasper focused on the right side of the face of TOM. This exposure is lowest of all, not having a symmetrical result with the focus on the left of the face. Each listed exposure value has an uncertainty of ±0.5% using a 95 percent confidence interval which translates to relative uncertainties between ±10% and ±17%. The uncertainty is again low because each of these values is an average of 180 separate measurements combining random uncertainty and the uncertainty obtained using the propagation of errors technique.

5.3 Manikin Tracer Gas Release

The results for evaluating the protection gaspers provide to passengers are presented below. The results for sampling within row 6 using both release points, and two-row sampling with both

release points within row 6 are presented in separate sections. All average normalized results had a relative uncertainty of less than ±10% using a 95 percent confidence interval.

5.3.1 Intra-row Method Seat 6B Release Point

The first tests performed using the manikin tracer gas release device placed the apparatus and release manikin near the aisle in seat 6B. TOM and the sampling tube were placed in seat 6A. The first set of tests was used to establish a baseline of tracer gas dispersal with only the cabin ventilation. The baseline condition was established by turning both gaspers 6A and 6B off. The baseline configuration is represented as configuration 1 in Table 4.1 as are all configurations mentioned in this section. The transient analysis for each of these runs is shown in Figure 5.11, Figure 5.12, and Figure 5.13. As can be seen, each run establishes a fairly consistent average normalized value and pattern of fluctuation in the normalized values. This pattern of normalized fluctuation indicates plumes of tracer gas consistently reaching the sampling location.

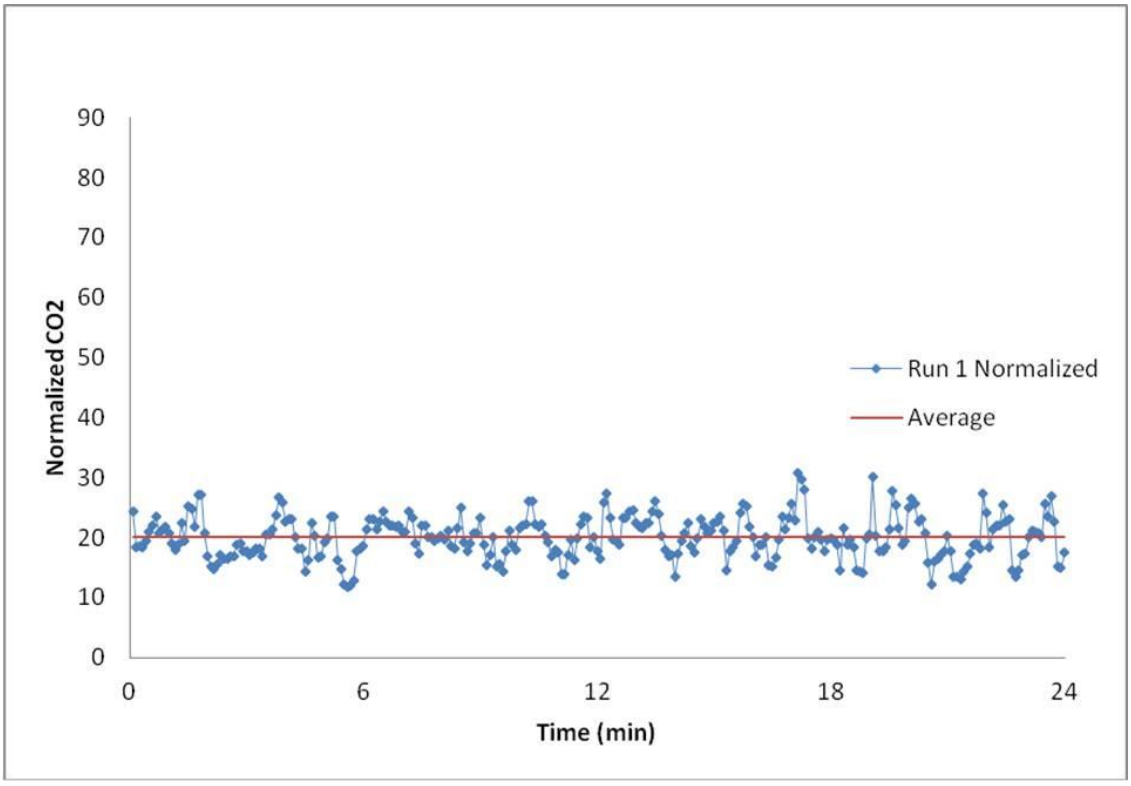

Figure 5.11 Run 1 Intra-row Method, Both Gaspers Off, Seat 6B Release

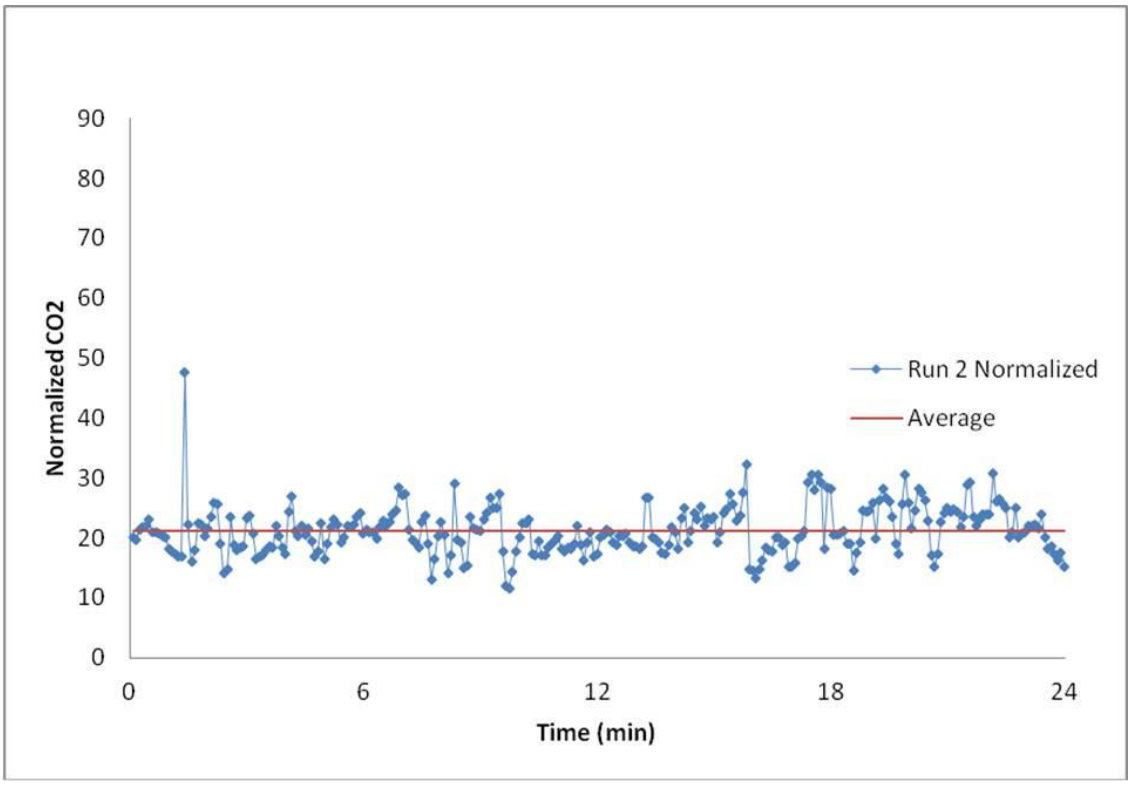

Figure 5.12 Run 2 Intra-row Method, Both Gaspers Off, Seat 6B Release

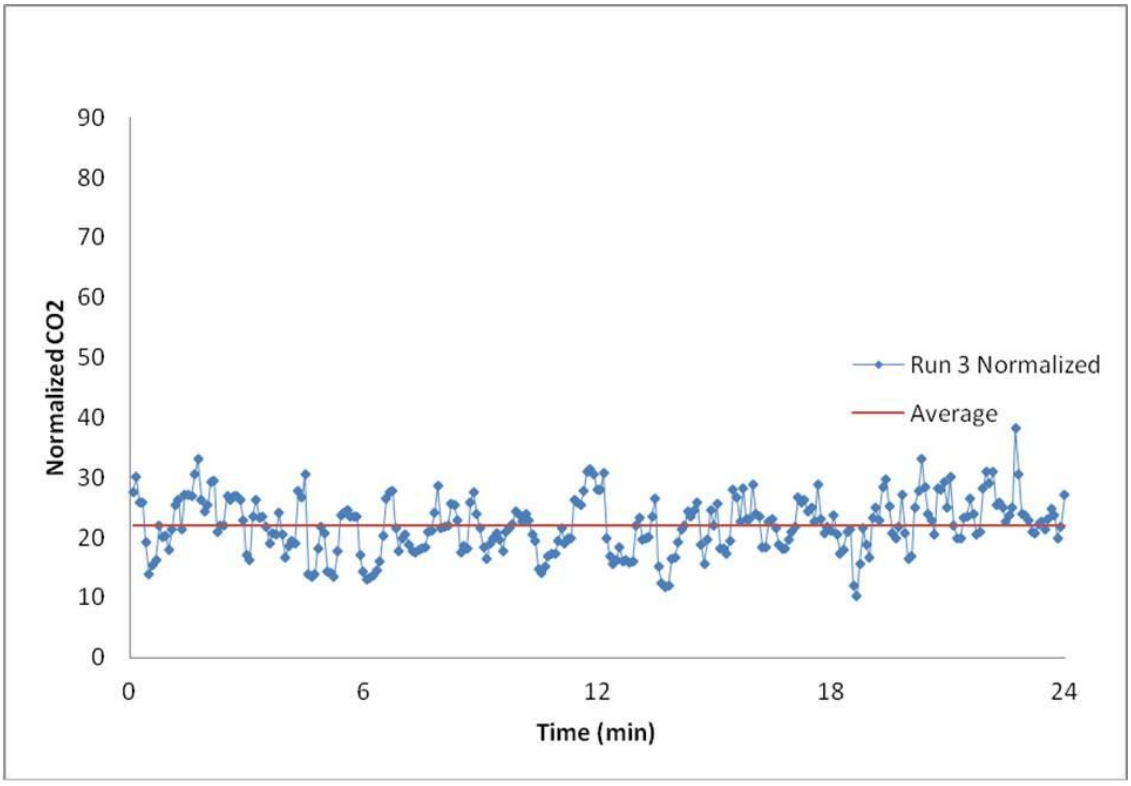

Figure 5.13 Run 3 Intra-row Method, Both Gaspers Off, Seat 6B Release

After the baseline test was performed, gasper configuration 2 was implemented, with the gasper above TOM on and above the release point off. The transient results from this configuration are shown in Figure 5.14, Figure 5.15, and Figure 5.16. Again, the results are consistent; having similar averages, but a reduction in the peaks of concentration can be seen. Similarly, the results of gasper configuration 3, with the release gasper on and gasper above TOM off, can be seen in Figure 5.17, Figure 5.18, and Figure 5.19. The use of the release gasper causes a significant decrease in sample concentration levels. The final test runs using gasper configuration 4, with both gaspers on, can be seen in Figure 5.20, Figure 5.21, and Figure 5.22. The utilization of the release gasper for seat 6B used in conjunction with the gasper above the sampling location causes a significant decrease in observed tracer gas concentration again.

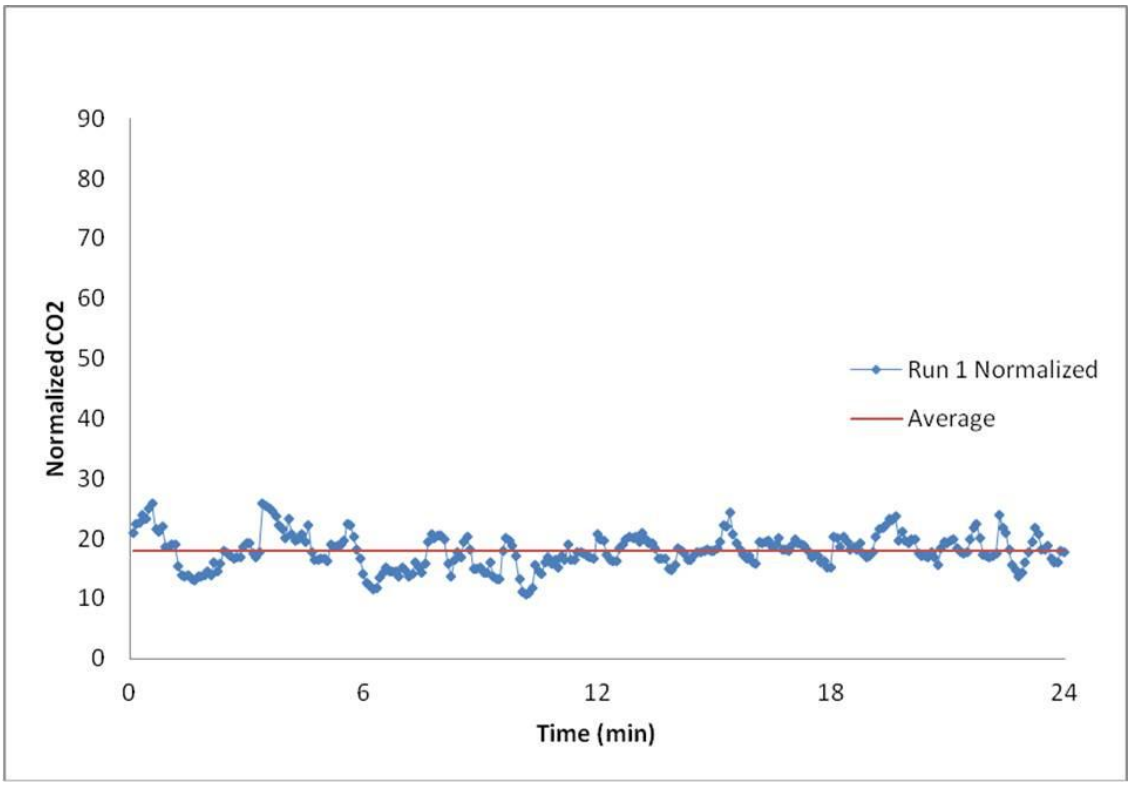

Figure 5.14 Run 1 Intra-row Method, Gasper 6A On, Seat 6B Release

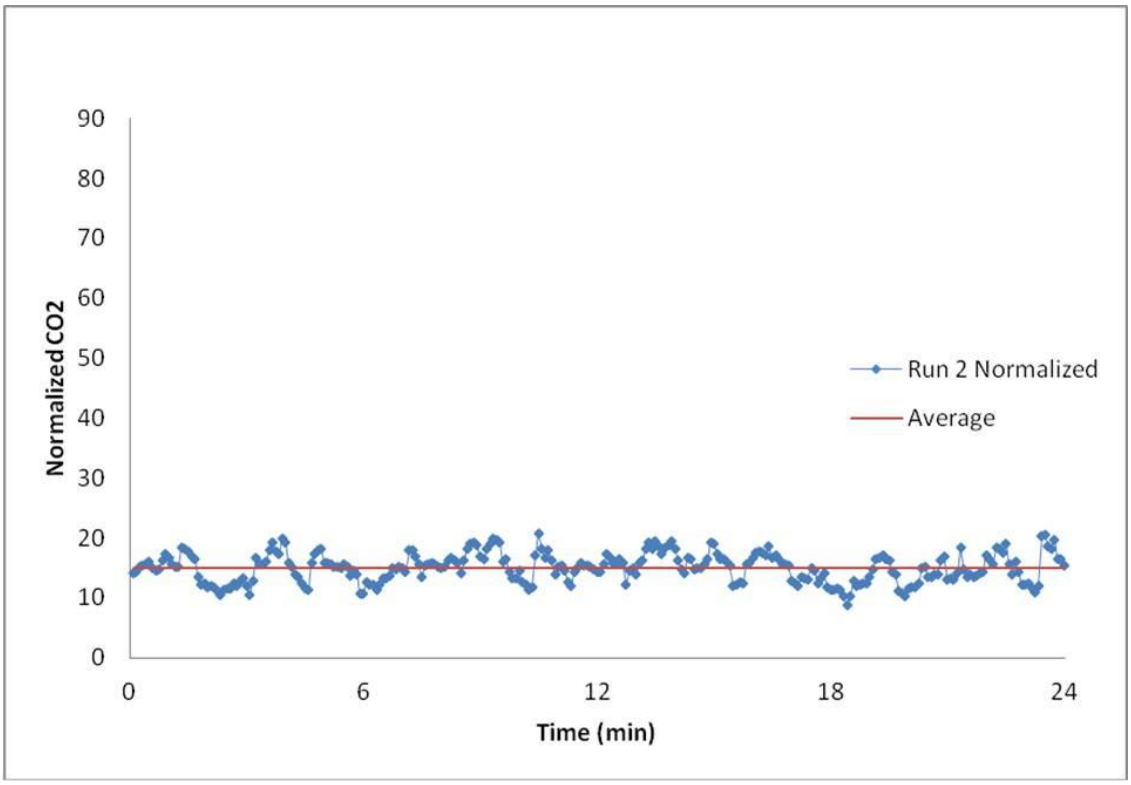

Figure 5.15 Run 2 Intra-row Method, Gasper 6A On, Seat 6B Release

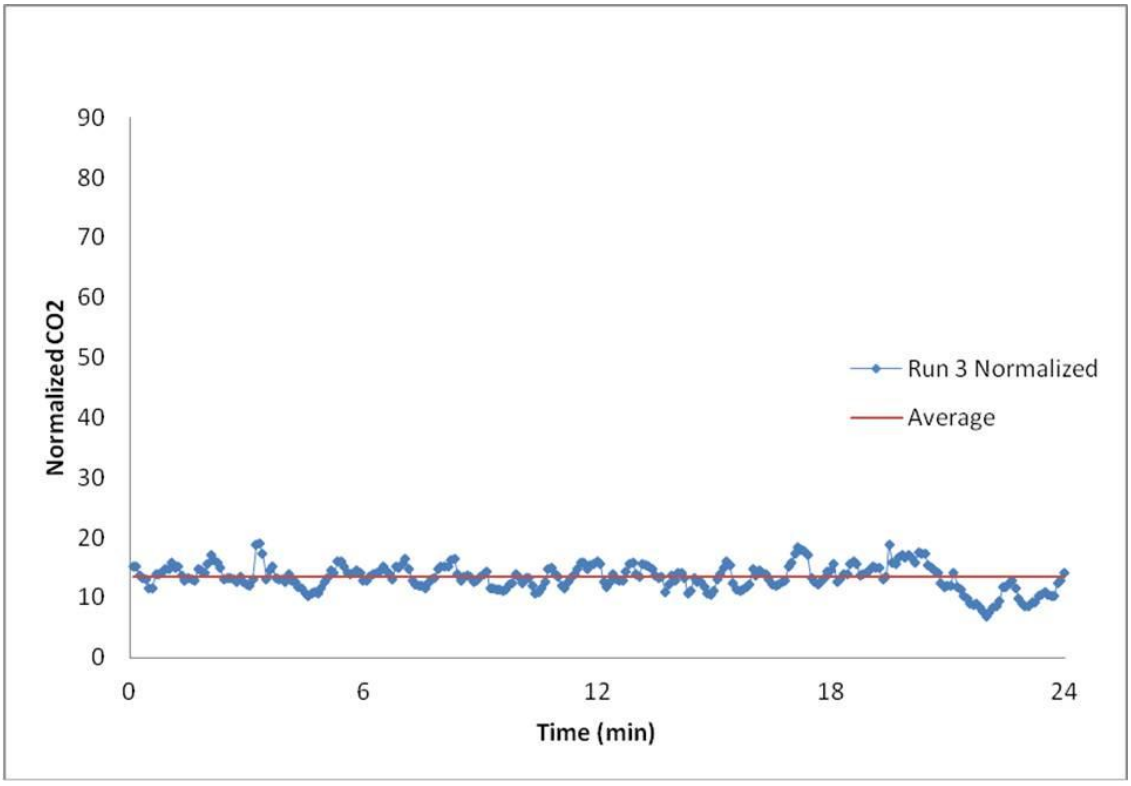

Figure 5.16 Run 3 Intra-row Method, Gasper 6A On, Seat 6B Release

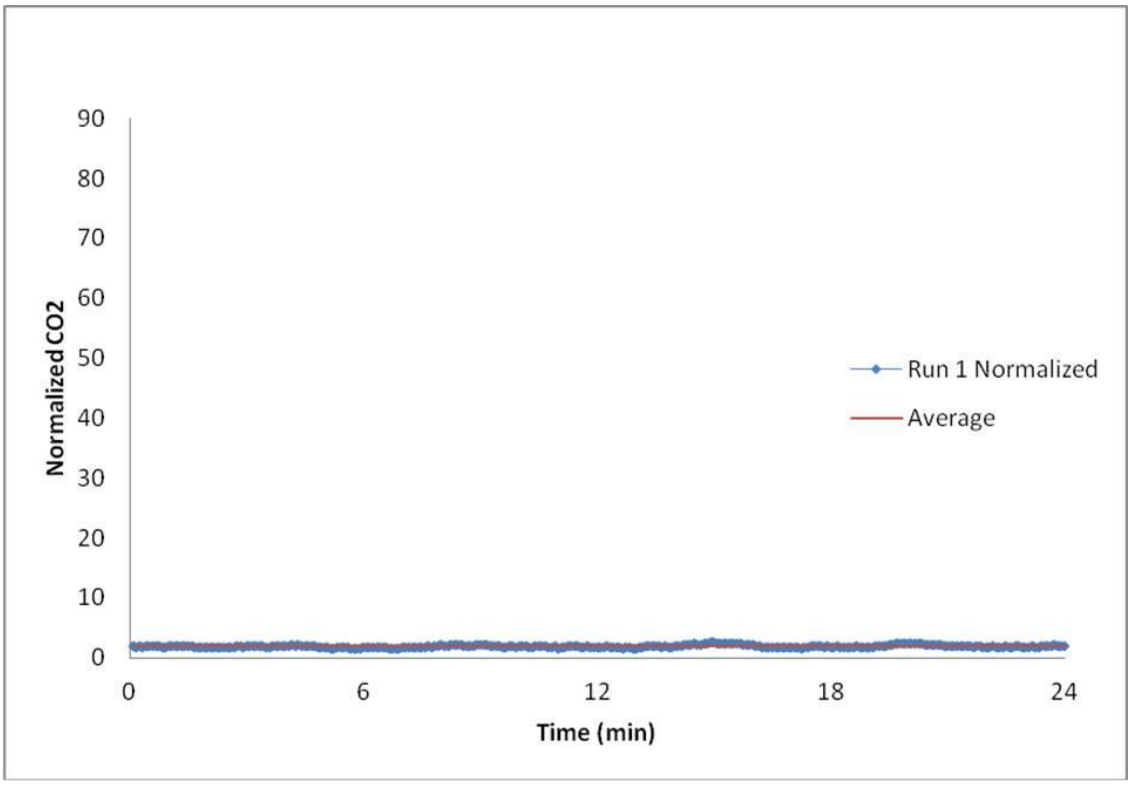

Figure 5.17 Run 1 Intra-row Method, Gasper 6B On, Seat 6B Release

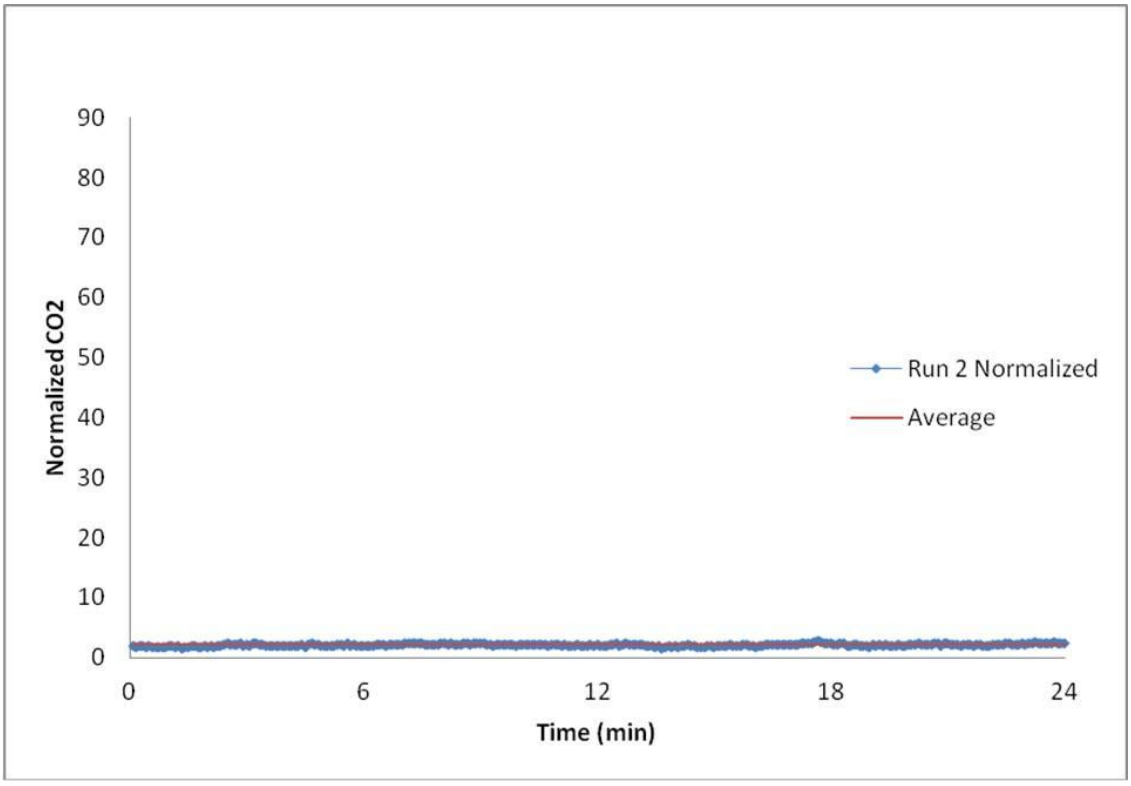

Figure 5.18 Run 2 Intra-row Method, Gasper 6B On, Seat 6B Release

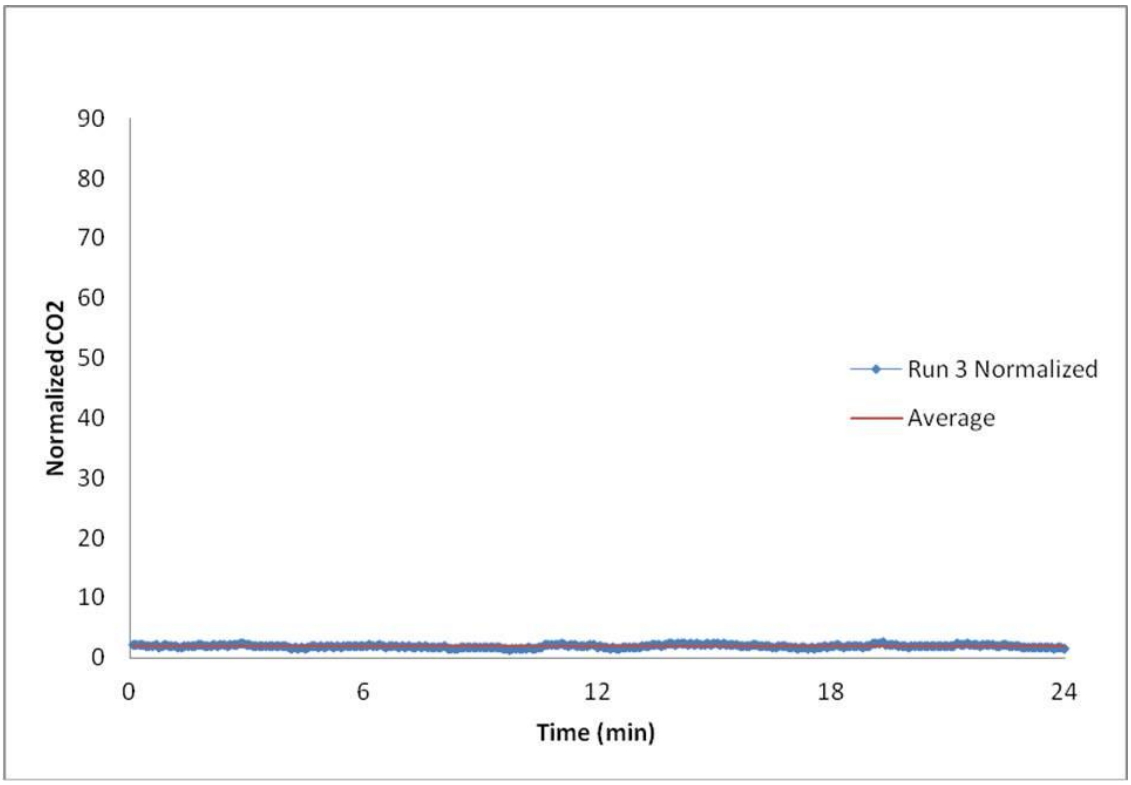

Figure 5.19 Run 3 Intra-row Method, Gasper 6B On, Seat 6B Release

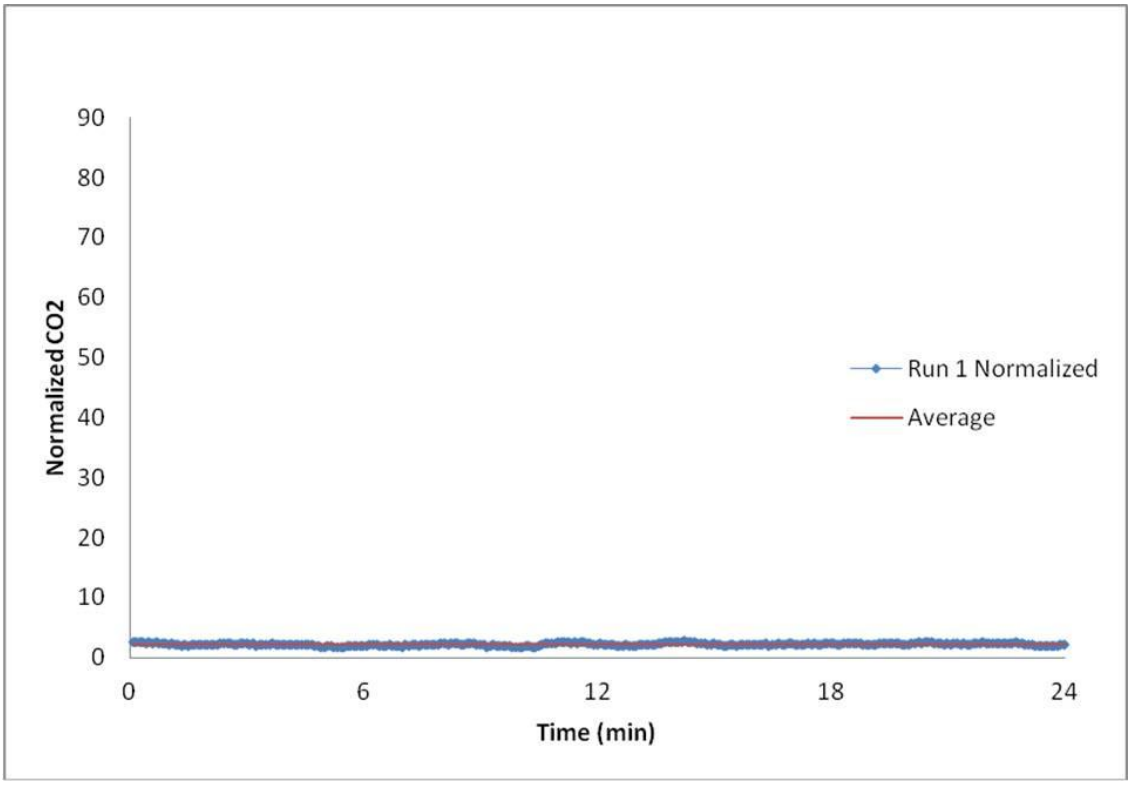

Figure 5.20 Run 1 Intra-row Method, Both Gaspers On, Seat 6B Release

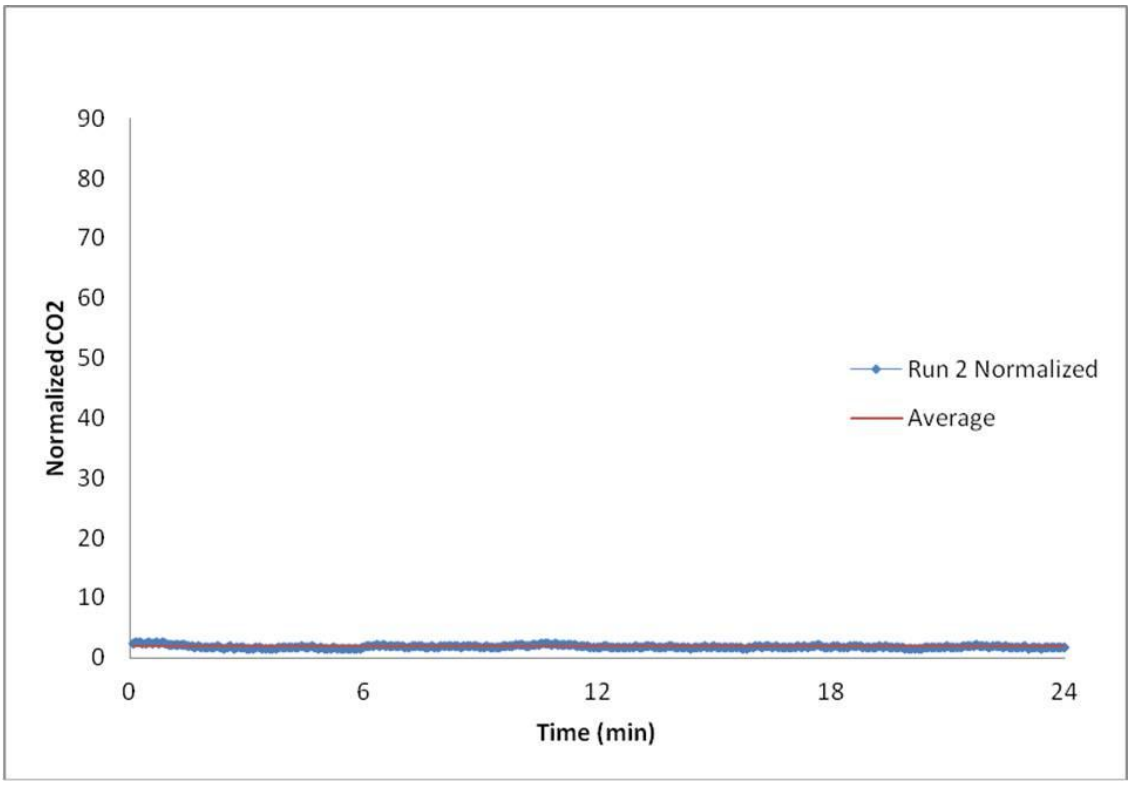

Figure 5.21 Run 2 Intra-row Method, Both Gaspers On, Seat 6B Release

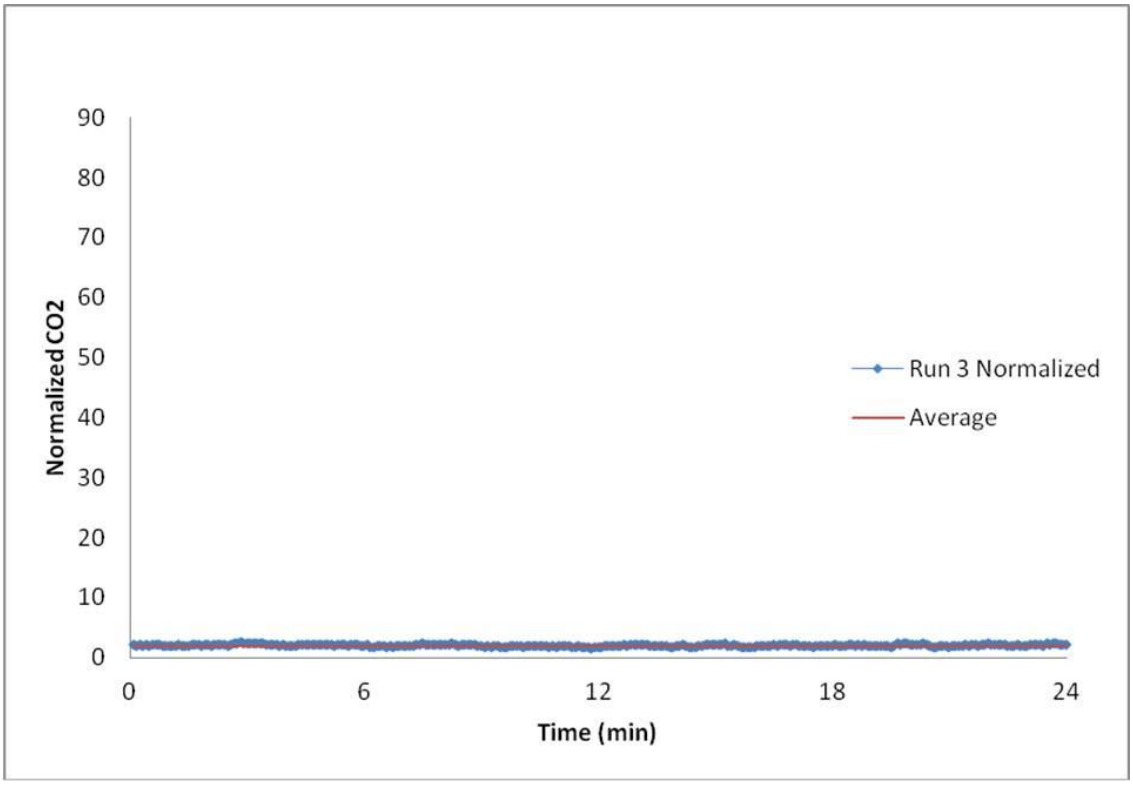

Figure 5.22 Run 3 Intra-row Method, Both Gaspers On, Seat 6B Release

The summaries of results for each gasper configuration are shown in Figure 5.23. The normalized values are organized by gasper configuration indicated on the x-axis. For each configuration, all three test runs are presented side by side and grouped together. All runs for a given configuration correlate well, showing the overall effect each configuration has compared to the baseline scenario with both gaspers off. These runs were then averaged together for a single comparison value for each gasper configuration. These values as well as the reduction in the amount of tracer gas reaching the sampling location compared to the baseline value (both gaspers off) are shown in Table 5.8.

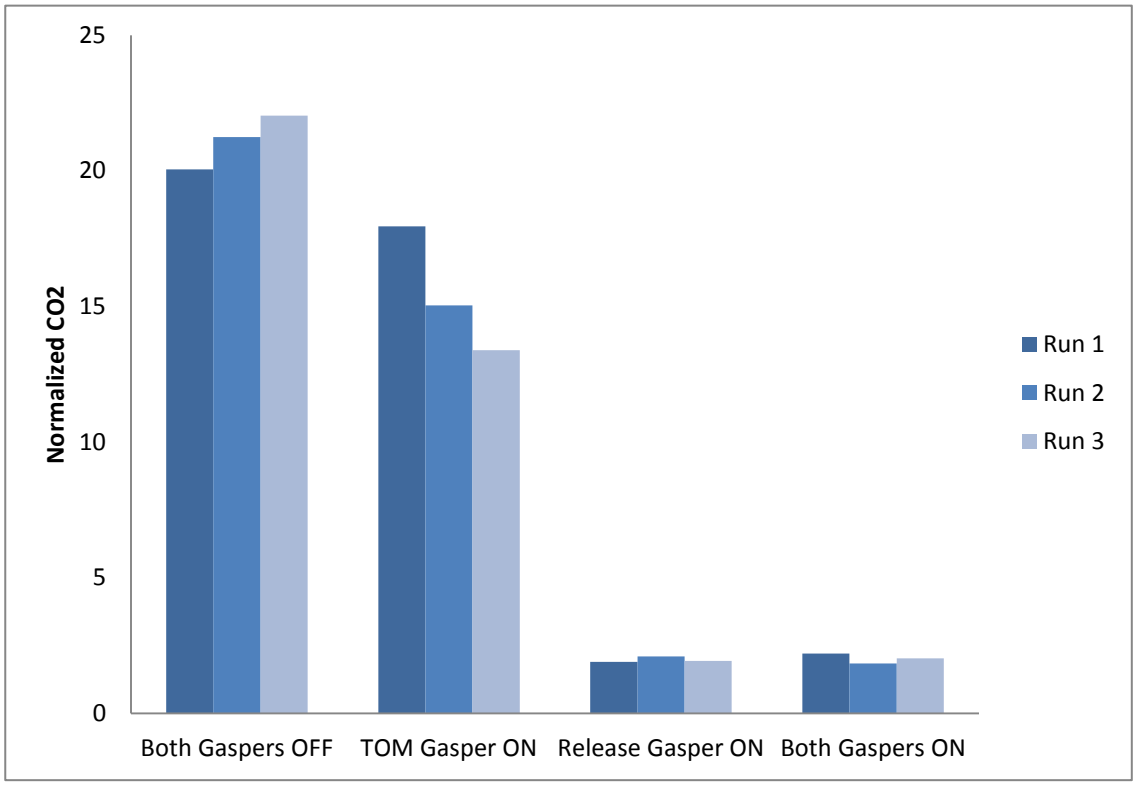

Figure 5.23 Intra-row Method, Summary of Seat 6B Release

Table 5.8 Intra-row Method, Averaged Values of Seat 6B Release

Gasper Configuration	Average Normalized CO2	Improvement over Baseline	Relative Uncertainty of Average
1	21.11		±9%
2	15.46	27%	±9%
3	1.97	91%	±15%
4	2.02	90%	±14%

5.3.2 Intra-row Method Seat 6A Release Point

The final tests performed using the Intra-row testing method placed the tracer gas release mechanism in seat 6A near the wall and placed TOM in seat 6B. The same gasper configurations were utilized again as indicated in Table 4.1. A baseline test was again performed first with both gaspers off. The transient results of these baseline runs can be seen in Figure 5.24, Figure 5.25, and Figure 5.26. The observed peaks are much higher for the seat 6A release point than they were with the release point in seat 6B.

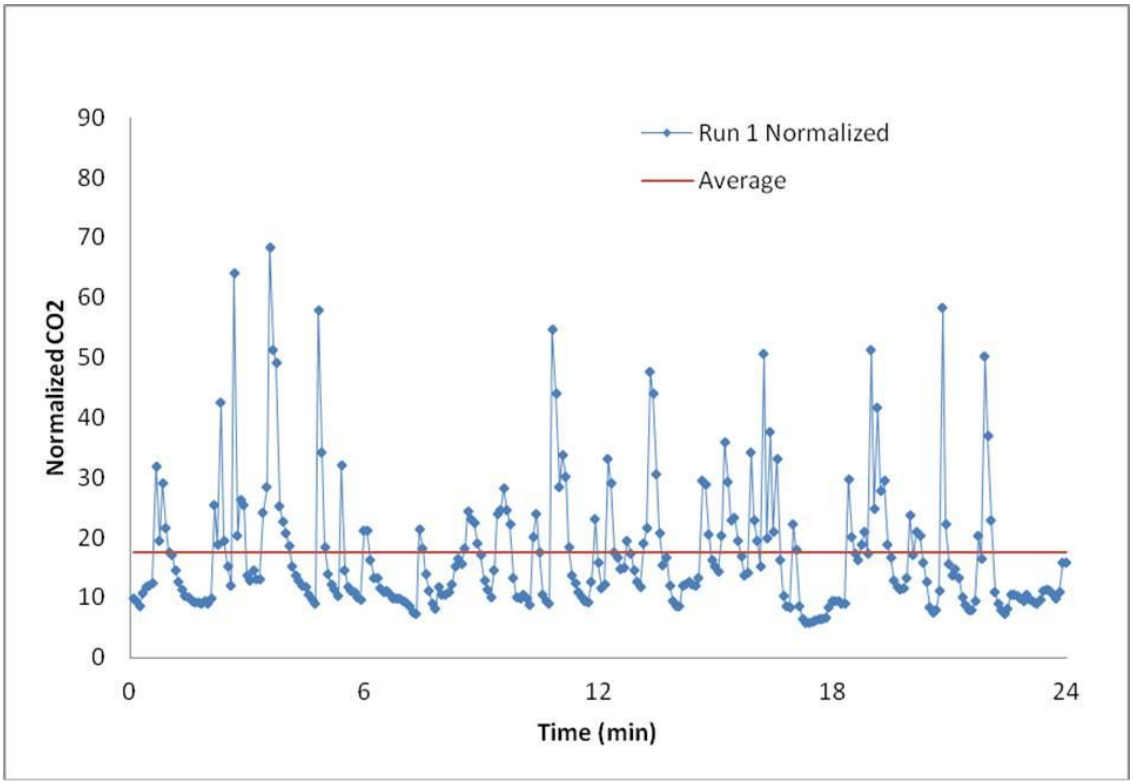

Figure 5.24 Run 1 Intra-row Method, Both Gaspers Off, Seat 6A Release

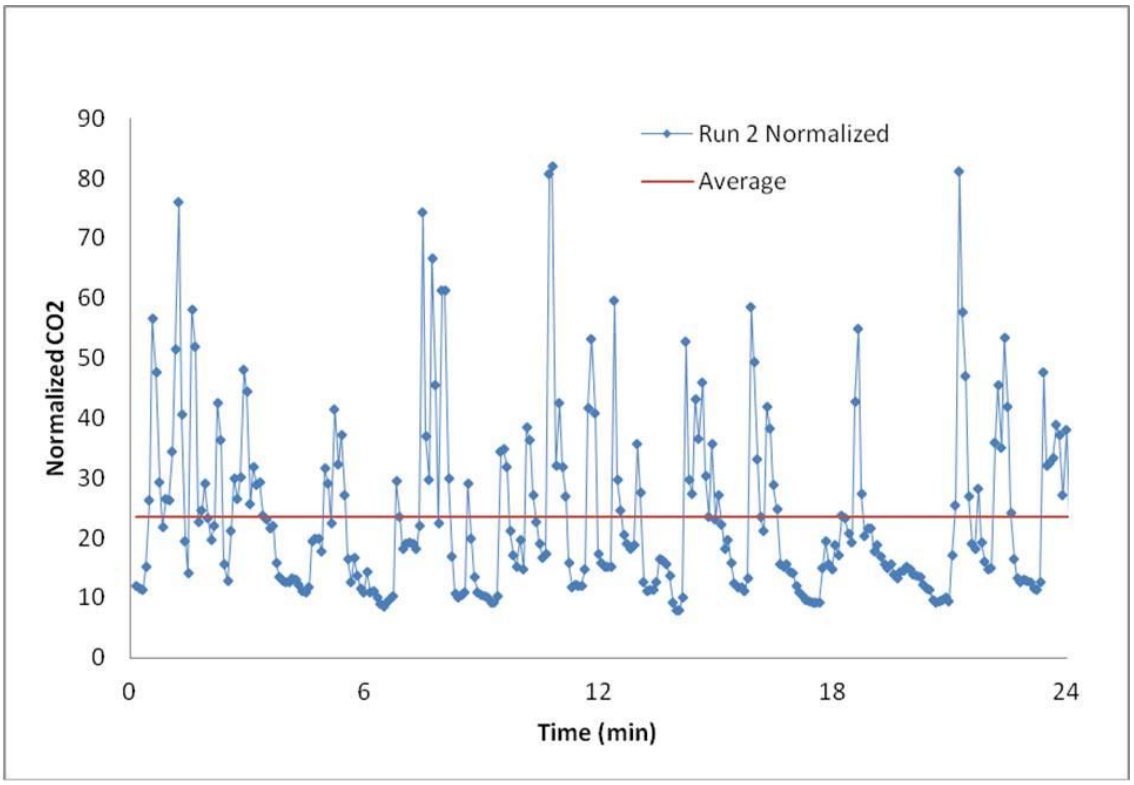

Figure 5.25 Run 2 Intra-row Method, Both Gaspers Off, Seat 6A Release

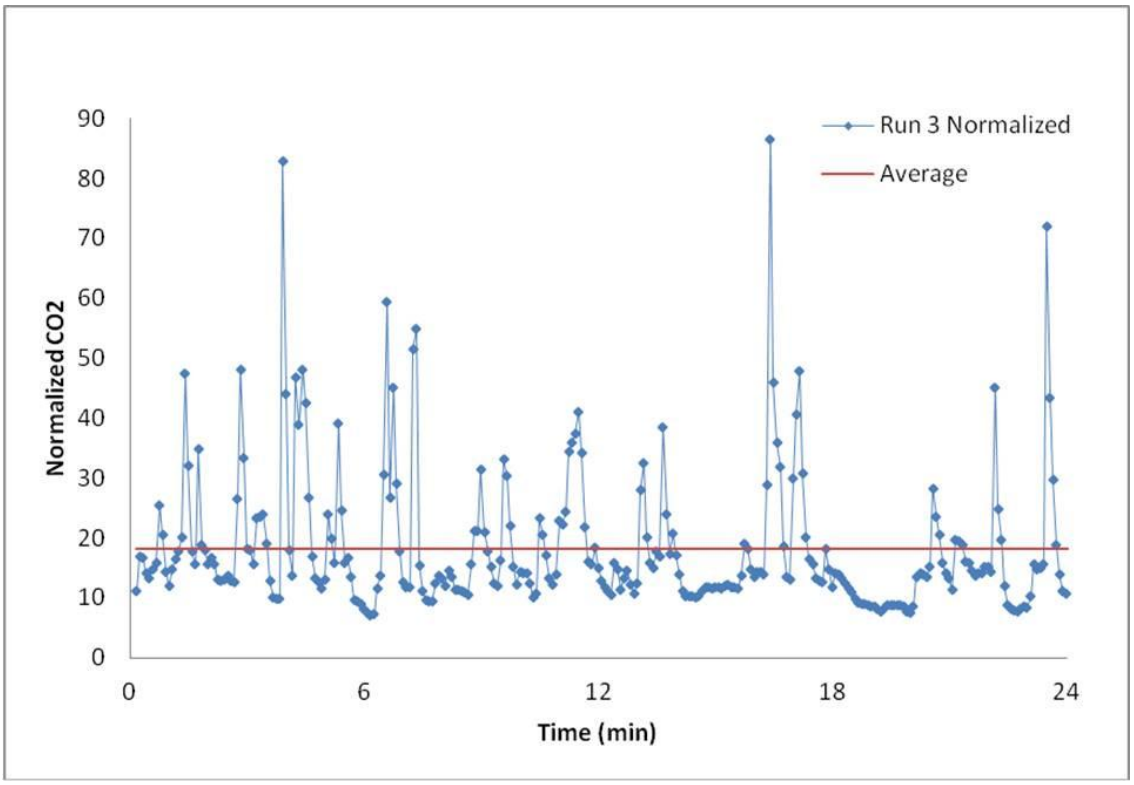

Figure 5.26 Run 3 Intra-row Method, Both Gaspers Off, Seat 6A Release

Configuration 2 with only gasper 6B on was implemented afterwards. Once again, a noticeable reduction in average normalized concentration and size of concentration peaks is observed. These results are shown in Figure 5.27, Figure 5.28, and Figure 5.29. The results of Configuration 3 with only gasper 6A on are shown in Figure 5.30, Figure 5.31, and Figure 5.32. Finally, the transient results of Configuration 4 with both gaspers on are shown in Figure 5.33, Figure 5.34, and Figure 5.35. The configuration of using both gaspers causes the greatest reduction in observed normalized concentrations and in size of concentration fluctuations.

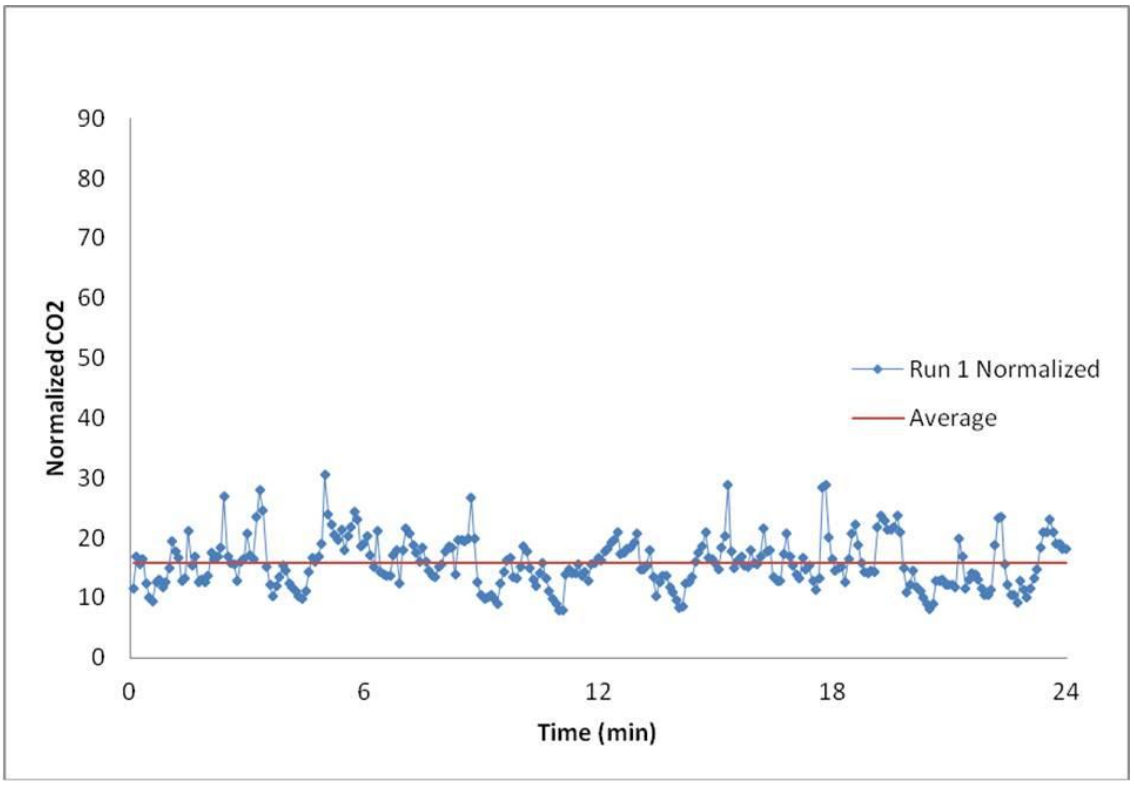

Figure 5.27 Run 1 Intra-row Method, Gasper 6B On, Seat 6A Release

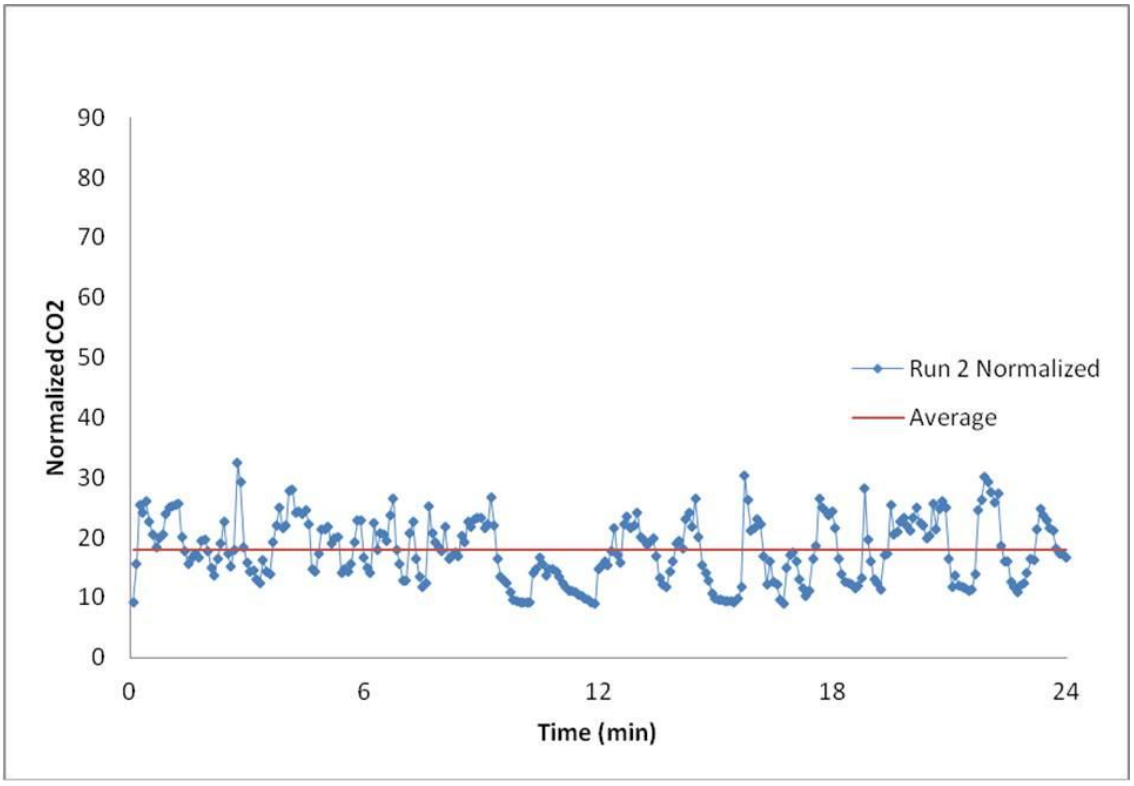

Figure 5.28 Run 2 Intra-row Method, Gasper 6B On, Seat 6A Release

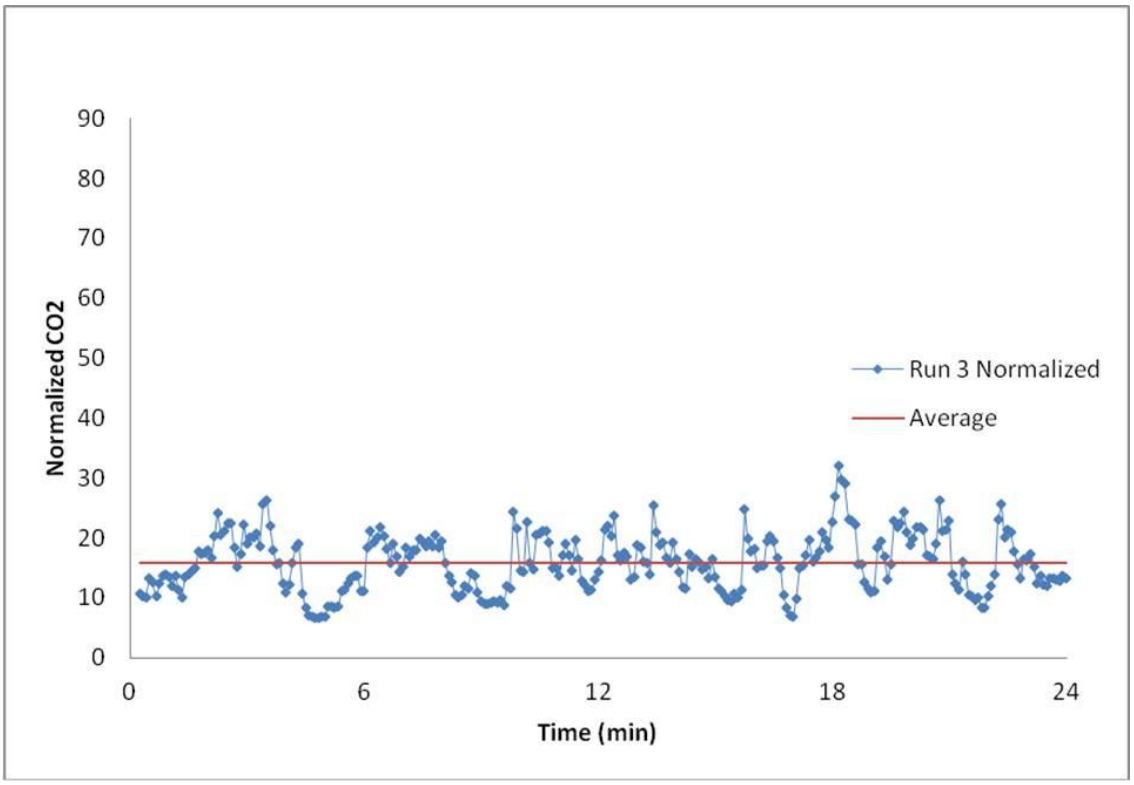

Figure 5.29 Run 3 Intra-row Method, Gasper 6B On, Seat 6A Release

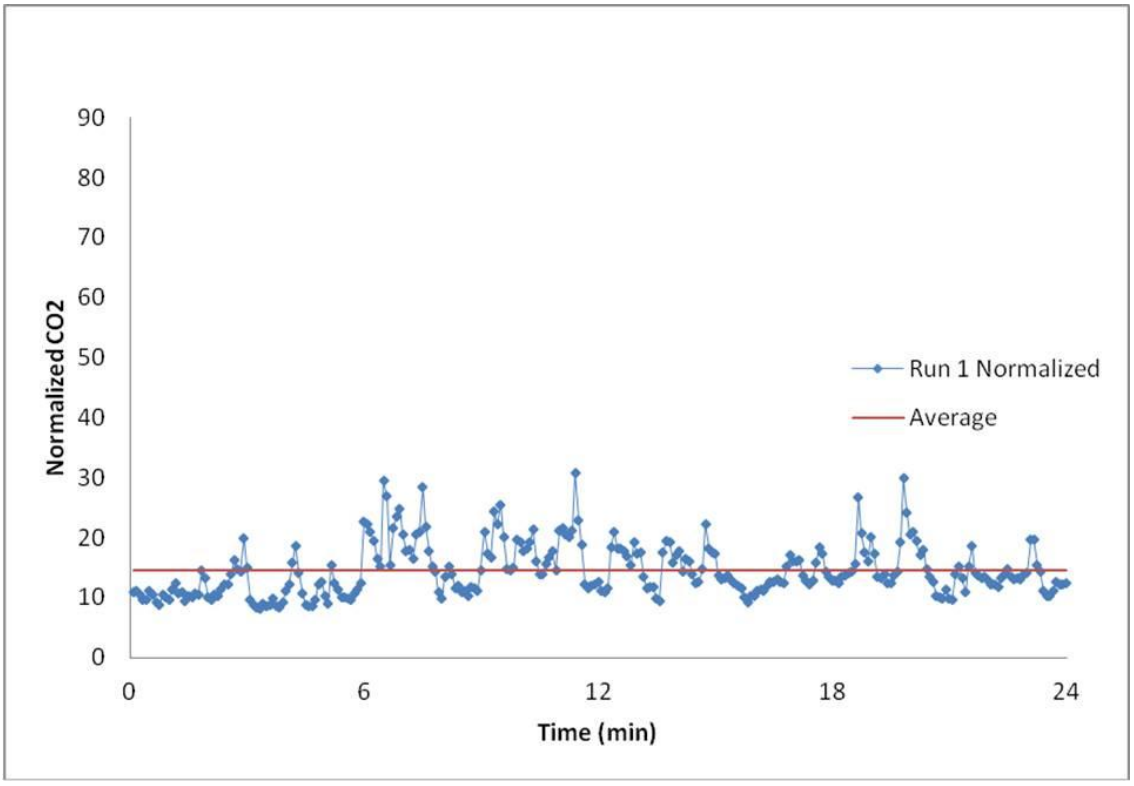

Figure 5.30 Run 1 Intra-row Method, Gasper 6A On, Seat 6A Release

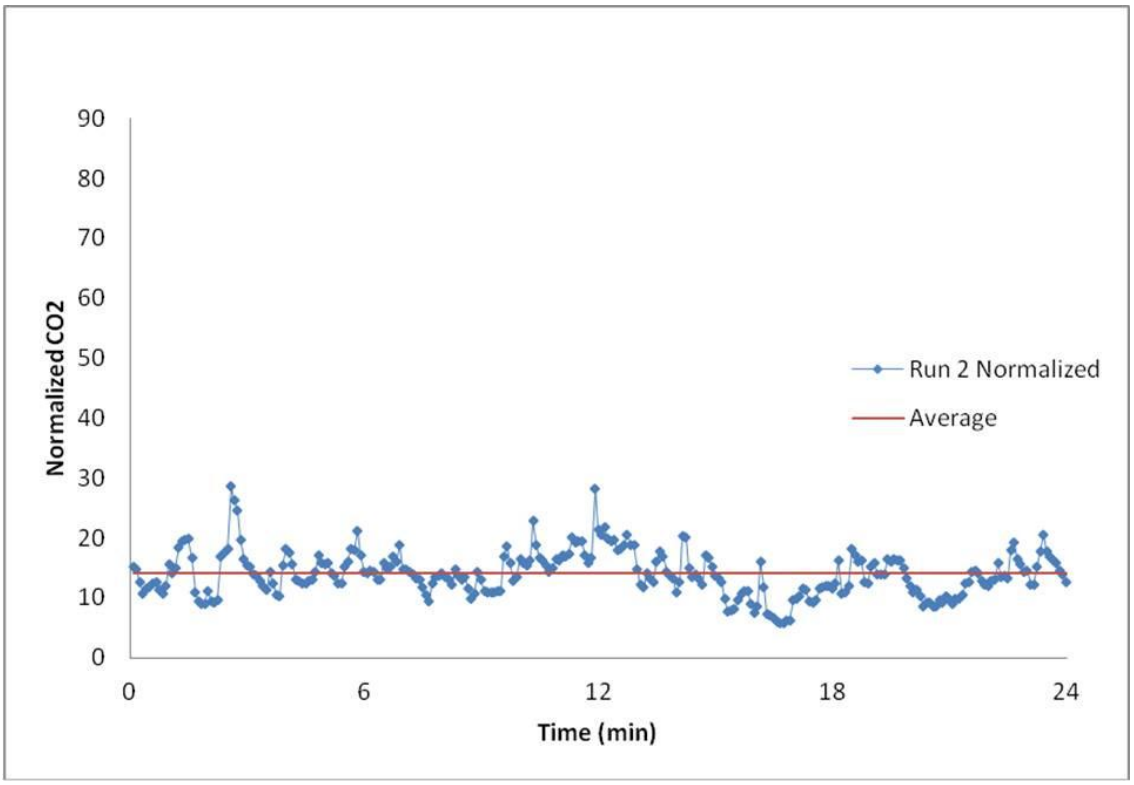

Figure 5.31 Run 2 Intra-row Method, Gasper 6A On, Seat 6A Release

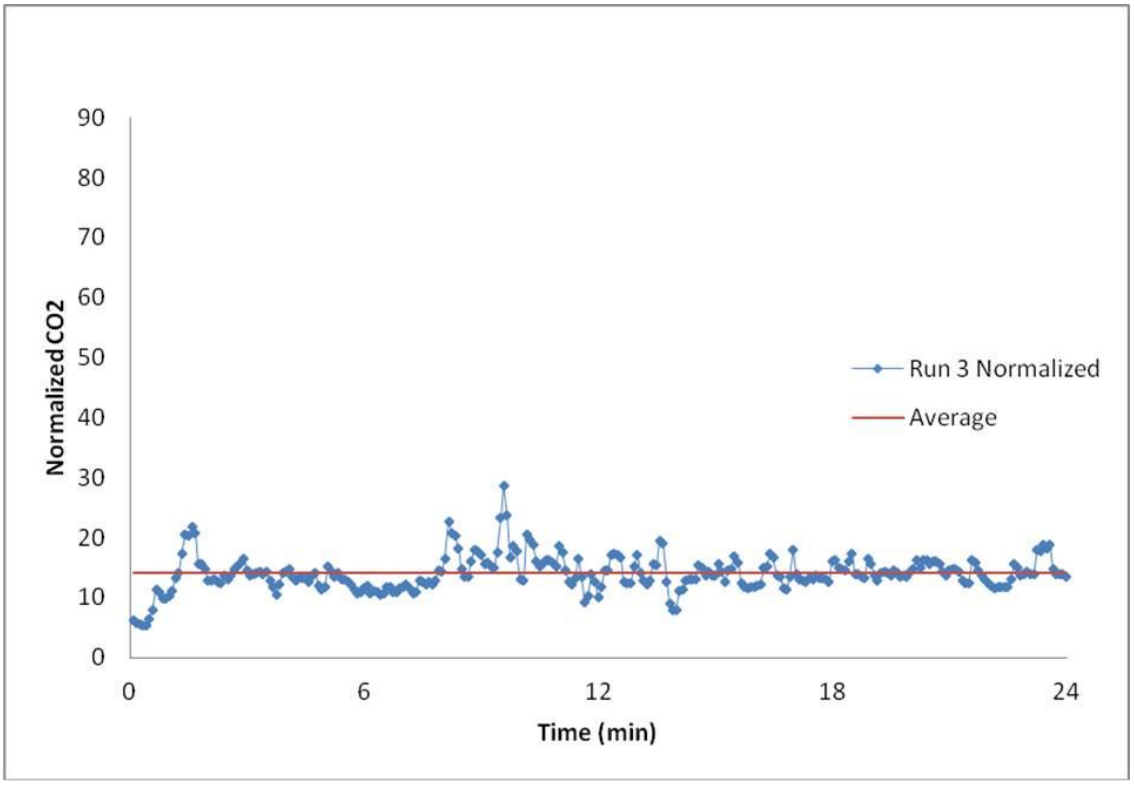

Figure 5.32 Run 3 Intra-row Method, Gasper 6A On, Seat 6A Release

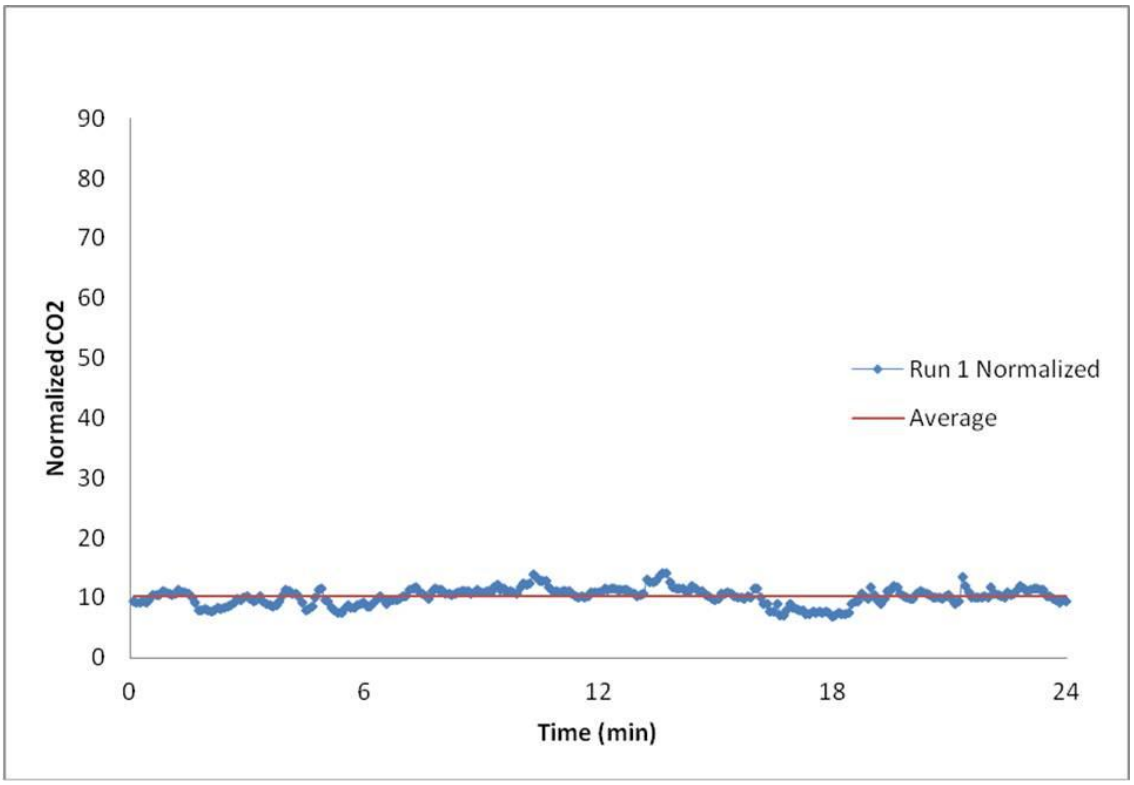

Figure 5.33 Run 1 Intra-row Method, Both Gaspers On, Seat 6A Release

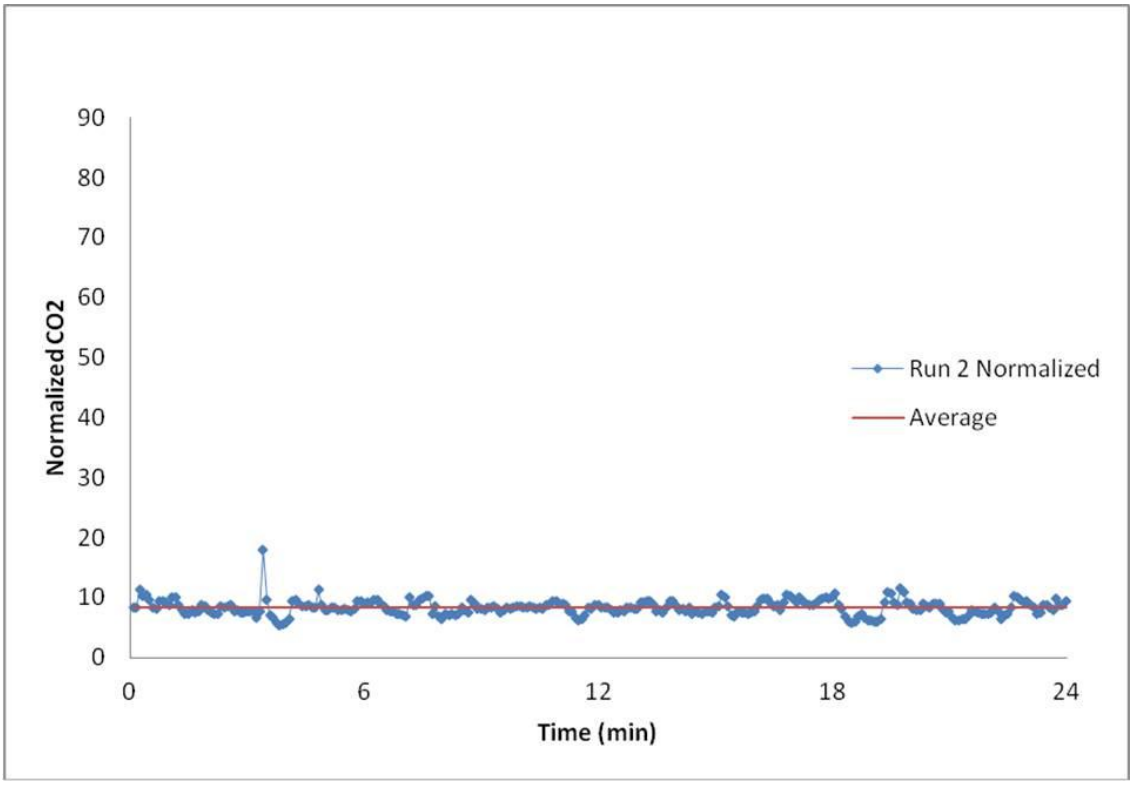

Figure 5.34 Run 2 Intra-row Method, Both Gaspers On, Seat 6A Release

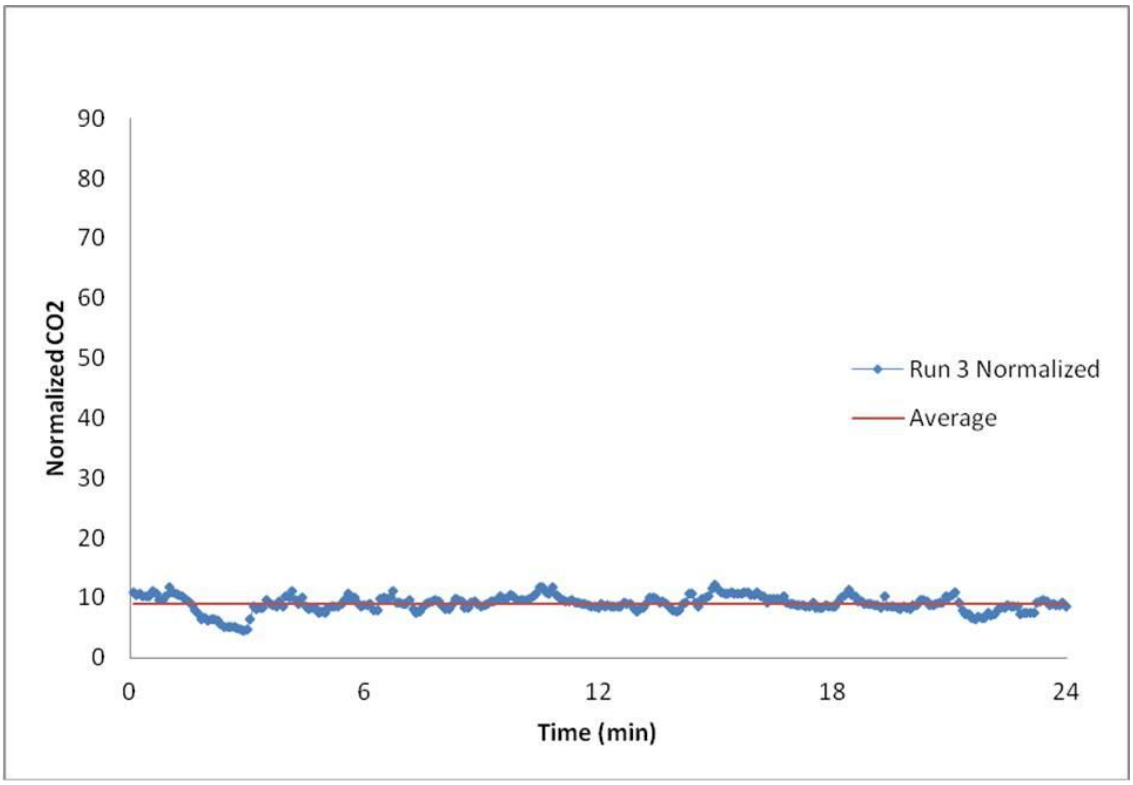

Figure 5.35 Run 3 Intra-row Method, Both Gaspers On, Seat 6A Release

A summary of averaged transient runs is shown in Figure 5.36. As with the previous summary chart, it enables the magnitude of the difference between each configuration to be visualized. Table 5.9 lists the average normalized value of all three runs at a given location, along with the improvement over the initial baseline test where both gaspers were turned off.

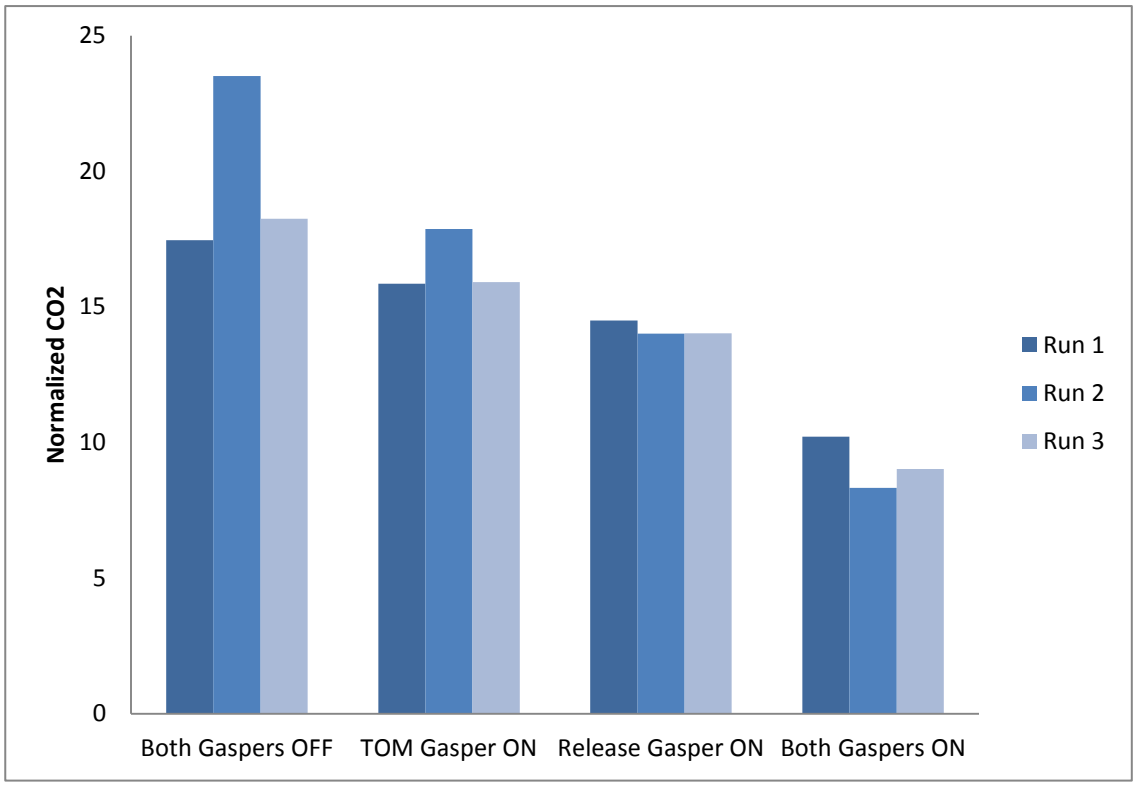

Figure 5.36 Intra-row Method, Summary of Seat 6A Release

Table 5.9 Intra-row Method, Averaged Values of Seat 6A Release

Configuration	Average Normalized CO2	Improvement over Baseline	Relative Uncertainty of Average
1	19.74		±11%
2	16.54	16%	±9%
3	14.18	28%	±9%
4	9.19	53%	±9%

5.3.3 Two-row Sampling with Seat 6A Release

Due to the increased distance from the tracer gas release point of the sampling locations in this testing, there were fewer instances of the sudden transient concentration peaks as seen in the intra-row testing. Because of the lack of transient peaks, results are presented first as the average normalized concentration for each sampling location during a given set of tests. Then, a summary plot is used for a given gasper configuration comparing the effect of the gasper's usage to the baseline test where no gasper was used. The values in the summary plot are averages of the three transient averaged values at each location together. The locations in the x-axis correspond to the testing layout in Figure 4.9.

The initial baseline test conducted was again the scenario where all gaspers were off; the results of this test can be seen in Figure 5.37. The three sampled runs at each location were averaged to use as comparisons for when other gaspers were activated. Figure 5.38 presents the results of each sampling location for when gasper number 1 (seat 7B) was turned on. Similarly, Figure 5.39 corresponds to the situation where the gasper above the release manikin was activated, Figure 5.40 for the gasper at location 2 (seat 7A) being turned on, Figure 5.41 for the gasper at location 3 (seat 5B), and Figure 5.42 for the gasper at location 4 being on (seat 5A).

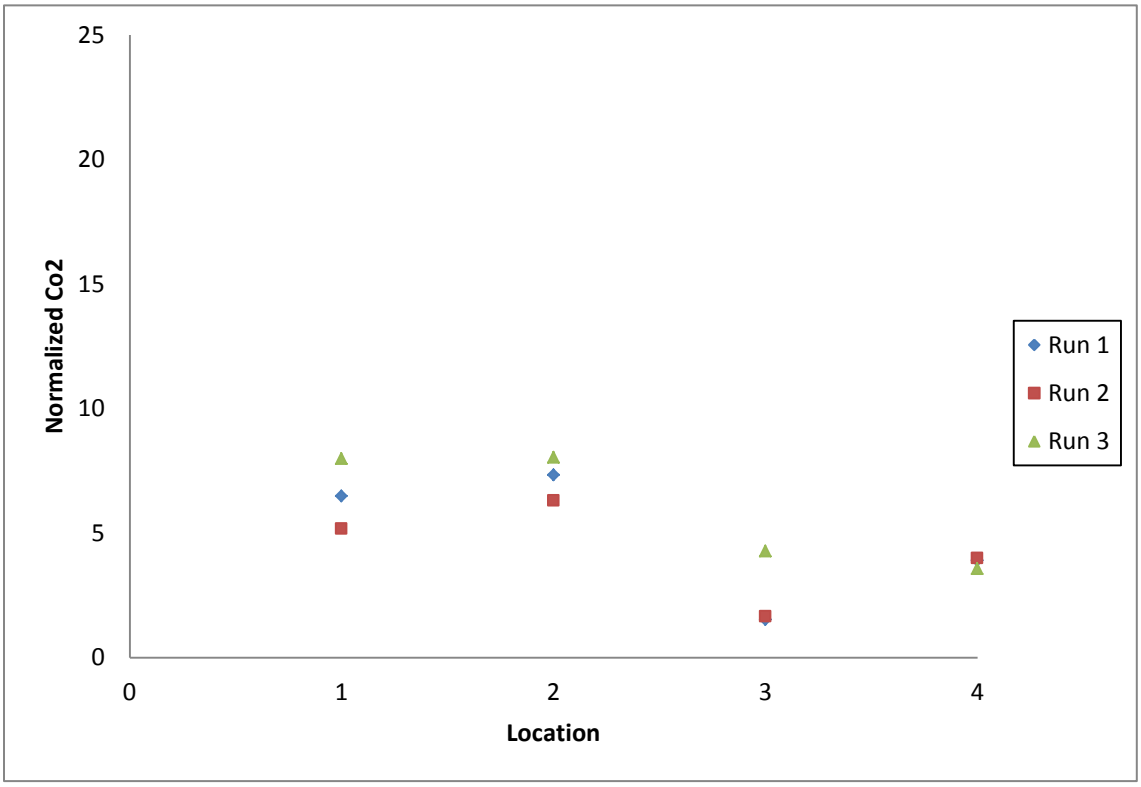

Figure 5.37 Two-row testing, All Gaspers Off, Seat 6A Release

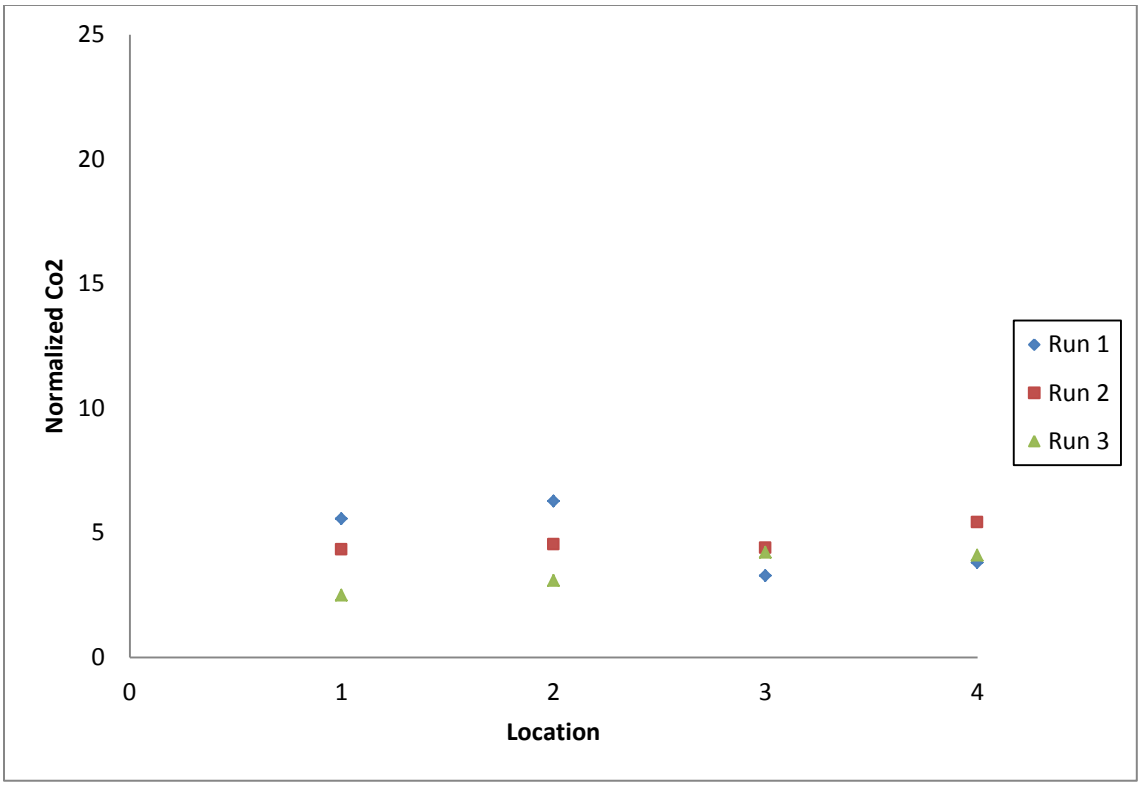

Figure 5.38 Two-row testing, Gasper Location 1 On, Seat 6A Release

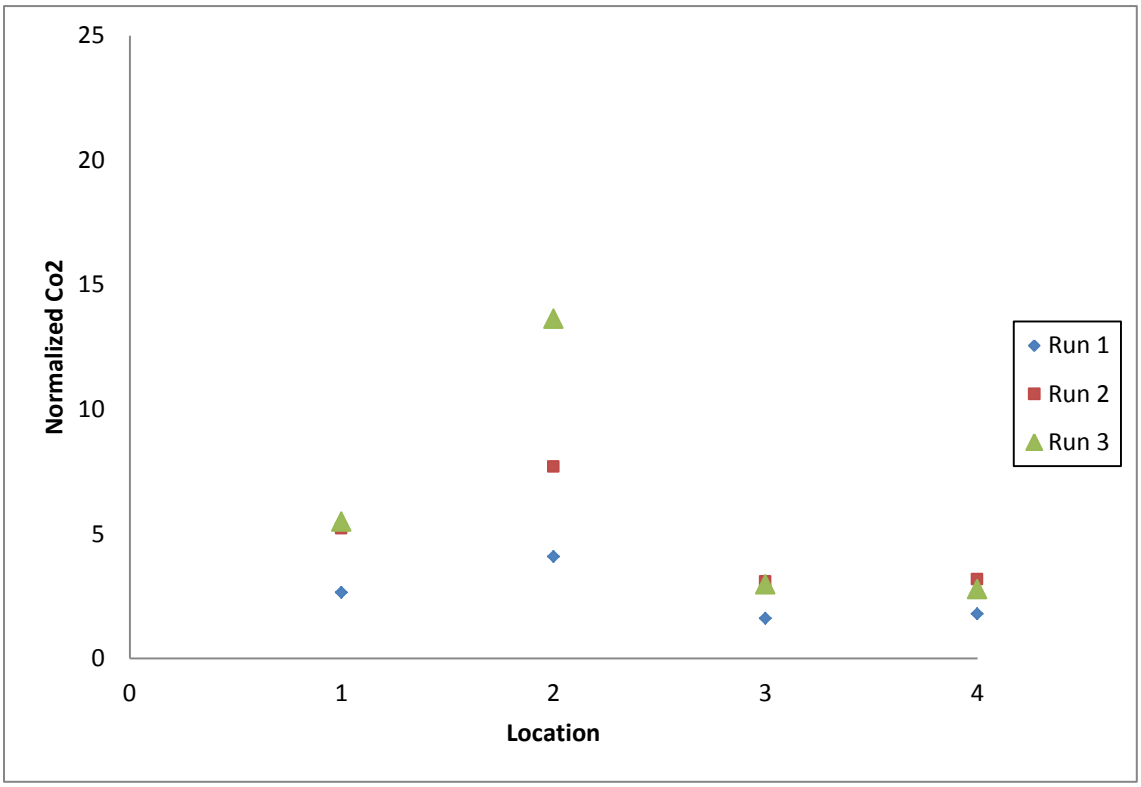

Figure 5.39 Two-row testing, Release Gasper On, Seat 6A Release

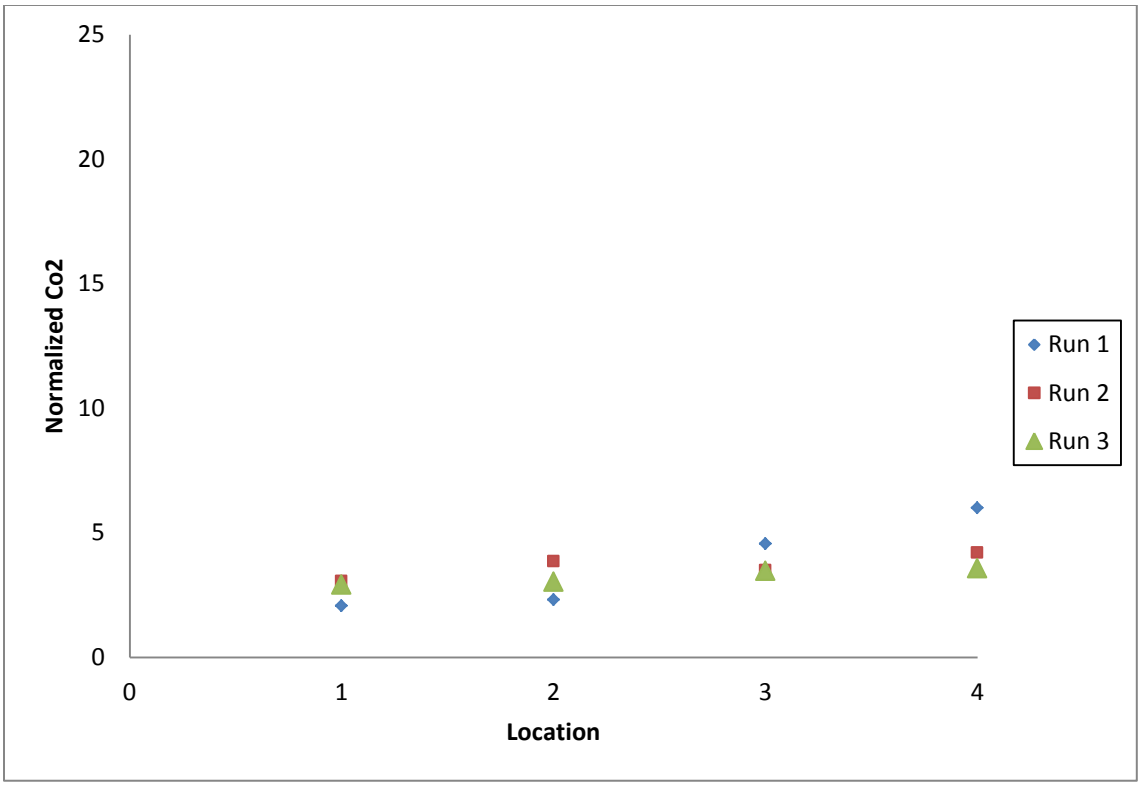

Figure 5.40 Two-row testing, Gasper Location 2 On, Seat 6A Release

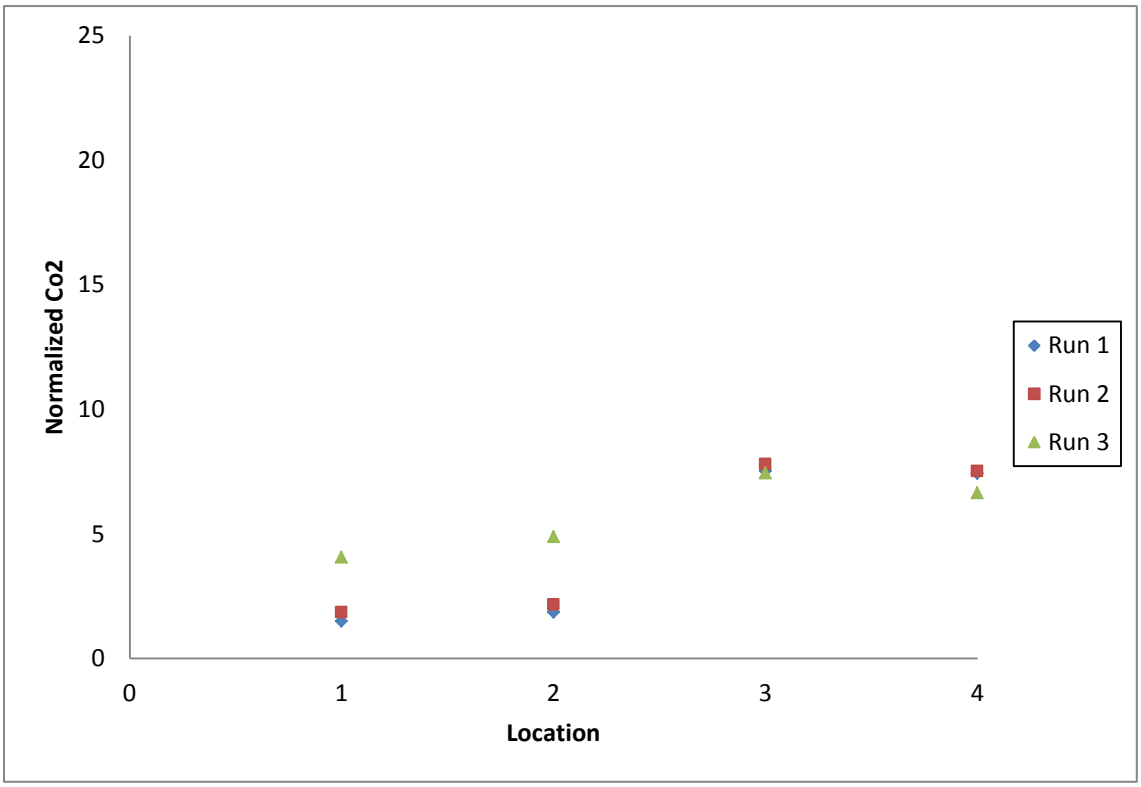

Figure 5.41 Two-row testing, Gasper Location 3 On, Seat 6A Release

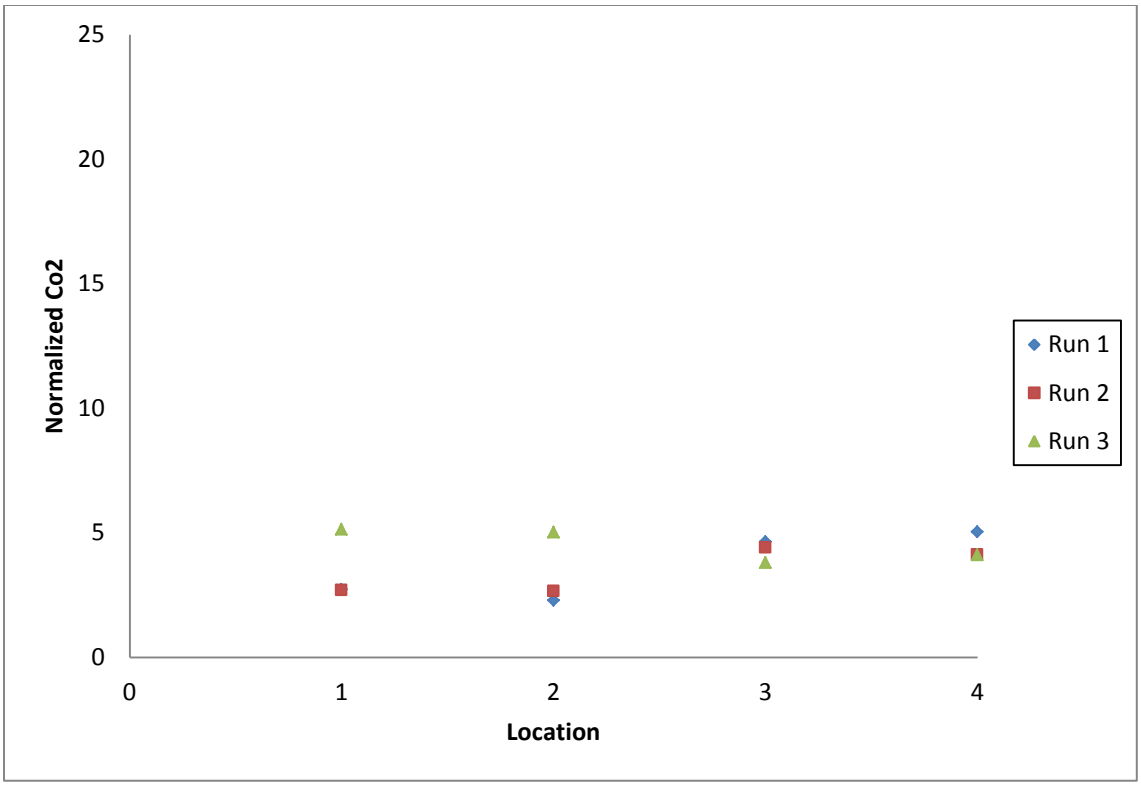

Figure 5.42 Two-row testing, Gasper Location 4 On, Seat 6A Release

Figure 5.43 shows the average normalized tracer gas concentration for the three runs occurring for each gasper configuration. The plot is laid out in the same orientation as the sampling locations, indicating the release and sampling points. Six seats are shown in the plot, as would be observed with an overhead view facing the front of the cabin. The two rectangles in the middle are representative of the seats in row 6. Each of the four plots corresponds to the results of all gasper configurations at one particular sampling site. This plot enables better visualization of how the tracer gas is moving between seats from the release location. Table 5.10 lists the normalized concentrations for each gasper configuration and sampling location. The table is organized by location and configuration, allowing for easy visualization of the impact a gasper had on a particular location in comparison to other measured concentrations at the same location for different configurations. All relative uncertainties for these values can be seen in Appendix A.

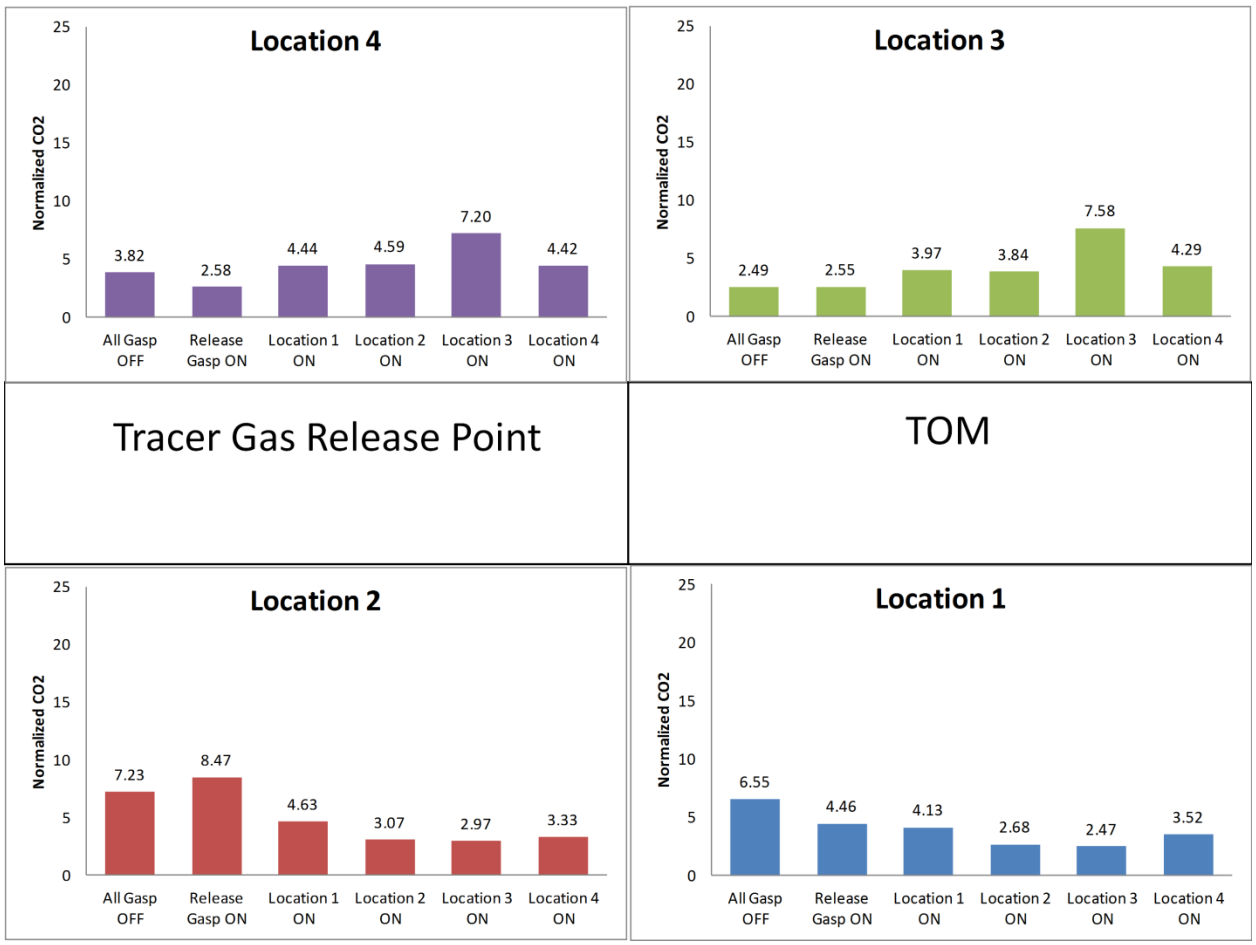

Figure 5.43 Summary of Average Normalized CO_2 for Rows 5 and Sampling with Seat 6A Release

Table 5.10 Normalized Values for Rows 5 and 7 Sampling with Seat 6A Release

	Location 1	Location 2	Location 3	Location 4
All Gaspers OFF	6.55	7.23	2.49	3.82
Release Gasper ON	4.46	8.47	2.55	2.58
Location 1 ON	4.13	4.63	3.97	4.44
Location 2 ON	2.68	3.07	3.84	4.59
Location 3 ON	2.47	2.97	7.58	7.20
Location 4 ON	3.52	3.33	4.29	4.42

5.3.4 Two-row Sampling with Seat 6B Release

The results for the moved release point were plotted in the same way as for the seat 6A release point. Again, there were no differing transient results due to the sampling locations being one

row removed from the release location in both directions. Figure 5.44 gives the baseline results with all gaspers off. Similarly, Figure 5.45 provides the results for gasper 1 (seat 5B) turned on. Figure 5.46 for the release manikin gasper turned on above seat 6B, Figure 5.47 corresponds to gasper 2 (seat 5A) on, Figure 5.48 with gasper 3 (seat 7B) on, and finally Figure 5.49 is for gasper 4 (seat 7A) on. Figure 5.50 is a summary plot of results, the same layout as the summary plot for seat 6A release. The normalized values for each location and gasper configuration are given in Table 5.11 allowing for easy comparison between turning the various gaspers on and the baseline configuration with all gaspers off.

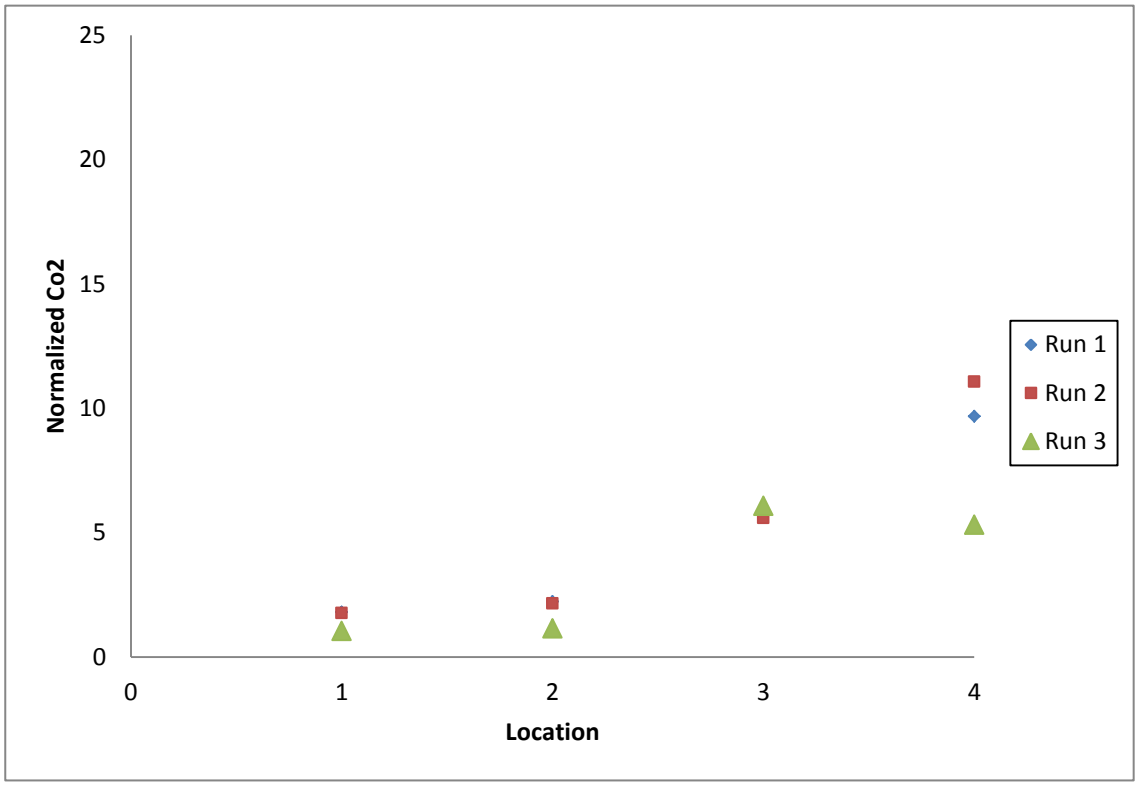

Figure 5.44 Two-row testing, All Gaspers Off, Seat 6B Release

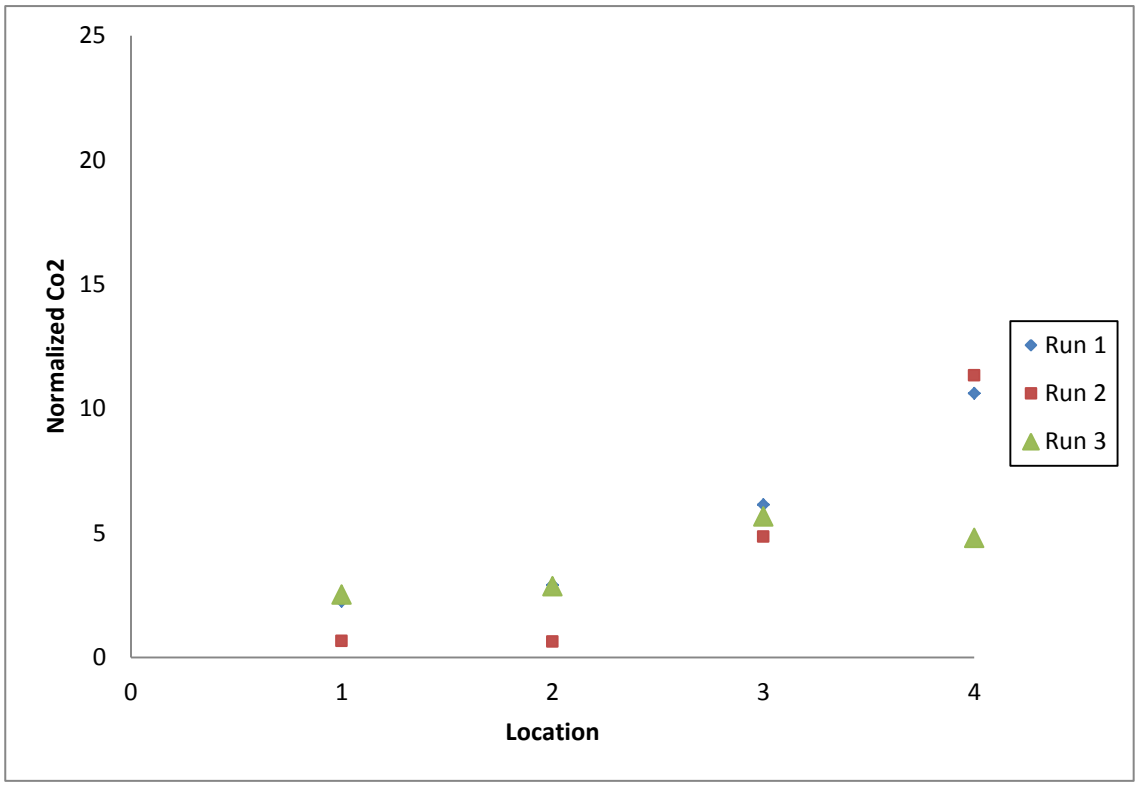

Figure 5.45 Two-row testing, Gasper Location 1 On, Seat 6B Release

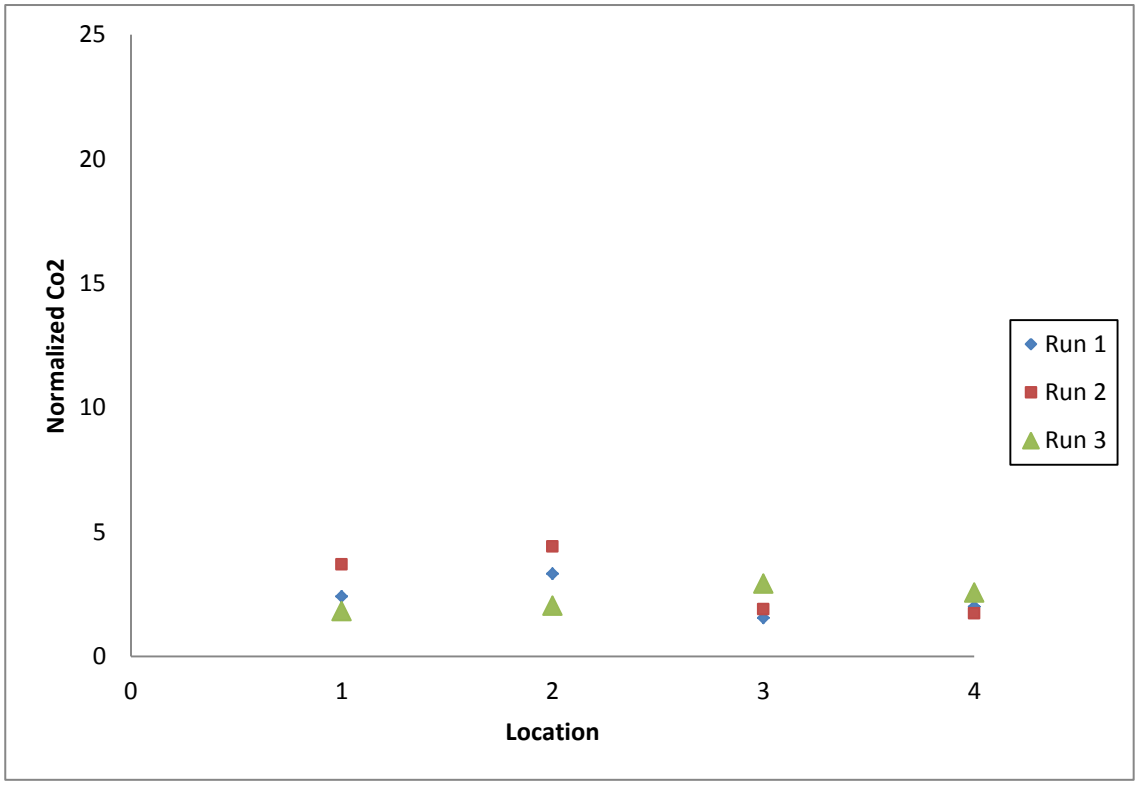

Figure 5.46 Two-row testing, Release Gasper On, Seat 6B Release

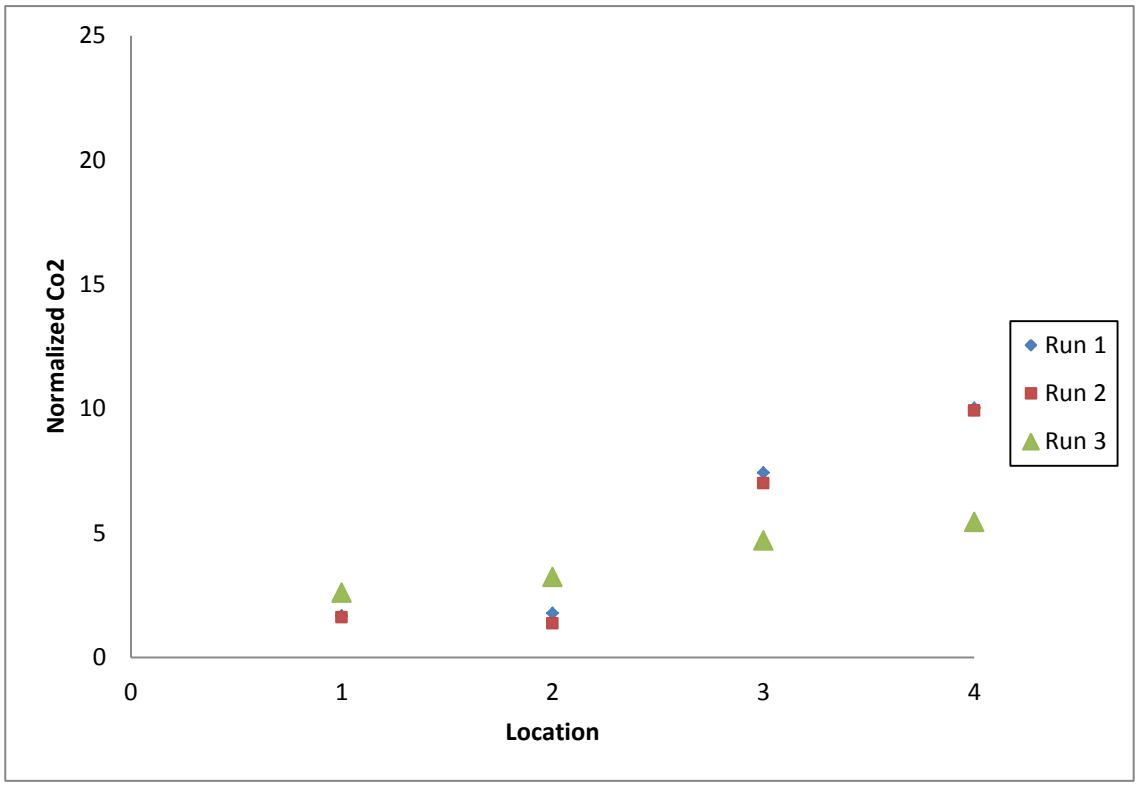

Figure 5.47 Two-row testing, Gasper Location 2 On, Seat 6B Release

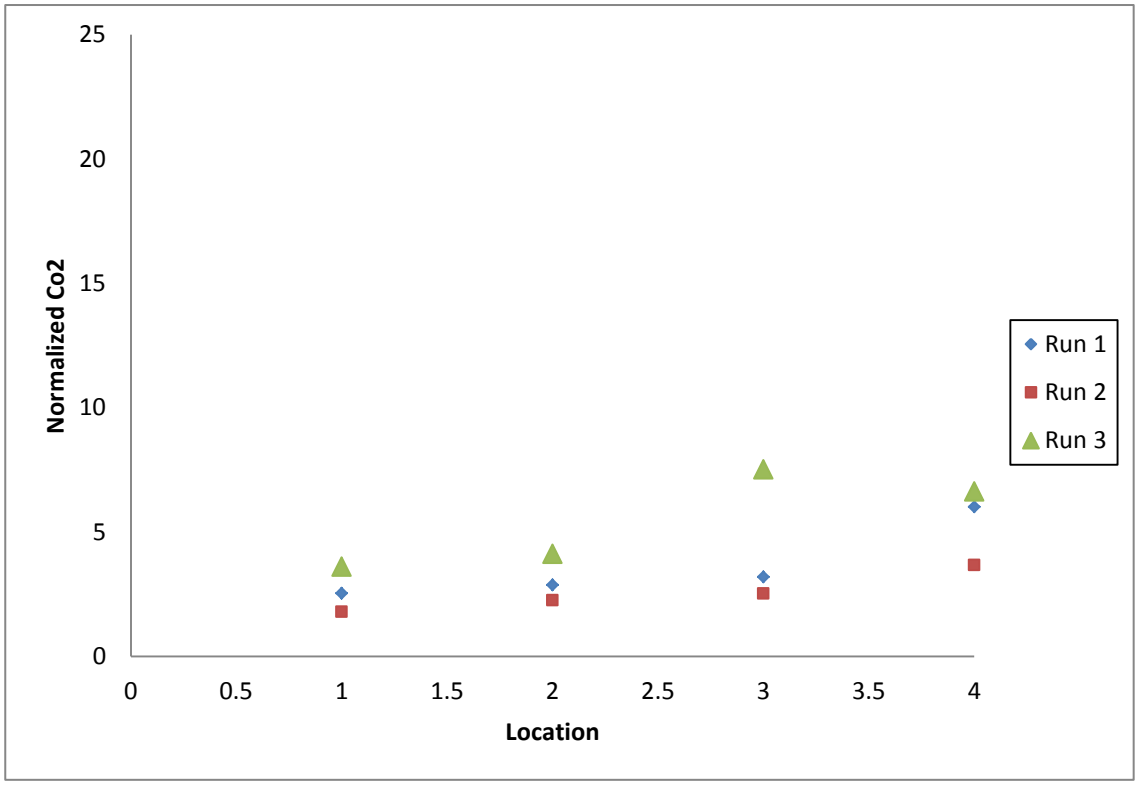

Figure 5.48 Two-row testing, Gasper Location 3 On, Seat 6B Release

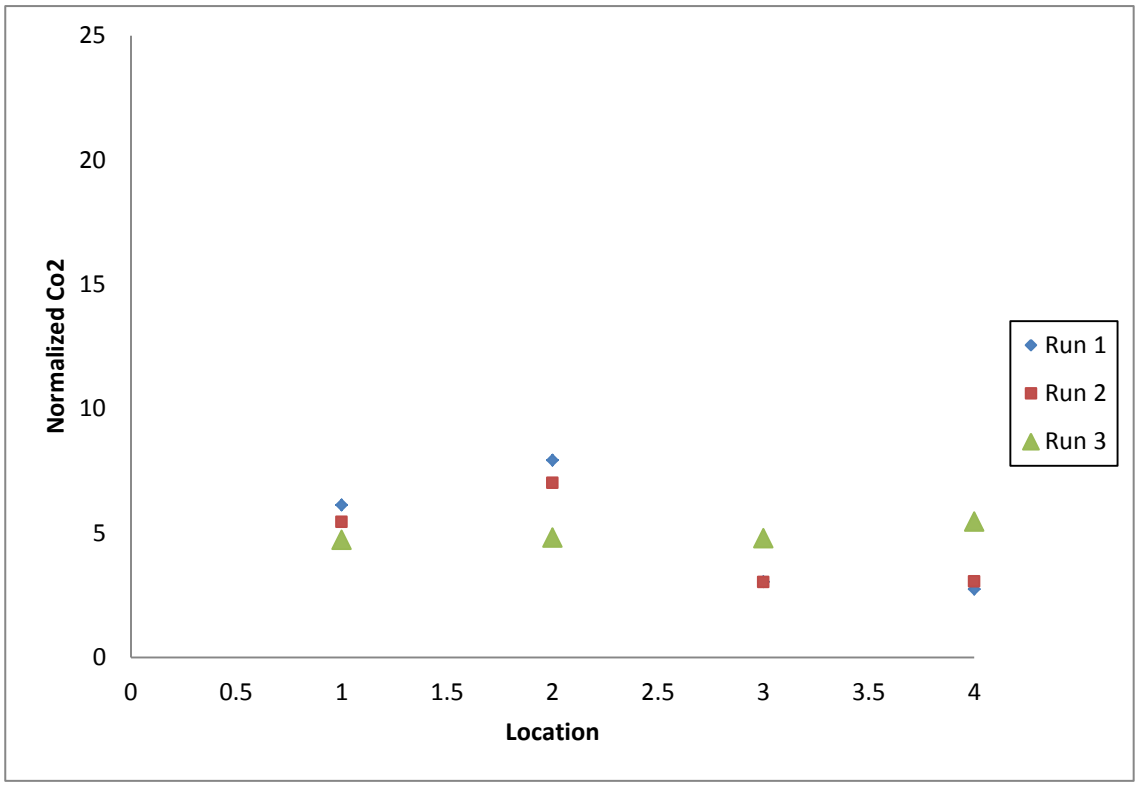

Figure 5.49 Two-row testing, Gasper Location 4 On, Seat 6B Release

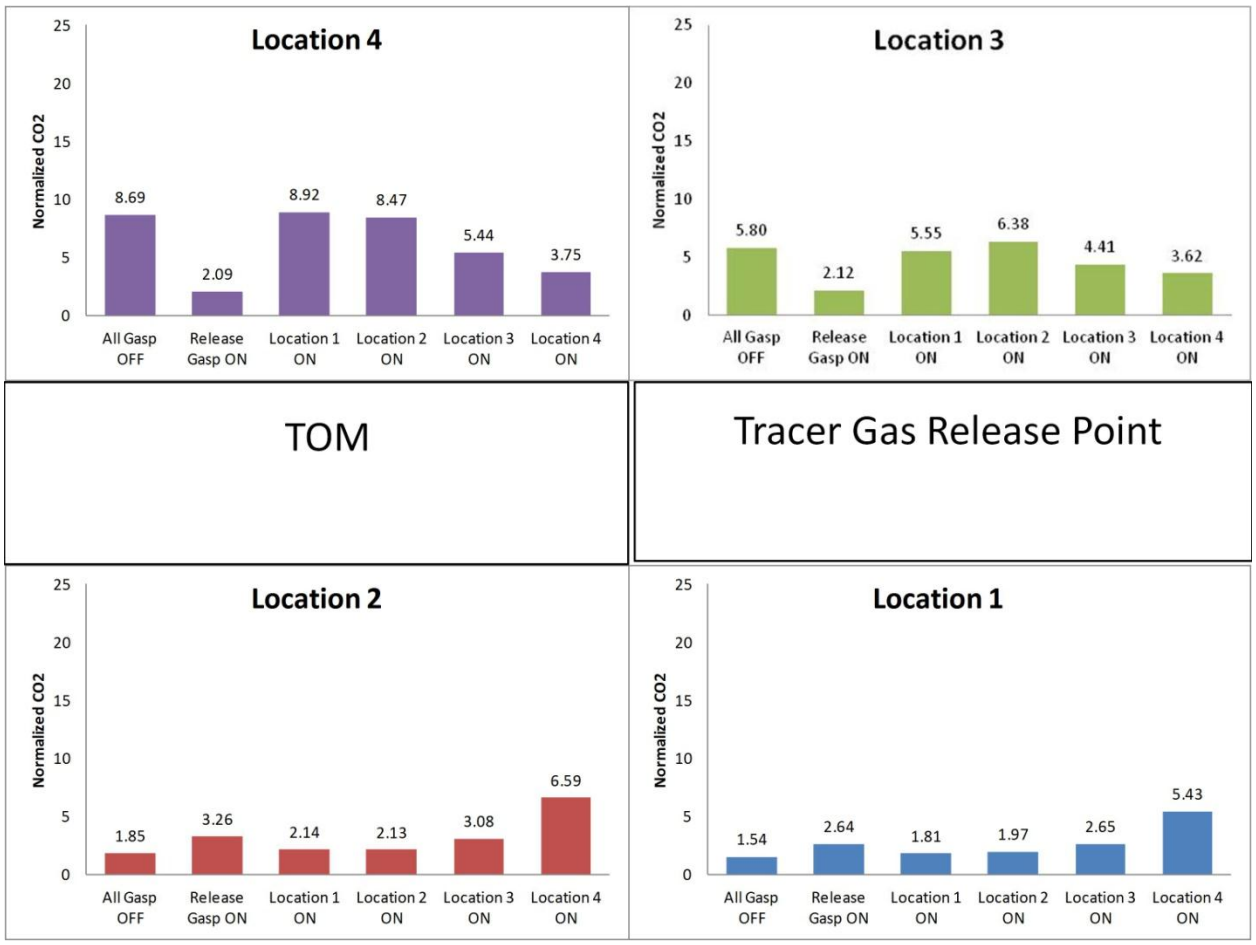

Figure 5.50 Summary of Average Normalized CO_2 for Rows 5 and 7 Sampling with Seat 6B Release

Table 5.11 Normalized Values for Rows 5 and 7 Sampling with Seat 6B Release

	Location 1	Location 2	Location 3	Location 4
All Gaspers OFF	1.54	1.85	5.80	8.69
Release Gasper ON	2.64	3.26	2.12	2.09
Location 1 ON	1.81	2.14	5.55	8.92
Location 2 ON	1.97	2.13	6.38	8.47
Location 3 ON	2.65	3.08	4.41	5.44
Location 4 ON	5.43	6.59	3.62	3.75

Chapter 6 - Discussion

The discussion of result and summary and/or conclusions below is again presented in separate sections based on the testing method utilized.

6.1 Cabin Traverse Testing

A careful review of the results presented for the cabin traverse testing reveals that a pattern may have developed indicating turning on the gasper system had an effect on the dispersal of the tracer gas. For each injection location it can be seen that the tracer gas exists in a higher concentration near the injection site with the gasper system on. However, after moving a distance away from the injection point, readings for both the gaspers on and off are nearly identical. This observation appears to indicate that with the gasper system off, the tracer gas distributes throughout the length of the cabin more effectively, possibly confirming the presence of a secondary airflow pattern rotating along the length of the cabin that is altered by the use of gaspers. This potential secondary airflow pattern was also observed in previous testing conducted at ACER (Beneke, 2010; IER, 2008).

Different maximum normalized values were observed with each injection location likely due to local airflow phenomena in the separate parts of the cabin. A symmetric distribution could be expected in a large enough cabin; however, in the 11-row simulator an eddy may be stopped abruptly by the presence of end walls in the cabin preventing it from developing fully. Prior research results using tracer gas in aircraft cabin simulators also show these asymmetric airflow patterns (Trupka, 2011; IER, 2008; Wang et al., 2006). These preliminary results are very important as researchers can further investigate the influence of gaspers on the general airflow pattern and contaminant transport in an aircraft cabin, both experimentally and numerically.

6.2 Gasper Air Inhalation Testing

The results of the gasper air inhalation testing show that a gasper provides marginal protection as a clean air source for passengers. Even with a gasper fully on and aimed directly at a passenger's face, 95% of the air the passenger is inhaling is entering through the diffusers of the cabin air distribution system. This is not to say the gasper does not provide protection, this simply shows

the gasper air mixes quickly in a short distance before reaching a passenger's inhalation zone. It also shows even with an operating gasper, passengers have a high dependence on the effectiveness of the cabin ventilation system providing clean air. The highly turbulent nature of the gasper air mixing with cabin diffuser air can be seen in Figure 6.1 taken from a smoke visualization video.

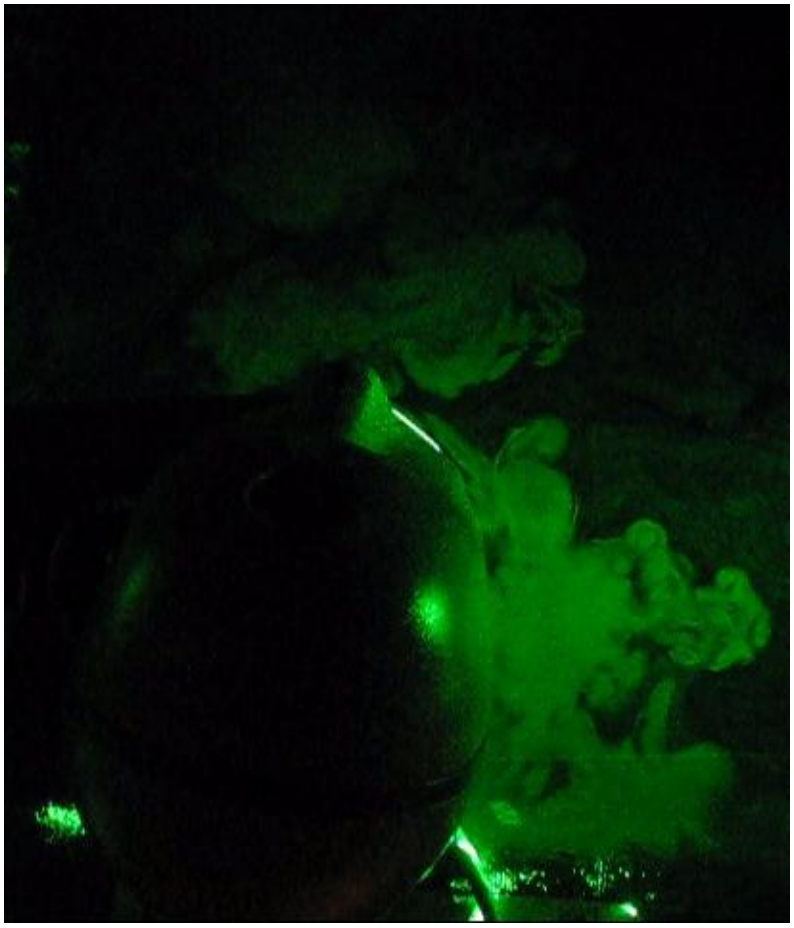

Figure 6.1 Top View of TOM with Smoke Visualization of Airflow

Figure 6.1 is a top view looking down on TOM being used as the sampling manikin. Smoke was being released from gasper 6B and visualized using a green laser sheet. As can be seen in the figure, a large number of eddies exist in the short distance between the gasper and sampling tube. These eddies cause the gasper air to quickly mix with the cabin air.

Research conducted using personal ventilation with dramatically increased airflow rates and decreased distances from the passenger's inhalation zone to the personal air outlet shows a large increase in the percentage of gasper air inhaled to nearly 60% in some cases (Zhang & Chen,

2007; Gao & Niu, 2008; Zhang et al., 2012). As these technologies are not yet fully developed, they have not yet taken into account passenger thermal comfort or practicality of replacing existing gasper systems in commercial aircraft. The results discussed in this section and those mentioned above simply address gasper air being inhaled by passengers. Gasper air inhalation does not necessarily correlate with prevention of contaminant spread within an aircraft cabin as was examined in the manikin tracer gas release testing.

6.3 Manikin Tracer Gas Release

With the dominant airflow pattern within an aircraft cabin moving from side to side, it was expected that the majority of the tracer gas would travel to a sampling location directly next to the release point within the row. The side-to-side airflow is indicated by the fact that the normalized concentrations are much higher for the sampling next to the tracer gas release using the intra-row sampling as opposed to the sampling taking place in rows 5 and 7 for the two-row sampling. With no gaspers on, the CO_2 concentration in-front and behind the release point is at most only 30-40% of the value sampled next to the release point. Typically this value was only 10-20% of the intra-row normalized concentration.

Each sampling and release method demonstrated that gaspers do have an impact on local airflows in the described configurations. It is important to note that all results are for a specific configuration in one location within the aircraft cabin, performing similar tests in another portion of the cabin would likely yield different results due to the nature of the airflows within the cabin. However, one would expect the overall nature of the results to be similar.

6.3.1 Intra-row Method, Seat 6B Release

The results from having the sampling location in seat 6A show that the use of gaspers does have an effect on the movement of tracer gas within the row in a transient manner. Peaks on the plots indicate a plume of tracer gas from the release location reaching the sampling point. The baseline test shows that over the course of a test, the normalized concentration is highest of all the gasper configurations utilized. Use of the gasper above the sampling manikin in seat 6A (configuration 2) caused a 27% decrease in this averaged concentration as well as a decrease in the magnitude of observed concentration peaks.

The use of the release gasper (seat 6B) in both configurations 3 and 4 caused an even greater decline of the average value over a test run, a reduction of over 90% in both cases. This fact appears to show that the release gasper has the greatest effect in reducing the dispersion of the tracer gas to the seat immediately next to the tracer gas release mechanism. As seen in smoke videos taken, when the gasper is focused on the release location, the tracer gas is immediately diluted with the clean air from the gasper, causing the tracer gas to disperse more quickly than in configurations 1 and 2 with the release gasper above seat 6B turned off. This prevents the tracer gas from reaching the sampling location as potently, and completely nullifies any peaks that can be attributed to stray plumes of the tracer gas. For this specific test setup, the release gasper provides the greatest reduction in tracer gas transport to seat 6A.

6.3.2 Intra-row Method, Seat 6A Release

This test was identical to the test with seat 6B being used as the release point, with the release point and sampling location being switched. The observed transient behavior was quite different however. For the baseline scenario, the peaks in normalized concentration were much higher, indicating larger plumes of tracer gas reaching the sampling location. As a result, simply turning on the gasper above the sampling location (configuration 2) caused a much more pronounced decrease in the magnitude of concentration of the peaks. Despite the apparent greater reduction in peak magnitude, the average concentration over the entire testing period only decreased 16%. Less than previously recorded, but still a sizable change.

The most noticeable difference in results occurred with the utilization of the release gasper. With only the release gasper on above seat 6A (configuration 3), the averaged concentration was reduced by 28%, a greater reduction than using only the sampling gasper, but not nearly as impactful as the results when seat 6B was the release point. Using both gaspers simultaneously caused the average concentration reduction to increase to 53%. Again a sizable reduction but still less of a reduction than the previous intra-row test with seat 6B as the release location. This is likely due to the location of the sampling in relation to the exhaust of the cabin along the walls. Want et al. (2006) noticed similar reductions in tracer gas values measured near the exhaust. A portion of the tracer gas is possibly mixing with an exhaust current as opposed to reaching the sampling location. The increased reduction between configurations 3 and 4 would indicate that

in this release configuration, dilution and dispersion of the tracer gas by the release gasper is not the only tangible effect. For this release scenario, the reduction in concentration shows the release and sampling gaspers complementing each other in terms of preventing the tracer gas from spreading within the row of seats.

6.3.3 Two-row Sampling, Seat 6A Release

The sampling of tracer gas in rows 5 and 7 in-front and behind the release location showed a lower normalized CO_2 concentration than the sampling location directly next to the release location within the release row, as expected. The results of these tests showed both increases and decreases in tracer gas concentration, dependent upon which gasper was turned on. This shows that the effect the gaspers have on airflow between rows in this release and sampling scenario is complex, a slight reduction in concentration at one sampled location is countered by a slight increase in concentration at another sampled location.

The effect a gasper has varies depending on its location, turning any gasper on caused an increase in the concentrations at locations 3 and 4 compared to the baseline test with all gaspers off, with no real difference seen with the release gasper being turned on. Turning on gasper 3 caused the concentration sample at locations 3 and 4 to be the highest of any configuration. Yet turning on gasper 4 caused the values to decrease nearly 50% while increasing the measured concentrations at locations 1 and 2. The only location the use of the release gasper improved protection over the baseline test was location 1, located in seat 5B diagonally behind the release point in seat 6A. This would indicate an airflow pattern causing the tracer gas to travel between these locations was disrupted.

The use of a gasper in this release case did not appear to follow any truly direct pattern. Turning on a gasper did not generally cause a decrease in measured concentration at its corresponding sampling site, but could create a decrease elsewhere in the sampling within rows 5 and 7. For instance turning on gasper 4 did not cause the concentration to decrease at location 4 from the baseline test but caused the concentrations at locations 1 and 2, located directly behind the release point, to decrease. However, it can be stated with certainty that the gaspers do have a measurable impact on the local airflow patterns within these three rows. Relative to the effect of

gaspers on intra-row travel of the tracer gas, the effect of the gaspers on the movement of the tracer gas is minimal.

6.3.4 Two-row Sampling, Seat 6B Release

Sampling within rows 5 and 7 with a near aisle release point (seat 6B) yielded results that showed a more direct link between gasper location and a reduction in averaged tracer gas concentration at that location. With gaspers off, a minimal amount of tracer gas reached the sampling locations in row 5, an amount barely above typical steady-state background CO_2 levels. The concentration in row 7, especially in seat 7A (location 4), was considerably higher.

The use of the release gasper caused a significant reduction in measured concentration in row 7, but increased the tracer gas level observed in row 5. With the use of gaspers 1 and 2, essentially no effect was observed on concentration levels observed at location 1 and 2 because barely any tracer gas was present in those locations to begin with. Overall, these gaspers had little effect on tracer gas transmission. Gasper 3 caused a decrease in concentration at locations 3 and 4, but a slight increase in concentration at locations 1 and 2. Gasper 4 again caused a decrease in concentrations at locations 3 and 4 while causing an even greater increase in concentrations observed at locations 1 and 2. Again this shows these gaspers have a tangible effect on the transmission of tracer gas between rows as seen with using seat 6A as the release point.

6.3.5 Additional Discussion

The intra-row and two-row experiments looked only at the impact on person-to-person transport for nearby passengers. If reductions in exposure are accomplished simply by increasing the dispersion of the contaminants into the rest of the cabin, then these reductions in exposure are achieved at the expense of small but widespread increases in exposure in the rest of the cabin. However, if the reductions are achieved by moving the contaminants downward where they are more rapidly exhausted, then the local reduction is not necessarily achieved at the price of higher exposure elsewhere. The mechanism of the reductions was not addressed in this project.

Chapter 7 - Summary and Conclusions

The results of testing conducted show gaspers have an impact on both lengthwise contaminant transport within a commercial aircraft as well as disrupting the typical dispersal of contaminants. It was also shown that the amount of gasper air inhaled by a passenger is minimal due to the turbulent mixing of the air jet with the normal ventilation within the cabin. At the testing location chosen, the use of gaspers greatly reduces the transmission of contaminants amongst passengers. However, these results are specific to one location tested within the aircraft cabin simulator. Further testing in a different location within the cabin may yield different results. Overall, it was shown that gaspers play a role in the overall transport of contaminants within an aircraft.

For the cabin traverse testing it was quite evident that the use of gaspers affected the longitudinal dispersion pattern present within the cabin. This effect was evident in the increased concentrations of tracer gas around the injection location when the gaspers were turned on as opposed to when they were off. The results show that a system of gaspers can disrupt the transmission of contaminants within an aircraft cabin.

The gasper inhalation testing demonstrated that the air emanating from individual gaspers mixes rapidly with the overall cabin ventilation. This was shown by the fact that only around 5% of the sampled air at the simulated passenger originated from the gasper used for testing. This would indicate that the gasper air mixes quickly with the cabin ventilation which was proven through the use of smoke visualization showing numerous eddies and recirculation patterns between the gasper and sampling location.

The results of manikin tracer gas release testing indicated that gaspers can appreciably reduce the transmission of contaminants between passengers. The reduction in exposure was most pronounced in transmission within a row with the gasper above the release manikin turned on, reducing transmission to the sampling manikin by as much as 90%. Between rows, the impact of the gaspers was mixed, dependent upon what airflow patterns local to those rows were being disrupted. No correlation could be determined between a certain gaspers usage and reduction of tracer gas transmission in-front of and behind the release location.

The uncertainty values associated with each test were relatively low due to the large number of data points used to obtain average normalized concentration values. This reduction in uncertainty was possible because tests were conducted in steady-state conditions meaning the dispersal patterns of the tracer gas were constant for a given testing run. These uncertainties were reduced even more when the individual test runs for a certain location were averaged together.

Chapter 8 - Recommendations

Based upon the results obtained for all testing scenarios and configurations it is recommended to conduct more tests investigating the impact of gaspers on disease and contaminant transmission within an aircraft cabin. The number of possible combinations of activated gaspers and release locations made it necessary to limit the scope of the research. As a result, more release locations could be investigated for all testing methods utilized to obtain a more complete picture of how contaminants disperse in all parts of the aircraft cabin.

Since gaspers were shown to provide local protection to passengers from the transmission of contaminants it is recommended to conduct future testing on the gaspers themselves. These tests could look into ways to further increase the protection gaspers provide. This testing would be necessary after verifying gaspers provide protection in all zones within an aircraft cabin.

References

ASHRAE. 2004. *ANSI/ASHRAE Standard 55-2004, Thermal Environmental Conditions for Human Occupancy*. Atlanta: American Society of Heating, Air-Conditioning and Refrigeration Engineers, Inc.

Beneke, J.M. 2010. Small Diameter Particle Dispersion in a Commercial Aircraft Cabin. *M.S. Thesis, Kansas State University, Manhattan, KS.*

Beneke, J.M., B.W. Jones, and M.H. Hosni. 2011. Fine Particle Dispersion in a Commercial Aircraft Cabin. *HVAC&R Research* 17(1):107-17.

Bolashikov Z.D., and A.K. Melikov. 2009. Methods for air cleaning and protection of building occupants from airborne pathogens. *Building and Environment* 44:1378-1385.

BTS. 2012. BTS Data. www.bts.gov/press_releases/2012/bts014_12/pdf/bts014_12.pdf

FAA. 1996. *FAR Section 25.831, Ventilation.* Washington, DC: Federal Aviation Administration.

Gao, N.P., and J.L. Niu. 2008. Personalized ventilation for commercial aircraft cabins. *Journal of Aircraft* 45:508-12.

Hunt, E. H., and D.R. Space. 1994. The airplane cabin environment, The Boeing company. *International In-Flight Service Management Organization Conference*. Montreal, Canada.

IER. 2008. Draft Final Technical Report, Contaminant Transport in Airliner Cabin. Kansas State University, Manhattan: FAA Cooperative Agreement 04-C-ACE-KSU, Institute for Environmental Research.

Jones, B.W. 2009. Advanced models for predicting contaminants and infectious disease virus transport in the airliner cabin environment: Experimental data. Proceedings of the Transportation Research Board, Research on the Transmission of Disease in Airports and Aircraft, A Symposium, The National Academies, September, 2009.

Lebbin, P. 2006. Experimental and numerical analysis of air, tracer gas, and particulate movement in a large eddy simulation chamber. *Ph.D. Thesis, Kansas State University, Manhattan, KS.*

Mangili, A., and M.A. Gendreau. 2005. Transmission of infectious diseases during commercial air travel. *The Lancet* 365:989-96.

Mazumdar, S., P.A. Priyadarshana, A. Keshavarz, Q. Chen, and B.W. Jones. 2008. Flow characteristics from air supply diffusers and their effect on airflow and contaminant transport inside an aircraft cabin. *Proceedings of the 11th International Conference on Indoor Air Quality and Climate: Indoor Air 2008*. Copenhagen, Denmark. p. 669.

Melikov, A.K., R. Cermak, and M. Majer. 2002. Personalized ventilation: Evaluation of different air terminal devices. *Energy and Buildings* 34:829-36.

Morawska, L. 2006. Droplet fate in indoor environments, or can we prevent the spread of infection? *Indoor Air* 16:335-47.

National Research Council. Committee on Air Quality in Passenger Cabins of Commercial Aircraft, Board on Environmental Studies and Toxicology. 2002. *The Airliner Cabin Environment and the Health of Passengers and Crew*. Chapter 2, Environmental Control. Washington, DC: The National Academies Press.

O'Donnell A., D. Giovanna, and V.H. Nguyen. 1991. Air quality, ventilation, temperature, and humidity in aircraft. *ASHRAE Journal* April:42-46.

Olsen, S.J., H.-L. Chang, T.Y.-Y. Cheung, A.F.-Y. Tang, T.L. Fisk, S.P.-L. Ooi, H.-W. Kuo, D.D.-S. Jiang, K.-T. Chen, J. Lando, K.-H. Hsu, T.-J. Chen, and S.F. Dowell. 2003. Transmission of severe acute respiratory syndrome on aircraft. *The New England Journal of Medicine* 349(25):2416-22.

Radim, C., A.K. Melikov, L. Forejt, and O. Kovar. 2006. Performance of personalized ventilation in conjunction with mixing and displacement ventilation. *HVAC&R Research* 12:295-311.

Shehadi, M. 2010. Experimental Investigation of Optimal Particulate Sensors Location in an Aircraft Cabin. *M.S. Thesis, Kansas State University, Manhattan, KS.*

Trupka, A.T. 2011. Tracer gas mapping of beverage cart wake in a twin aisle aircraft cabin simulation chamber. *M.S. Thesis, Kansas State University, Manhattan, KS.*

Wang, A., Y. Zhang, J.L. Topmiller, J.S. Bennett, and K.H. Dunn. 2006. Tracer study of airborne disease transmission in an aircraft cabin mock-up. *ASHRAE Transactions* 112(2):697-705.

Zhang, T., and Q. Chen. 2007. Novel air distribution systems for commercial aircraft cabins. *Building and Environment* 42:1675-1684.

Zhang, T., P. Li, and S. Wang. 2012. A personal air distribution system with air terminals embedded in chair armrests on commercial airplanes. *Building and Environment* 47:89-99.

Appendix A - Uncertainty Analysis

The uncertainties of each testing method were evaluated, taking into account the uncertainties within the entire testing system. All uncertainties were evaluated about the true mean for each testing run since the average normalized values were the values used for comparisons. In the equations below, K is used to denote the number of data points as to not be confused with the normalized CO_2 concentration which is abbreviated as N.

A.1 Measurement and Random Uncertainties

In order to obtain the measurement uncertainty for each sampled value, the propagation of errors technique was utilized. The propagation of errors equation is seen in Equation (A.1).

$$U_f^2 = \left(\frac{\partial f}{\partial x_1} U_{x1}\right)^2 + \left(\frac{\partial f}{\partial x_2} U_{x2}\right)^2 + \ldots + \left(\frac{\partial f}{\partial x_n} U_{xn}\right)^2 \quad \text{(A.1)}$$

Where the total uncertainty in a function $f(x_1,x_2,...,x_n)$ is a function of all uncertainties associated with values in that function. Using this equation on the normalization function used for most calculations seen in Equation (4.1), the measurement uncertainty becomes Equation (A.2).

$$\frac{U_N}{N}^2 = \left(\frac{U_{Interior}}{(C_{Interior} - C_{Inlet})}\right)^2 + \left(\frac{U_{Inlet}}{(C_{Interior} - C_{Inlet})}\right)^2 + \left(\frac{U_{Vent}}{V_{Vent}}\right)^2 + \left(\frac{U_{VCO2}}{V_{VCO2}}\right)^2 \quad \text{(A.2)}$$

Meaning four individual uncertainty values need to be known to calculate the measurement uncertainty; the uncertainty in the inlet and outlet CO_2 measurements, the uncertainty in the cabin ventilation airflow rate, and the uncertainty in the injection rate of CO_2.

The measurement uncertainty associated with Equation (4.2) utilized in the gasper air inhalation testing is shown in Equation (A.3).

$$U_{Exp}{}^2 = \left(\frac{U_{Manikin}}{(C_{gasper} - C_{background})}\right)^2 + \left(\frac{-(C_{Manikin} - C_{background})}{(C_{gasper} - C_{background})^2} U_{gasper}\right)^2 + \left(\frac{(C_{Manikin} - C_{gasper})}{(C_{gasper} - C_{background})^2} U_{background}\right)^2 \quad \text{(A.3)}$$

This time only three uncertainties are necessary, the uncertainty of the CO_2 measurement at each sampling location used during testing.

Since the average normalized values for each location over a period of time are of most importance, the random uncertainty about the true mean was used. This is seen in Equation (A.4) where $t_{95,N-1}$ is the associated value based on a 95 percent confidence interval, and S_x is the standard deviation for a given test run.

$$U_{Random} = \frac{t_{95,K-1} S_x}{\sqrt{K}} \quad \text{(A.4)}$$

To obtain the total uncertainty for a test run, the random and measurement uncertainties were combined using the root-sum-squared equation given in Equation (A.5).

$$U_{total} = \sqrt{U_{Random}{}^2 + U_{Measurement}{}^2} \quad \text{(A.5)}$$

The random uncertainty is inversely proportional to the number of samples taken while the measurement uncertainty varies only by the changes in CO_2 concentrations measured.

A.2 Testing Equipment Uncertainties

As indicated in section A.1, in order to calculate the measurement uncertainty associated with each test, the uncertainties in the measurement of each variable in Equation (4.1) need to be known. The uncertainty associated with the cabin ventilation airflow rate and the airflow rate of

CO_2 has been previously calculated in Trupka (2011). Since the same cabin ventilation airflow rate measurement equipment and CO_2 airflow rate measurement equipment were used in this testing as in Trupka (2011), these uncertainty values were used in calculations. However, the uncertainties associated with the CO_2 sensors were again calculated since these values are based upon CO_2 analyzer calibrations. These calibrations were independent of those conducted by Trupka (2011).

A.2.1 Cabin Ventilation Airflow Rate Uncertainty

The airflow rate into the aircraft cabin is 39,660 lpm (1400 cfm). To ensure that this amount of air is reaching the aircraft cabin, the airflow rate within the vent is calculated and recorded over 5 second intervals for the duration of a test. The airflow rate is calculated based on pressure and temperature readings of the air within the duct along with correction factors based upon the duct size. The series of calculations leading to the overall uncertainty again uses propagation of errors of the associated uncertainties with pressure and temperature measurements within the duct. The exact calculations can be seen in Trupka (2011), with the final value for the cabin ventilation airflow rate uncertainty being ±1.1%.

A.2.2 CO_2 Injection Rate Uncertainty

Since the mass flow controller was used for long series of tests, the repeatability of the instrument was the uncertainty used in calculations. This uncertainty was ±0.2% of the full scale flow rate of 100 lpm (3.53 cfm). This repeatability was combined using a root-sum square with the purity of the CO_2 used for injection which was ±0.5%. For the cabin traverse testing this meant the uncertainty in the injection rate of 7 lpm (0.247 cfm) was ±2.9%, and for the manikin tracer gas release with a flow rate of 2.5 lpm (0.089 cfm) the uncertainty was ±8.0%.

A.2.3 CO_2 Sensor Uncertainty

The measurement uncertainties associated with each CO_2 sensor used in testing is a RSS combination of the repeatability, calibration, DAQ and linearity uncertainties associated with each instrument. The uncertainties specified by the manufacturer for each CO_2 analyzer are given in Table A.1 below along with the uncertainty of the Agilent DAQ used for reading and

recording samples. The repeatability uncertainties given were used in calculating the overall sensor uncertainty. The DAQ uncertainty used in the calculation is also given in Table A.1.

Table A.1 CO_2 Analyzer and DAQ Uncertainties

Model	Uncertainty	Range
Edinburgh Gascard NG	2% of range (accuracy)	0 to 3000 ppm
	0.3% @ zero 1.5% @span (repeatability)	
NOVA Analytical 420	50 ppm (accuracy)	0 to 5000 ppm
	0.3% @ zero 1.5% @span (repeatability)	
PP Systems WMA-4	20 ppm (accuracy)	0 to 2000 ppm
	<1% @span (repeatability)	
Agilent 34970a DAQ	0.0040% of reading + 0.0007% of range	1 V
	0.0035% of reading + 0.0005% of range	10 V

For the calibration process outlined in Section 3.3.3, each calibration gas had an associated uncertainty: ±2% for the 500 ppm calibration cylinder and ±1% for the 1000 and 2000 ppm calibration cylinders. These values were combined using RSS again to obtain a calibration uncertainty of ±2.5%.

The final uncertainty value needed to calculate the total uncertainty of each analyzer was the linearity uncertainty, based on the calibration curve of each analyzer. Since the sensors were calibrated over regular intervals, the linearity uncertainty of each sensor was an average of the linearity uncertainties for each individual calibration. The linearity uncertainty for each sensor is given in Table A.2. The repeatability uncertainty is also given for each sensor, based on a linear interpolation of the span and zero repeatability for each instrument, using estimates of 1000 ppm for the interior reading and 400 ppm for the inlet reading. Since the PP Systems analyzer was the newest of the three analyzers and only used once, it was not calibrated as often as the other sensors. The NOVA sensor eventually began to have issues, necessitating replacing it with the PP Systems analyzer for interior cabin sampling.

Table A.2 R-squared Values and Uncertainties of CO_2 Analyzers

Calibration Date	Edinburgh R^2	NOVA R^2	PP Systems R^2
8/2/2012		0.999999	0.999993
7/20/2012	1.000000	0.999999	
7/6/2012	0.999920	0.999918	
6/19/2012	0.999773	0.998519	
5/7/2012	0.999798	0.999977	0.999925
2/24/2012	0.999467	0.999751	0.999880
12/12/2011	0.999634	0.999735	
9/6/2011	0.999690	0.998782	
8/15/2011	0.999781	0.999153	
7/18/2011	0.999976	0.999711	
5/27/2011	0.999735	0.999841	
Average R Squared	0.999777	0.999539	0.999933
Average Linearity Uncertainty	**0.022%**	**0.046%**	**0.007%**
Repeatability	**0.45%**	**0.54%**	**1.0%**
Total Uncertainty	**2.5%**	**2.5%**	**2.7%**

Once all uncertainty values were obtained for each sensor, the total uncertainty value was then calculated. The total uncertainty for each sensor is given at the bottom of Table A.2. These values were calculated using the RSS method of addition again. The NOVA analytical sensor will be used for a sample calculation shown in Equations (A.6) and (A.7).

$$U_{NOVA} = \pm\sqrt{{U_{Linearity}}^2 + {U_{Repeat}}^2 + {U_{DAQ}}^2 + {U_{Cal.Gas}}^2} \quad \text{(A.6)}$$

$$= \pm\sqrt{0.0512\%^2 + 0.539\%^2 + 0.0047\%^2 + 2.45\%^2} = \pm 2.5\% \quad \text{(A.7)}$$

These calculated uncertainties for each analyzer are the final values needed to perform measurement uncertainty calculations based on Equations (A.2) and (A.3).

A.3 Uncertainty Calculations

Calculating the uncertainties of the different testing procedures is a matter of using the uncertainty values and equations outlined in sections A.1 and A.2. Though the calculation methods are the same, handling of the data for uncertainty calculations varies slightly between testing scenarios.

A.3.1 Cabin Traverse and Manikin Release Uncertainty Calculation

For the cabin traverse testing, the tests conducted with tracer gas being released in row 11 and samples being taken in row 10 for the second test run will be used as a calculation example. The first step in performing the calculations was to average all normalized values for the 360 data points and take the standard deviation of the data set. These values are shown below.

Table A.3 Statistical Values for Row 11 Injection, Row 10 Sampling, Test Run 2, Gaspers Off

Average Normalized Concentration	4.58
$S_{\bar{x}}$	±0.10
$t_{95,359}$	1.97
Random Uncertainty	±0.21
Measurement Uncertainty	±0.31
Total Uncertainty	±0.37

The standard deviation allows the random uncertainty to be calculated for the average normalized concentration using Equation (A.8).

$$U_{Random} = \frac{t_{95,359}(1.98)}{\sqrt{360}} = \pm 0.21 \tag{A.8}$$

The average measurement uncertainty for the entire test was then calculated. A measurement uncertainty existed at each normalized data point, a sample calculation of one of these uncertainties is shown in Equation (A.9) using Equation (A.2).

$$\begin{aligned} U_{Measure} = \ & \pm\sqrt{\left(\frac{0.0251 * 1601}{(1601-399)}\right)^2 + \left(\frac{0.0249 * 399}{(1601-399)}\right)^2 + (0.0108)^2 + \ (0.0209)^2} \\ & = \pm 0.042 * N = \ \pm 0.28 \end{aligned} \tag{A.9}$$

Where N is the normalized value based on the measured concentrations for that data point. The average of all measurement uncertainties in the data set was then taken, resulting in a value of:

$$\overline{U_{Measurement}} = \pm 0.31 \quad \text{(A.10)}$$

The random and measurement uncertainties of the average normalized concentration were then summed together.

$$\sqrt{0.31^2 + 0.21^2} = \pm 0.37 \quad \text{(A.11)}$$

In relative uncertainty form, this uncertainty for this particular test run becomes ±8%. Two other test runs were performed for this sampling location, also with resultant relative uncertainties of ±8%. Since the relative uncertainty was the same for all three test runs, it was assumed to be the representative relative uncertainty for that location.

It is important to note that the systematic uncertainty is inversely proportional to the difference between the sampled concentration and the concentration of the inlet air. This can be seen in Equation (A.3) as the concentration difference is in the denominator of the systematic uncertainty equation. The test cases in which the normalized tracer gas value is reduced the most are the cases with the highest relative uncertainty.

A.3.2 Gasper Inhalation Uncertainty Calculation

Calculating the uncertainty for the gasper exposure measurements was a different process than for the normalized concentration uncertainties. Equation (4.2) is composed of three separate concentration values that while taken with the same CO2 analyzer, were not taken simultaneously. The values used were averages of samples taken when the cabin reached a steady state condition. As such, each concentration value used had a different uncertainty despite being taken with the same CO2 analyzer, mostly due to the random uncertainty. Calculating the uncertainty of each concentration was again a RSS of the measurement and random uncertainties. The uncertainty of the gasper air concentration will be used as an example. For this case there were 180 samples taken for each concentration averaging.

Table A.4 Example Values for Gasper CO_2 Concentration Measurement

Average CO_2 Concentration	3204 ppm
$S_{\bar{x}}$	±1 ppm
$t_{95,180}$	1.97
Random Uncertainty	±2 ppm
Measurement Uncertainty	±81 ppm
Total Uncertainty	±81 ppm

The same calculation procedure as in section A.3.1 was used to obtain these values, using the uncertainties associated with the NOVA analytical CO_2 analyzer. As can be seen the measurement uncertainty is the dominant uncertainty when calculating the total uncertainty this time. This procedure was repeated for the background and manikin CO_2 concentrations. The total uncertainties associated with each measurement are summarized in Table A.5.

Table A.5 Uncertainties of Averaged CO_2 Concentrations

Gasper Concentration Uncertainty	±81 ppm
Manikin Concentration Uncertainty	±14 ppm
Background Concentration Uncertainty	±11 ppm

These uncertainties were then used with the corresponding average concentrations and Equation (A.3) to determine the total uncertainty in the exposure value calculation. All values are in ppm.

$$U_{Exp}{}^2 = \left(\frac{14}{(3204-432)}\right)^2 + \left(\frac{-(557-432)}{(3204-432)^2} * 81\right)^2 + \left(\frac{(557-432)}{(3204-432)^2} * 11\right)^2 \quad \text{(A.12)}$$

In examining the equation, it is easy to see that the final two terms have no significance in the calculation as they are several orders of magnitude less than the first term. The final uncertainty in the gasper exposure is then ±0.5% for this test run. The uncertainty is in units of percentage because those are the units of the exposure equation. Due to the constant values of the background and gasper concentrations in all calculations, the uncertainty value was the same for all test runs. The relative uncertainty varied from ±10% to ±17% depending on the final exposure value.

A.4 Manikin Release, Two-row Testing Uncertainties

Tables A.6 and A.7 list the relative uncertainties for the results obtained using the two-row testing method with manikin release. The relative uncertainties calculated for the averages of the three testing runs for each configuration and location of the two-row manikin release testing are listed below. The values are organized within the tables corresponding to sampling location and configuration of the gaspers used.

Table A.6 Relative Uncertainties for Manikin Release, Two-row Testing Method, Seat 6A Release

	Location 1	Location 2	Location 3	Location 4
All Gaspers OFF	±11%	±11%	±10%	±10%
Release Gasper ON	±8%	±7%	±10%	±10%
Location 1 ON	±11%	±10%	±8%	±7%
Location 2 ON	±10%	±9%	±9%	±8%
Location 3 ON	±12%	±10%	±7%	±7%
Location 4 ON	±11%	±11%	±8%	±8%

Table A.7 Relative Uncertainties for Manikin Release, Two-row Testing Method, Seat 6B Release

	Location 1	Location 2	Location 3	Location 4
All Gaspers OFF	±14%	±12%	±7%	±6%
Release Gasper ON	±9%	±8%	±14%	±15%
Location 1 ON	±11%	±11%	±8%	±6%
Location 2 ON	±11%	±11%	±7%	±6%
Location 3 ON	±12%	±11%	±10%	±10%
Location 4 ON	±8%	±7%	±10%	±10%

Appendix B - Changing of Interior CO_2 Sensors

The NOVA Analytical CO_2 analyzer used for analyzing air from the sampling tree began having technical issues before the final set of testing for the two-row testing method seat 6B release. The analyzer was replaced with the PP Systems WMA-4 analyzer with specifications described in Chapter 7. All test runs demarcated as 'run 3' in the two-row testing results were obtained using the WMA-4 analyzer. All other results presented were obtained using the NOVA Analytical CO_2 sensor. As all results were similar to the sets obtained with the NOVA analyzer and the associated measurement uncertainties with the sensors were essentially the same values it is evident that changing the sensors did not have any impact on the two-row testing results.

.